THE UNIVERSITY OF CALGARY

An Evaluation of Closed Flux Chamber Technique for Gas Emission Measurement from Landfills

by

M.D. Nandana Perera

A THESIS

SUBMITTED TO THE FACULTY OF GRADUATE STUDIES

IN PARTIAL FULFILLMENT OF THE REQUIREMENTS FOR THE DEGREE OF

MASTER OF SCIENCE

DEPARTMENT OF CIVIL ENGINEERING

CALGARY, ALBERTA

JANUARY, 2000

ABSTRACT

This thesis presents a critical evaluation of the closed flux chamber technique for gas emission measurements at landfills and a methodology to minimize errors associated with such measurements. Field and laboratory experiments were conducted to evaluate the effects of factors such as soil conditions, gas flux rates, and chamber configuration, on chamber measurements. A two-dimensional gas migration model incorporating advection and diffusion was developed to simulate various scenarios that could arise during closed flux chamber measurements.

The field and laboratory experiments showed that the gas flux is under-estimated when a closed flux chamber was used for measurements. The same conclusion was drawn by the model. The model was used to understand gas migration patterns and to determine the measurement errors caused by gas accumulation within the chamber. The research concludes that accurate results could be obtained economically and conveniently if the closed flux chamber technique is used in association with the mathematical model simulations.

ACKNOWLEDGEMENTS

I would like to express my sincere gratitude to Dr. J.P.A. Hettiaratchi under whose supervision this work was carried out. It has been a rewarding experience to work with Dr. Hettiaratchi and his guidance, encouragement, and constructive criticism throughout all stages of the research program contributed to the success of this work. I also appreciate the role of the Department of Civil Engineering in providing me with the financial assistance and a supportive working environment.

I would like to thank Dr. Gopal Achari, Dr. Sukru Sumer, Simant Upreti, and Dr. Larry Bentley for their enlightening discussions on modeling. Dr. Doug Phillips' assistance in computing and graphics is also greatly appreciated.

I express my gratitude to Kiran Dave, Manager, and Harry Friessen, Head Mechanic, of Grounds Department for their generous assistance in constructing the field lysimeter. Heather Mills, and other technicians in the Department of Civil Engineering and Claudine Curnow of Department of Chemical Engineering should also be mentioned for their support for this research.

This work would not have been a success without the support of my friends and colleagues, Vanita Shroff, Prasanna Amatya, Kanishka Perera, Vince Stein, Mallika Gunarathne, and other students of the Engineering for the Environment program. Last but not the least, I would like to express my deep gratitude to my beloved parents and sisters for their inspirational support without complaining about lapses of my responsibilities.

Dedicated to my beloved parents

- for their endless love and care

TABLE OF CONTENTS

LIST OF TABLES

LIST OF FIGURES

CHAPTER ONE
INTRODUCTION

1.1 General

Although integrated waste management, the hierarchical method of waste management, ranks landfilling as the last option; low cost and simplicity make it the preferred method in most countries (Tchobanoglous et al., 1993). About 75.5 % of the solid waste excluding construction and demolition waste generated in Canada ended up in landfills in 1992 (Environment Canada, 1996). However, the overall amount of waste landfilled has decreased in developed countries over the last few years. In United States, the percentage of waste disposed of in landfills decreased to 55% in 1996 as opposed to 83 % in 1986 (US EPA, 1998). This decrease is in response to waste minimization, recycling, and other waste diversion activities. Although there is a reduction in developed countries, the global amount of landfilled waste is likely to increase significantly, as developing countries produce more waste in response to rapid urbanization and industrialization (Bogner et al., 1998).

The inevitable consequences of the practice of solid waste disposal in landfills are leachate and gas generation, because of microbial decomposition of waste. The off-site migration of leachate and landfill gas, and their release into the surrounding environment, present serious environmental concerns. These concerns include landfill settlement, groundwater pollution, fires and explosions, vegetation damage, unpleasant odors, air pollution, and global warming. Scientists throughout the world are conducting research to predict and control landfill processes to reduce their impacts on the environment. Understanding gas emissions from landfills especially requires a vast amount of research work, as the present knowledge base related to landfill gas is very limited.

Methane and carbon dioxide are the terminal products of anaerobic decomposition of organic carbon in the biodegradable fractions of landfilled waste. The landfill gas consists of approximately 50% CH_4 and 50% CO_2, and traces of numerous other gases. Methane in

landfills must be controlled to prevent the formation of explosive mixtures; because CH_4 causes explosions at 5%-15% (by volume) in air. Methane can be exploited commercially as an alternative energy resource.

In recent years, landfills have been implicated in greenhouse warming scenarios as significant sources of atmospheric CH_4. Although CH_4 is a trace gas in the atmosphere, its contribution to global warming is estimated to be about 17% (Princiotta, 1992). Global landfill CH_4 emissions have been estimated to be in the range of 30-70 Tg/year (Bingemer and Crutzen, 1987). The national estimates for landfill CH_4 emissions have been based on approaches using the assumed mass of landfilled solid waste for a given country multiplied by assumed rates of CH_4 production (Bingemer and Crutzen, 1987). This is an over-simplification, because a significant portion of the CH_4 produced within a landfill is biologically oxidized before it is emitted to the atmosphere (Bogner et al., 1997). In addition, uncertainties associated with CH_4 generation potential and the lack of field data from developing countries reduce the credibility of the global CH_4 emission estimations.

To be credible, the CH_4 emission estimations need to be supported by actual field measurements. Over the last few years attempted researchers have tried to develop acceptable techniques to measure gas emissions from landfills. At present flux chamber techniques are the most popular methods used at landfills. However, limitations in these techniques require additional research to refine them.

1.2 Objectives and Scope

The primary objective of this thesis is to critically evaluate the closed flux chamber technique as a means of measuring gas emissions from landfills and to develop methods to increase the accuracy of this technique. Specific objectives are; to investigate the advantages and disadvantages of the closed flux technique under field conditions, to identify and quantify the errors involved with it, and to develop methods to improve the accuracy of field measurements.

Therefore, the study involved the following components:

- a literature review to identify the available methods to measure gas emissions from soils and compare these methods with closed flux chamber technique.
- Field lysimeter studies to assess the suitability of closed flux chamber technique under field conditions.
- Laboratory experiments to determine the accuracy of the technique.
- Develop a computer model to simulate gas migration in soil when a closed flux chamber is employed for landfill gas measurement.

1.3 Thesis Organization

This thesis contains eight chapters. Chapter one is the introduction. Chapter two presents a review of literature on available techniques for gas emission measurement. It also discusses previous mathematical models that were developed to simulate gas migration in soils. In Chapter three, the experimental setup and methodology are described for both field and laboratory experiments. Results of these experiments are presented in Chapter four. Chapter five describes the theoretical aspects of the new mathematical model and the model development is included in chapter six. Chapter seven presents the model results. Conclusions and recommendations for further research are included in Chapter eight.

CHAPTER TWO
LITERATURE REVIEW

2.1 Impact of Landfill Gas on Atmospheric CH_4

The presence of methane in the atmosphere has been known since the 1940's, when strong bands in the infrared region of the electromagnetic spectrum caused by the presence of atmospheric CH_4 were discovered. Concentrations of CH_4 in the troposphere vary from 1.7 ppmv in the Northern Hemisphere to about 1.6 ppmv in the Southern Hemisphere (Rassamussen and Khalil, 1986). The global average CH_4 concentration has been increasing by about 18 ppbv per year, or about 1% per year. Atmospheric measurements and measurements in ice cores have indicated a 100% increase in atmospheric CH_4 in the past 200 years (Khalil et al., 1992). It is estimated that about 70% of the increase of methane over the past 200 years is probably due to the increase of emissions while about 30% may have been caused by depletion of hydroxyl (OH) radicals in the atmosphere (OH reacts with methane and forms CO_2). Schutz et al. (1990) stated that methane accounts for approximately 20% of the greenhouse warming of 0.7^0C over the last 100 years. Methane has a shorter atmospheric lifetime compared to CO_2 and its global warming potential is 21 with respect to a 100-year time horizon (IPCC, 1996).

Anthropogenic sources account for about sixty percent of the 500-600 Tg/year global CH_4 budget (Hogan and Kruger, 1992). Rice paddies, coal mining, natural gas industry, and livestock are the main anthropogenic sources of atmospheric CH_4. Landfill CH_4 emissions account for 30-70 Tg/year or 4-13% of global emissions (Bingemer and Crutzen, 1987). However, the amount of research conducted on CH_4 emissions from landfills is comparatively less than for the other CH_4 sources.

2.2 CH_4 Generation in Landfills

Solid waste provides both substrate and substratum for the growth and succession of diverse microbial communities. Many aspects in a landfill are conducive to the growth of microorganisms; surfaces are available for colonization, organic and inorganic nutrients are abundant, moisture is usually adequate (at least in sections of the waste matrix), and temperatures are often elevated with respect to the atmosphere (Palmisano and Barlaz, 1996).

A complex series of microbiological and chemical reactions begins with the burial of refuse in a landfill, and the production of CH_4 and CO_2 from landfills is well documented (Emcon Associates, 1980; Barlaz et al., 1990; Barlaz, 1996). When solid waste is placed in a landfill, biological decomposition does not occur immediately or in one step. Decomposition occurs at different stages and a period ranging from months to years may be necessary for the proper growth conditions and the required microbiological system to become established. Barlaz (1996) identified solid waste decomposition in a landfill in an aerobic phase, an anaerobic acid phase, an accelerated CH_4 production phase and a decelerated CH_4 production phase.

Oxygen entrained in the void space when solid waste is buried and the O_2 dissolved in the refuse associated moisture, support aerobic decomposition of soluble sugars and other hydrolyzed monomers. Gas produced during the aerobic phase is almost totally CO_2. However, depending on the compaction of waste, initial moisture content and the permeability of the cover, the aerobic phase declines with time as O_2 is depleted and fermentation begins.

The anaerobic acid phase begins following the depletion of O_2 from the refuse ecosystem. Rapid O_2 depletion has been measured in the laboratory and can be expected in the field

because once a mass of waste is covered by another layer of waste, replenishment of oxygen becomes insignificant (Barlaz et al., 1989). The acid phase is characterized by the rapid accumulation of carboxylic acids and a decrease in refuse pH from around 7.0 to below 6.0. Beginning of the anaerobic phase is marked by the hydrolysis of polymers, including carbohydrates, fats, and proteins into sugars, amino acids, long-chain carboxylic acids, and glycerol. Fermentative microorganisms then ferment these products to short-chain carboxylic acids, carbon dioxide, and hydrogen. Acetate, a direct precursor of CH_4, and alcohols are also formed. The terminal step in the conversion of complex polymers to CH_4 is carried out by methanogenic bacteria. Methanogens convert either acetate, or H_2 plus CO_2 to CH_4. Although the methanogens are most active in the pH range 6.8 to 7.4 (Barlaz, 1996), an increase of methanogenic bacteria too can be seen during the anaerobic acid phase. With progression through the acid phase, the CO_2 concentration decreases as the CH_4 concentration increases.

In the accelerated methane production phase, there is a rapid increase in the rate of CH_4 production rate to its maximum value. Methane concentrations of 50 to 70% are typical of this phase, with the balance of the gas being CO_2 (Barlaz, 1996). Carboxylic acid concentrations decrease sharply, and subsequently, the pH of the refuse ecosystem increases. These favorable conditions cause the CH_4 generation rate to be at its maximum. The final phase of refuse decomposition is described as the decelerated CH_4 production phase. It is characterized by a decrease in CH_4 production rate while the CH_4 and CO_2 concentrations remain constant at about 60% and 40%, respectively. The decrease in the CH_4 production rate correlates with a decrease in carboxylic acid concentrations. With the depletion of carboxylic acid concentrations, there is a further increase in pH of the ecosystem.

2.3 CH_4 Generation versus CH_4 Emissions from Landfills

Quantification of CH_4 generation within landfills and emissions from them are both necessary to control the impacts of landfill gas. As extraction is a primary gas control measure, accurate estimations of gas generations are sought by many waste managers. Additionally, power generation is becoming an attractive option, and its economic feasibility could be assessed only with accurate estimations of gas generation.

Gas generation rates are usually determined from either field measurements or using simple mathematical models. Field measurements are carried out using landfill gas pumping tests. Pumping tests are expensive and a large number of tests are required for a typical landfill. Scholl Canyon model (Emcon Associates, 1980) is the most widely used mathematical model to estimate CH_4 generation within landfills. In addition, global CH_4 generations could be estimated using gas generation potentials of various waste components (Bingemer and Crutzen, 1987) or regression models (Doorn and Barlaz, 1995). These global CH_4 emission models have not been validated in the field.

Although the amount of gas generation within a landfill provides an indication of the emissions from the landfill surface, these two amounts are not equal, the reason being a significant portion of CH_4 produced could be biologically oxidized before it is emitted to the atmosphere (Bogner et al., 1998). Importance of landfill gas emissions has increased during the last few years because of its implications on global warming phenomenon. However, there is no single model to determine gas emission rates, but labor intensive or costly field techniques. Therefore in many instances, estimated CH_4 generation is being used as a surrogate for estimated CH_4 emissions. If it is possible to determine the amount of CH_4 oxidized, gas generation rates provide a good means of determining landfill gas emissions. Unfortunately, at present, there is no method to quantify CH_4 oxidation. U.S. EPA (1998b) recommends using a 10% oxidation rate after calculating the generation rates

from the Scholl Canyon model. Many researchers question this approach because oxidation rates are dependent on environmental conditions and vary from one landfill to the other.

Since there is no satisfactory method to determine landfill gas emissions developing a new technique or improving an existing one is required. Existing methods are examined in the next section.

2.4 Measurement Techniques for Gas Emissions

Measuring landfill gas emissions involves a very high uncertainty because of the complexity of generation, transport processes and other reactions. The gases produced within a landfill are usually emitted into the atmosphere through the landfill cover. Therefore, landfill gas emission involves mass transfer between the soil and the atmosphere. For decades soil scientists have studied nitrous oxide and carbon dioxide emissions from agricultural soils. Concerns of harmful gas emissions from contaminated soils also have attracted the attention of researchers. In all such situations, similar principles are applicable for emission measurements.

Field measurements of landfill CH_4 emissions with different techniques indicate a variability spanning more than seven orders of magnitude, from less than 0.0004 to more than 4000 g m^{-2} day^{-1} (Bogner et al., 1997). Because of the complex dynamics resulting in high spatial and temporal variability of CH_4 generation, consumption and transport in landfills Bogner et al. (1997) recommended that two or more techniques be used in tandem, ideally chosen to focus on different scales.

The techniques reported in the literature to measure gas emissions from landfills are discussed below. The amount of information on techniques used for landfill gas emissions is limited because of the short period of time landfill gas emission monitoring has been in

existence. However, there is a wealth of information on other trace gas emissions measurements, especially from agricultural soils. Soil scientists have studied in emissions of nitrous oxide (N_2O) and carbon dioxide (CO_2) from agricultural soils since 1940s (Kanemasu et al., 1974). Since the techniques used to determine any tracer gas emissions into the atmosphere could be applicable for CH_4 emissions from landfills, this discussion is carried out in a broader sense to incorporate all information in this field. Surface exchange studies range in scale from investigations of specific microbial biochemistry to projections of changes in the composition of the global atmosphere (Dabberdt et al., 1993). The resulting fluxes are of importance in studying the budgets of trace gas species.

The available techniques include the following:

1. Above-ground techniques for large areas
    - e.g. micrometeorological techniques, tracer methods
2. Ground surface – less than 1 m^2
    - e.g. chamber methods
3. Below-ground
    - e.g. diffusive flux calculation from vertical concentration

Although the emphasis of this research is on flux chamber methods, for completeness, other methods are also discussed briefly.

2.4.1 Micrometeorological Techniques

The basic concept of micrometeorological approaches for measuring trace gas flux to or from the soil surface is that gas transport is accomplished by the eddying motion of the atmosphere which displaces parcels of air from one level to another (Mosier, 1990). For the distance scales over which measurements are practical (i.e. a few millimetres above the surface), turbulent transport is the dominant mechanism. These methods consider various aspects of atmospheric turbulence in relation to trace gases. The micrometeorological

methods can be broadly classified as equilibrium and non-equilibrium methods. Eddy correlation method, gradient methods, and Bowen ratio method fall under the equilibrium method, while mass balance method is a non-equilibrium method.

2.4.1.1 Eddy Correlation

The most direct micrometeorological approach for determining surface constituent exchange is the measurement of the vertical turbulence near the surface. The flux is the average of the instantaneous product of vertical velocity and constituent density (species mass per unit volume) or mixing ratio with respect to air (species mass per mass of air). In statistical terms, flux is determined by calculating the covariance between the concentration fluctuations of that entity and the fluctuations in vertical wind speed (Clement et al., 1995). Although the eddy correlation is the most direct flux measuring technique, it can be difficult to implement because it requires concurrent and contiguous measurements of velocity and concentration with high-frequency response (e.g. for tower measurements, typically > 1Hz: for airplane measurements, typically > 10Hz).

2.4.1.2 Gradient Method

Direct measurement of fluxes of trace species requires fast-response concurrent measurements of both the vertical and the trace species. Indirect measurements generally require some empirically determined relationship to estimate the flux. The most common derived technique is the gradient method. Here, the flux is estimated from the difference in concentration between two or more levels (Fowler and Duyzer, 1989). The turbulent flux is proportional to the product of the mean vertical mixing ratio gradient of the gas and an eddy diffusivity (Mosier, 1990). Gradient methods have been used to determine trace gas emissions more than the other micrometeorological techniques.

2.4.1.3 Bowen Ratio (Energy Balance)

The Bowen ratio is defined as the ratio of sensible to latent surface heat fluxes. It was originally used, together with the other terms in the surface energy budget, to estimate these fluxes at the surface (Fowler and Duyzer, 1989). Advantages of this approach are that eddy flux measurements and stability corrections are not required: a drawback is that it requires measurements of the incoming net radiation at the surface and the soil heat flux.

2.4.1.4 Mass Balance

Another approach for estimating surface flux is the use of mass balance or budget techniques. In contrast to variance and profile techniques, this is an absolute technique in that no empirical relationships are necessary to estimate the flux (Lenschow, 1995). Gas flux rate is related to the horizontal distance from the upwind edge of the measurement area and the top of the air layer influenced by the emission of the gas. The method assumes that the mean horizontal turbulent flux is much smaller than the mean horizontal advective flux (Mosier, 1990). One attraction of this technique is that it does not demand such precision in gas concentration measurement as the other techniques.

Micrometeorological techniques can provide accurate flux estimates, but have relatively large personnel demands and sophisticated instrumentation and data-processing requirements. Perhaps, a reasonable compromise for ground-based measurements may be obtained through the application of automated conditional sampling techniques (which are under development); conditional sampling results to-date are encouraging but not yet definitive. Similar considerations must be given to trade-off between surface-based and airborne measurements. The former are more easily obtained but frequently are limited in their spatial representativeness and ideally require flat sites with homogeneous source sink

characteristics. Airborne flux measurements are spatially representative but are more difficult and do not provide good temporal resolution or continuity.

The history of observational micrometeorology is one of the experiments carried out over horizontally homogeneous sites, as demanded by similarity theory. Unfortunately, in most practical situations, surfaces are not horizontally homogeneous. Overland, hills and scattered trees are obvious sources of heterogeneity. However, other more subtle effects may contribute towards such sources.

2.4.2 Atmospheric Tracer Methods

Atmospheric tracer methods also use the measurements of atmospheric mixing to determine trace gas fluxes. In this case, a tracer (e.g. sulfur hexafluoride - SF_6 has been used by most researchers) is released from the emitting surface to simulate gas emissions (Czepiel et al., 1996a; Tregoures et al., 1997). If the released tracer is well mixed in the source plume, then the CH_4 emission rate can be obtained directly by the ratio method, as:

$$Q_m = Q_t \frac{C_m}{C_t} \quad \text{.....} \quad (2.1)$$

where

Q_m = Gas flux rate

Q_t = Tracer flux rate

C_t, C_m = Concentrations of tracer and the gas of interest respectively.

However, this method is restricted to situations with no interfering sources, a sufficient signal to be measured against the background, and a source strong enough to be measured far enough downwind to ensure adequate mixing with the tracer gas under circumstances of stable atmospheric conditions (Czepiel et al, 1996a).

2.4.3 Diffusive Flux Calculation

Diffusive calculation of trace gas emissions from soils is based on the Fick's first law of diffusion. This approach assumes the gas flux is at one-dimensional steady state. It requires the coefficient of diffusion and concentration gradient of interested gas in the soil. The flux is given by the Fick's law;

$$F = -DA\frac{dC}{dz} \quad \text{.....} \quad (2.2)$$

where,

F = Flux rate ($gm^{-2}s^{-1}$)

D = Coefficient of diffusion (m^2s^{-1})

A = Area (m^2)

$\frac{dC}{dz}$ = Concentration gradient closer to the surface (gm^{-2})

The concentration gradient is determined by field measurements. However, uncertainties associated with both concentration gradient and coefficient of diffusion restrict the application of this technique.

2.4.4 Chamber Methods

Chamber or enclosure methods involve isolating gases emitted from the soil surface using an enclosure. The flux chamber is a non-intrusive technique and offers advantages of accuracy, simplicity, and flexibility over other measurement techniques. Chamber methods have been used by soil scientists to determine CO_2 and N_2O fluxes from agricultural soils (Kanemasu et al., 1974; Denmead, 1979; Hutchinson and Mosier, 1981). Emission measurements using flux chambers have also been performed to assess the need to control gas emissions from subsurface contamination, to define the levels of air emissions from

hazardous waste treatment, storage and disposal facilities at a number of remedial action sites (Eklund et al, 1985). These methods recently gained popularity in landfill settings (Lu and Kunz, 1981; Jones and Nedwell, 1990; Bogner et al., 1995; Czepiel et al., 1996a). An inherent drawback of these methods is that perturbations of the gas concentration profile in the soil occur as a result of concentration in the chamber. The shape of the chamber used mostly is cylindrical. Some of the designs are cylindrical with a hemispherical top (Klenbusch, 1986, Eklund et al., 1985). Although, Jones and Nedwell (1990) and Clement et al. (1995) have used square shaped box chambers, they are not popular.

The deployment of the flux chamber requires isolating a volume of air adjacent to the surface with a minimal perturbation of natural processes governing trace gas exchange across the surface. This is usually accomplished by inserting the enclosure into the soil. Many researchers have come up with different insertion depths, but 1 to 2 inches is accepted by many (Reinhart et al., 1996; Matthias et al., 1978). However, this insertion might increase the pressure inside the chamber if requisite precautions are not taken. Installing a collar permanently in the soil is a solution for this if the measurements are repeated at the same spot. Then the chamber can be attached to the collar without affecting the soil or air atmosphere within the chamber. Care should also be taken to minimize the alteration of the enclosed air during the measurement. This includes the temperature and the humidity. When Plexiglas chambers are used, there is a potential of increasing the temperature inside the chamber. In such a situation, insulation of chamber walls might be required. Another criticism flux chambers encounter is that they alter the atmospheric boundary layer. As such, measurements under windy conditions may be comparatively less accurate.

Spatial variability of emissions is undoubtedly the greatest problem encountered in using chamber techniques to estimate a given gas flux from soils in a large area. Coefficients of variation of N_2O or CH_4 between measuring points within a "uniform" site location can range between 50 and 100% (Hutchinson and Mosier, 1981). On the other hand, the ability

to determine the heterogeneity of surface emissions is an advantage of flux chamber techniques. There are two different chamber designs; namely closed and open flux chambers based on the flow regime.

2.4.4.1 Closed flux Chamber

Closed flux chamber method is the most widely used technique in determining gas emissions from landfills. The closed flux chamber method involves capturing gas emitted by the soil using a closed enclosure. By measuring the change in concentration with respect to time, the flux rate is estimated.

Figure 2.1 shows the simple arrangement of a closed flux chamber. As shown in the figure, if an infrared analyzer is used, it is possible to circulate air to attain good mixing. If a gas chromatograph (GC) is used to analyze the gases, a gas port can be installed.

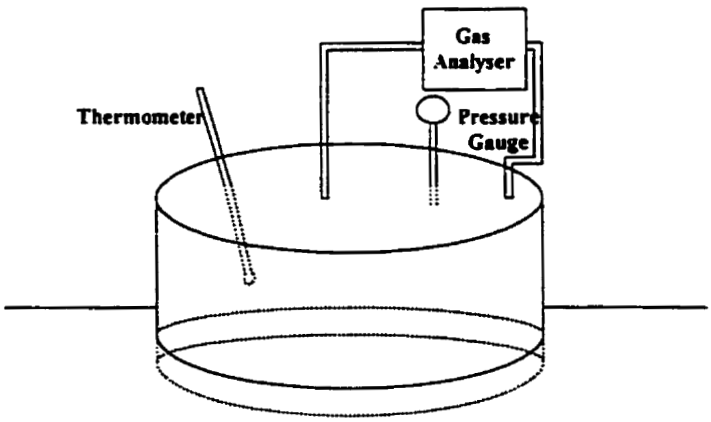

Figure 2.1: Diagram of a closed flux chamber

Flux rate is calculated using the following equation:

$$F = \frac{V}{A}\frac{dC_{Chamber}}{dt} \qquad \text{.....} \qquad (2.3)$$

where,

F = Flux rate ($g.s^{-1}m^{-2}$)

V, A = Volume (m^3) and basal area (m^2) of the chamber respectively

$\frac{dC_{Chamber}}{dt}$ = Concentration gradient inside the chamber, with respect to time ($gm^{-3}s^{-1}$)

The concentration gradient is obtained by measuring concentrations inside the chamber at different time intervals. Linear regression is used to determine the gradient.

The attraction for this method is mainly due to its simplicity, portability, and the ability to measure very small fluxes. The major disadvantage of this method is its underestimation of flux. As the accumulation of gases in the chamber changes the soil gas concentration gradient, the calculated fluxes tend to be under-estimated. Researchers have found different degrees of accuracy with the closed flux chamber technique. Matthias et al. (1978) reported that closed flux chamber flux values might under-estimate actual values by as much as 55% of the actual values. Jury et al. (1982) and Healy et al. (1996) also showed closed flux chambers could under-estimate fluxes by various amounts depending on soil type.

With the closed chamber, the time rate of change of gas concentration should be evaluated as soon as the chamber is placed on the soil surface. Because of the precision restraints in the gas concentration measurement technique, this may not be feasible. Thus the time period of gas collection must be sufficient to allow for measurable gas accumulation. The trace gas concentration gradient beneath closed systems is ever diminishing in response to continual concentration changes within the chamber air. Enclosure dimensions and deployment times, therefore, should be carefully selected in each application so that this negative feedback on the rate of molecular diffusion is minimized.

Closed chambers often allow fluxes to be quantified over shorter deployment periods and are useful in quantifying low exchange rates, particularly if the minimum detectable flux is

limited by the precision of the concentration analysis. In measuring surface-atmosphere N_2O exchange beneath a corn canopy at various times throughout the growing season Hutchinson and Mosier (1979) found that a substantial proportion of the fluxes measured by open chambers were below the detection limits reported obtainable with closed systems.

Pressure vents are recommended by some researchers for most enclosures not only to transmit atmospheric pressure changes to the enclosed air volume, but also to compensate for air sample withdrawal and possible reduction in chamber volume during deployment. Flux chambers with vents are also referred here as closed chambers as there is no forced air flow through the system. Hutchinson and Mosier (1981) developed guidelines for calculating appropriate vent tube diameter and length as functions of chamber volume and wind speed. These guidelines were defined to minimize resistance to air flow in response to atmospheric pressure fluctuations and to minimize the quantity of air exchanged by advective flow between the enclose air volume and the atmosphere. Livingston and Hutchinson (1995) recommend that vented systems are especially required whenever the underlying soils are highly permeable or the trace gas sources or sinks are located near the soil-atmosphere interface. They assume exchange due to molecular diffusion through the vent as negligible over typical deployment times. However, the vent tube should be widely separated from the chambers sampling port to avoid unintended interactions.

Conen and Smith (1998) found that in a well-drained soil with a fairly large air permeability, vented chambers yielded fluxes as much as five times those of sealed chambers depending on wind speed. By contrast, on a heavier and wetter soil with smaller air permeability, vented chambers averaged only 88% of the fluxes observed with sealed chambers. It seems more likely that wind blowing over the vent depressurizes the chamber (venturi effect), resulting in significant gas flow from the more permeable soil into interior of the chamber. The opposite trend for the less permeable soil suggests that diffusion losses through the vent tube are greater than the increase in concentration due to soil gas flow. Conen and Smith (1998) have calculated a pressure deficit inside the chamber 2.4 Pa for a

steady wind of 2 ms^{-1}. Dimensions of their vent tube were length 16 cm and inner diameter 1 cm. According to them, venting can create larger errors than the ones it is supposed to overcome.

2.4.4.2 Open Flux Chamber

Open flux chamber is different from the closed one because a clean dry sweep air is added to the chamber at a fixed controlled rate. This flow rate should be at a rate significantly exceeding the gaseous release rate from the surface. The volumetric flow rate of sweep air through the chamber is recorded and the concentrations of the species of interest are measured at the exit of the chamber. The Figure 2.2 shows the essential components in an open chamber design,

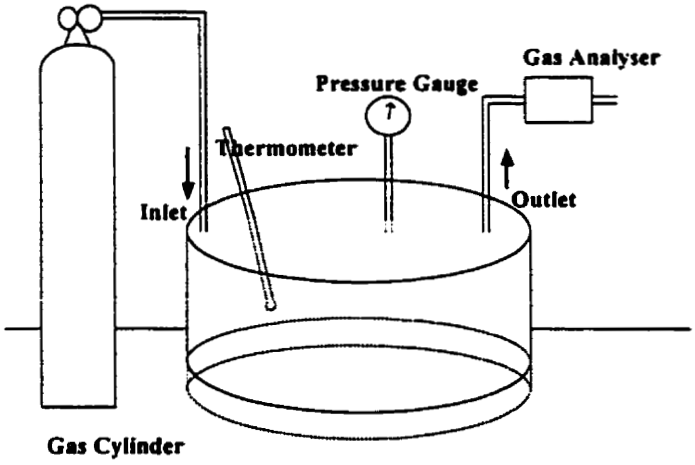

Figure 2.2: Diagram of the open chamber arrangement

The emission rate is expressed as;

$$F = \frac{Q_t C}{A} \quad \text{.....} \quad (2.3)$$

where;

F = Flux rate ($g .s^{-1}.m^{-2}$)

Q_t = Volume flow rate at the outlet (m^3s^{-1})

A = Basal area of the chamber (m^2)

C = Concentration at the outlet (gm^{-3})

In the open systems, the trace gas concentration gradient controlling molecular diffusion across the soil-atmosphere interface is assumed constant after an initial period of adjustment following deployment. This steady state condition is maintained by passive regulation of the trace gas concentration in the enclosed air volume, typically by employing an open-path circulation system to sweep the enclosed volume using a constant flow of external air with known concentration of the species of interest. Although the steady state concentration gradient that is established will likely differ from pre-deployment conditions, the perturbation can be minimized by optimizing the flow rate and make-up of the sweep air such that the difference in trace gas concentration inside and outside the enclosure is minimized.

Because of low perturbations to the soil atmosphere, open chambers may be a preferred design for monitoring trace gas exchange at fixed locations over extended or repeated time periods. In comparison between closed and open enclosures deployed over the same period, Denmead (1979) demonstrated that open systems induced smaller changes in the subsurface trace gas concentration gradient, thereby resulting in not only smaller bias in observed gas transport rates, but also more rapid recovery to near pre-disturbance conditions between consecutive measurement periods.

However, the sweep air should be pumped in or pumped out in order to keep a constant airflow rate. The pressure within the chamber is lowered in case of pumping out and it is increased when air is pumped in. This change in pressure ultimately affects the gas emissions (Denmead, 1979). Kanemasu et al. (1974) reported variations in chamber

pressures when air is circulated through the chamber under suction and under pressure. They measured the chamber pressure to be approximately –25 μbars when under suction and +10 μbars when under pressure. Their measurements show the CO_2 flux from the soil surface inside the "pressure" chamber was nearly an order on magnitude lower than the soil surface inside the "suction" chamber. Kanemasu et al. (1974) conclude the flux from the soil surface under natural conditions is probably between the suction and pressure diffusion values. Hartless (1995) also found 1 Pa of pressure change in the chamber could distort the flux rates by about 40%. This can be overcome by ensuring that the size of the inlet gas orifices are large compared to the size of the outlet orifice (Denmead, 1979).

An additional consideration in open chambers is the time required for gas concentration in the soil and the chamber air to adjust to new equilibrium values. The time for the steady state depends on the flux rates, soil characteristics, and the air flow rate. Predicting this could be difficult as the time to reach the steady state may be quite long or poorly defined under many site conditions (Jury et al., 1982). If not established, the true flux rate may be significantly underestimated, so open chambers often incorporate in-line sensors to monitor the concentration of the species of interest in real time. When there is no longer a measurable concentration within the chamber, measurements assume an equilibrium flux between soil atmosphere and chamber atmosphere.

Reinhart et al. (1992) tried to optimize the design and operational parameters of open flux chambers in order to increase the accuracy of measurements of landfill gas emissions. Flux chamber operating parameters included: chamber pressure, sweep airflow rate, landfill insertion depth, and sweep air velocity. The effect of varying landfill cover type, operating procedures, climate, and waste composition and age on landfill gas emission rates were not evaluated. Their research has clearly shown that the sweep airflow rate has an impact on the measurements. Biasing shifted from positive to negative as the air flow rate is increased. The Table 2.1 shows the details of flux chambers used by several researchers.

Table 2.1. Details of Some Flux Chambers Used by Researchers

Reference	Chamber Type	Description	Operational Details	Application
Denmead (1979)	Open	Cylindrical, ϕ30 cm, 18 cm high	inserted 10 cm deep into soil	Used for N_2O emission measurement
Hutchinson and Mosier (1981)	Closed	Cylindrical, ϕ 12.1 cm, 13.6 cm high	vent tube (10 cm x ϕ0.5 cm)	For N_2O emissions
Ekland et al. (1985)	Open	Stainless steel cylinder with a Plexiglas dome	mixed air with an impeller	For various emissions
Klenbusch (1986)	Open	Cylindrical with a dome on the top, Vol. = 30 L, Area = 1300 cm^2	inserted 2-3 cm deep into the soil	recommended for RCRA facilities
Jones and Nedwell (1990)	Closed	Polyethylene box 24.5x21.5x7.5 cm	pressed into soil	Landfill gas emissions
Reinhart et al. (1992)	Closed	Stainless steel cylinder ϕ 71.1 cm, 30 cm high	inserted 1.5 cm deep	laboratory experiments
Erno and Schmitz (1996)	Open	Cylindrical, ϕ 61 cm, 12.7 cm high	Similar to Denmead (1979)	Gas leaks in oil / gas wells
Williams and Williams	Dyn.Dilu. Tube	Cylindrical ϕ 15 cm, 45 cm high	Inserted 4.5 cm deep	Used in landfills
Clement et al. (1995)	Closed	Aluminum box 6.24cmx62.4cmx3.7cm	Collars inserted into the peat	CH_4 emissions from wetlands
Czepiel et al., (1996)	Closed	ϕ25.4 cm, 18 cm high	air was mixed inside by a fan	Used in landfills
Bogner et al. (1999)	Closed	Hemispherical, V = 19 L, A = 1134 cm^2	Used collar to insert into the soil	Used in Landfills
Conen and Smith (1998)	Closed	ϕ40 cm, 20 cm high	Inserted 7 cm, vent tube (16cm xϕ1cm)	N_2O measurement

The insufficient accuracy holds against the usage of flux chambers. There have been many studies with the objective of increasing the accuracy of these methods. Two approaches are commonly adopted by scientists to refine the techniques. They are either physical and/or procedural modifications and/or attempts to interpret measurements by utilizing mathematical modeling. The first approach was explained earlier when the chamber methods were introduced. Modeling approach is discussed below. Modeling approaches that can be applied in a landfill setting are varied and depend on the processes one is interested and the size of the domain, the type and technique of modeling. However, reviewing the literature related to modeling of gas generation and emission will help to determine the techniques that should be used for a particular problem.

2.5 Simulation Models

Mathematical models have been presented as tools for assessing migration patterns for predicting the temporal and spatial distribution of gas production. Basic simulation models reported in the literature can be classified as:

- Models that predict gas generation only
- Models that combine gas generation and transport
- Models that include gas, moisture, and heat generation and transport
- Models simulating special situations (application of flux chambers)

These models consider various processes occurring within and in the surrounding region of a landfill. These include physical, chemical, and biological processes. A simplified representation of these processes is shown in Figure 2.3.

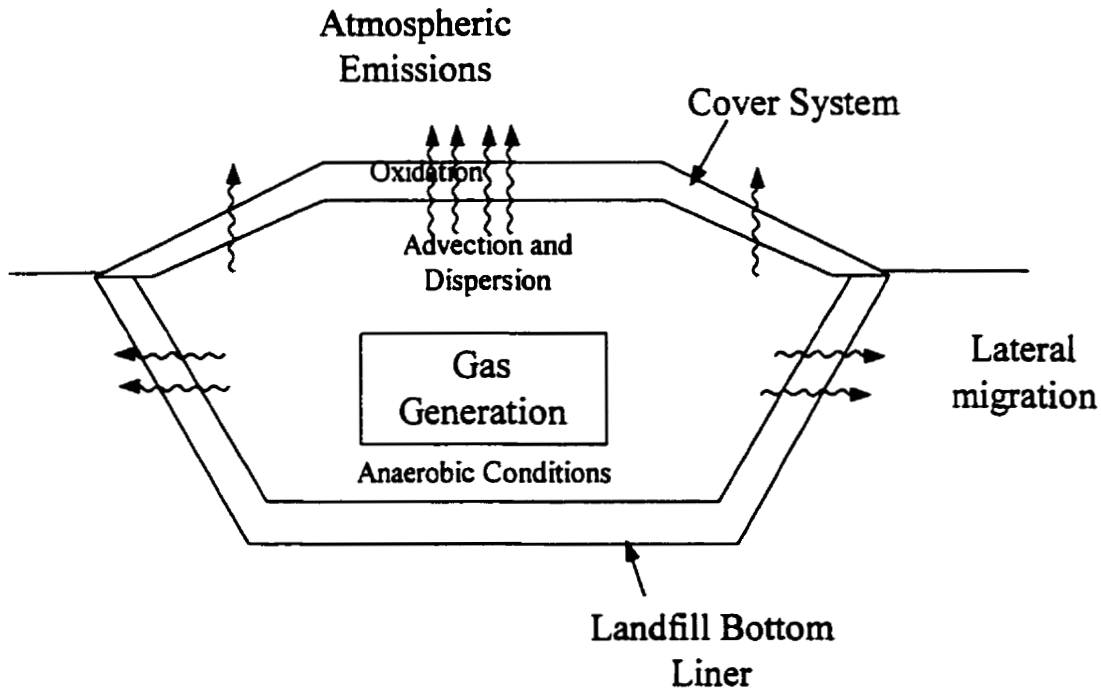

Figure 2.3: Processes in a landfill

2.5.1 Gas Generation Models

Because of the wide variety of biodegradable matter in municipal solid waste, no simple equation or rate constant can describe adequately the rate of biodegradation and the rate of gas generation in landfills (El-Fadel et al., 1996). Various factors affecting gas generation such as waste composition, moisture content, pH, temperature, other inhibitors, the age of the landfill and the landfilling practices make the modeling very complicated. The most widely used approaches are to use zero or first order kinetic reaction models. A second category of models using Monod kinetics incorporates the complete or sequential stages in anaerobic biodegradation of organic materials (Findikakis et al., 1988; El-Fadel et al, 1989; Young, 1989).

Emcon Associates (1980) discusses three theoretical kinetic models for gas production. These models use first order reaction kinetics. The Palos Verdes and the Sheldon Arleta models utilize two-stage first order kinetics. The most popular kinetic model, the Scholl Canyon model, is a single stage model. This model assumes that, after a lag time of negligible duration, during which anaerobic conditions are established and the microbial biomass is built up and stabilized, the gas production rate is at its peak. These gas generation models have not been validated using enough field data.

2.5.2 Gas Transport Models

The theory and governing equations of gas transport in porous media have been addressed by many researchers during the last few decades. Approximate closed form expressions and numerical solutions have been developed for different gas flow problems in the petroleum industry (Aziz and Settari, 1979) and more recently in connection with problems of assessment and remediation of subsurface contamination (Frind, 1982; Mendoza and Frind, 1990). Similar attempts have been made in modeling gas transport in landfills. With the awareness of impacts of landfill gas on local and global environment, there is an increased interest about fate and transport of landfill gas.

There have been many attempts to model fate and transport of gases within landfills. A wide variety of analytical and numerical techniques have been used. In a landfill setting, there are two distinct components important for gas migration. They are, a highly non-homogeneous waste layer and a fairly homogeneous soil cover on top of that. However, most of landfill gas transport models are based on the assumption that the landfill can be treated as a porous medium and the gas velocity is given by Darcy's law. Alzaydi et al. (1978) developed analytical and numerical models to simulate gas flow through soil formations adjoining sanitary landfill. They have used a parallel pore model where the porous medium was represented as an aggregation of parallel capillary tubes, each of

constant radius, which simulate the pore size distribution. Moore et al. (1979) applied these equations and numerical models to simulate data from existing landfills and developed design charts for CH_4 concentrations in the subsurface surrounding a landfill. Mohsen et al. (1979) developed a numerical axisymmetric flow model to simulate gas migration away from sanitary landfills.

Lu and Kunz (1981) developed an analytical radial flow model to determine the landfill's CH_4 production rate and gas flow permeability. They considered an extraction scenario. They were able to match the results with the flux chamber measurements. Their approach assumed that the landfill consists of a number of small cylindrical elements.

Young's (1989) model described gas transport in a rectangular cross section of a landfill with impermeable bottom and side walls. He considered pumping of gas from horizontal wells. He did not calibrate the model with field data. Arigala et al. (1995) developed a model to simulate pressure field inside and outside a landfill equipped with a gas extraction system consisting of vertical pipes placed at arbitrary points.

The usual practice in modeling subsurface contaminant transport is to solve the flow equations first and then solve the transport equations using solved flow velocities. This is sufficiently accurate for contaminants in water since their concentrations generally do not affect flow equations. However, gas migration is dependent on the composition of gas mixture and therefore its simulation is similar to modeling multi phase and/or multi component flow modeling. The result is the need to solve flow and transport equations iteratively (Mendoza and McAlary, 1990). Bear (1972) and Corapcioglu and Baehr (1987) derived equations for multiphase, multi-component flow and transport. There are other attempts made to develop models to simulate vapor transport in unsaturated zones that are important to review. Mendoza (1986) developed Vapour-T model, which is a two-dimensional finite element program, designed to simulate flow of gas and/or the transport of vapors in the unsaturated zone. It considers both advection and dispersion transport with

phase partitioning, but developed for only one vapor component. Mendoza and Frind (1990) showed that the simulations of laboratory experiments, for which the effects of advection are not immediately apparent, show improved results when advection is included. Their approach for solving the governing equations is similar to the conventional groundwater contaminant modeling.

Findikakis and Leckie (1979) used an approach that is different from conventional hydrogeologic transport models to simulate landfill gas generation and migration. They solved this problem by incorporating flow equations into the transport equations. That has been done by converting the pressure terms also into concentration terms. They used the equation of state for the gases to find a relationship between gas pressure and concentrations of individual gases. Findikakis and Leckie (1979) solved these final non-linear equations using Newton-Raphson method. Their model simulates one-dimensional flow of a mixture of CH_4, CO_2, and N_2.

Metcalfe and Farquhar (1987) developed a model that was similar to Findikakis and Leckie (1979) to model CH_4 migration through soils adjacent to a landfill. El-Fadel et al. (1996) went a step further than Findikakis and Leckie (1979) by incorporating heat generation and transport in landfills. Their model incorporates a set of biokinetic equations describing the dynamics of microbial landfill ecosystem. El-Fadel et al.'s (1996) model used three interdependent modules, namely gas generation module, gas transport module, and heat generation and transport module.

2.5.3 Methane Oxidation

Compared to the CH_4 sources, the sinks of CH_4 have not been well identified until very recently. The most important sink for atmospheric CH_4 is its reaction with free hydroxyl (OH) radicals (King, 1992; Dubey et al, 1996). Another sink of CH_4 is the uptake of CH_4 by

soils. Microbes in the soil play a major role in the CH_4 budget of the atmosphere. Although much is known about CH_4 production in natural and man made eco-systems, relatively little is known about CH_4 oxidation.

The term 'methanotrophs' has been used by the microbiologists to describe those bacteria that use CH_4 as the source of C and energy. Methanotrophs are a subset of a larger group of organisms, the 'methylotrophs', having the ability to use compounds other than CO_2 containing one or more carbon atoms but no carbon-carbon bonds as the sole carbon source for growth. Methanotrophs belong to the gram-negative eubacteria and are strict aerobes but survive frequently under reduced O_2 tension. Although numerous research works have been done on CH_4 oxidation in wetlands and rice paddies, research at landfills soils are rare. Only a few studies to determine the CH_4 oxidation rates in landfill covers are reported in literature.

Published data show that, methanotrophs can oxidize CH_4 up to 166.4 $gm^{-2}d^{-1}$ (Kightley et al, 1997) under favorable conditions. Most of the research is being done with the intention of understanding the microbiology and the factors that affect oxidation. This knowledge could be used in developing equations that represent the oxidation process. The studies on CH_4 oxidation in soils come under two categories, namely batch experiments and soil column experiments. Batch experiments are important in optimizing oxidation in soil. However, soil column or microcosm studies are more relevant in modeling CH_4 oxidation in landfill covers. That is because those studies simulate other physical processes such as diffusion and advection.

The major factors identified by many researchers are soil moisture content, O_2 and CH_4 availability, temperature, nutrients, and soil porosity. Boeckx and Cleemput (1996) found that optimum oxidation occurs between the temperatures 25-30 ^{0} C and at a moisture content around 15% for a sandy loam soil. Czepiel et al. (1996b) found that CH_4 oxidation rates decreased rapidly to zero when O_2 mixing ratios were below 3%. Most of the

researchers attempted to determine kinetic parameters for soil methanotrophy. Assuming Monod kinetics, they determined the maximum rate of CH_4 oxidation (V_{max}) and the half saturation constant (K_s). There are wide variations in the values generated by, on the studies different researchers. These parameters were determined assuming CH_4 to be the only control. The effect of O_2 concentration is not reflected in these values. There is a requirement for more research to obtain more information about the oxidation process. The kinetic parameters reported in literature are given in the Table 2.

Table 2.2. Kinetic parameters for CH_4 oxidation

Reference	**V_{max}**	**K_s**
Czepiel et al. (1996b)	40-2594 nmol h^{-1}g dry $soil^{-1}$	195-5847 ppmV
Whalen et al. (1990)	61 g $m^{-2}day^{-1}$	1800-4600 ppmV
Kightley et al. (1995)	998-2347 nmol.h^{-1}g $drysoil^{-1}$	233-1005 nmol ml^{-1}

However, all these modeling exercises have been done for a large area within or outside the landfills, under normal conditions. With the introduction of a flux chamber on the surface of a landfill, or any other contaminated site, the conditions of flow and transport of gases locally will change. This work involves modeling such situations to determine the perturbations in gas flux measurements. The difference between this specific case and the general emission scenarios are the smaller scale in space and time, and the different boundary conditions. There have been some attempts to model effects of the flux chambers on gas emissions. Most of them considered N_2O and CO_2 emissions from agricultural soils. Some of the previous work is reviewed below.

2.5.4 Modeling Gas Migration for Flux Chamber Measurements: Previous Attempts

There have been a few attempts to quantify the effects of perturbations in gas flux measurements when flux chambers are used. Some of these studies were aimed at quantifying the perturbations, but some others used modeling to propose corrections for the flux chamber techniques. The first attempt was by Kanemasu et al. (1974) to illustrate the change in flux due to the variation of pressure inside the chamber when air is swept through open flux chambers. Although they considered both diffusion and advection, their model was one –dimensional and their assumptions were not clearly defined. They demonstrated that advection plays a major role due to the pressure drops, or increases, when sweep air is pumped out or pumped in, respectively.

Rolston et al. (1978) proposed a method to correct the decrease in concentration gradient with time as N_2O gas accumulates inside the chamber. Their correction was based upon the steady state diffusion equation. They assumed the concentration at the soil surface was equal to the concentration beneath the cover and that the concentration at the shallowest sampling depth (2 cm in their case) did not change with time. They used the solution as given below to determine the soil gaseous diffusion coefficient. The equation they used was:

$$F = -D_p \frac{dC}{dz} \quad \text{.....} \quad (2.4)$$

$$\text{where } D_p = -\frac{(VL)}{At} \ln\left[\frac{(C_2 - C_0)}{C_2}\right]$$

where,

F = Gas flux rate (g $m^{-2}d^{-1}$)

D_p = Soil gaseous diffusion coefficient (m^2s^{-1})

C = Gas concentration (g m^{-3})

V, A = Volume (m^3) and area (m^2) of the chamber respectively

L = Depth of soil for which measurements were taken (2 cm)

t = Time (s) after covering the soil at which the concentration beneath the lid (C_0) was measured

C_2 = Measured concentration at a depth of 2 cm

The calculated diffusion coefficient and the measured concentration gradient at time = 0 were used to calculate the corrected flux. However, measuring the concentration at a depth of 2 cm cannot be done accurately. The assumption that it stays constant is also not realistic. Therefore, this method is difficult to apply.

Both linear and non-linear models have been proposed to describe the relationship between trace gas concentration and time in closed flux chambers. If the chamber dimensions, deployment period, and measurement protocol are suitably matched to the rate of gas exchange and site characteristics, a linear model may be adopted, which assumes a constant exchange rate over the period of observation.

In many common applications, such as when working with low exchange rates, or highly permeable soils or when the trace gas sources or sinks close to the surface, analytical limitations may preclude using a measurement period sufficiently short that a linear model may be considered appropriate. In such situations, a non-linear model of concentration change over time should be employed. Matthias et al. (1978) and Hutchinson and Mosier (1981) proposed separate non-linear models, each based on the theory of molecular diffusion in soils. The iterative approach required by the Matthias et al. (1978) model makes it difficult to apply. Hutchinson and Mosier (1981) developed a correction for decreasing concentration gradient in the closed chamber method. Considering one-dimensional diffusion of gases below a flux chamber, they came up with an equation for the flux rate. The solution described by them applies to the special case defined when observations over two successive time periods of equal length are available. The solution is as follows:

$$F = \frac{V(C_1 - C_0)^2}{At_1(2C_1 - C_2 - C_0)} \ln\left[\frac{C_1 - C_0}{C_2 - C_1}\right] \quad \text{if} \left[\frac{C_1 - C_0}{C_2 - C_1}\right] \rangle 1 \quad \ldots\ldots\ldots \quad (2.5)$$

where,

F = Gas flux ($gm^{-2}s^{-1}$)

C_0, C_1, C_2 = Concentrations measured at two successive periods of equal length (gm^{-3})

V = Chamber volume (m^3)

A = Covered soil area (m^2)

t_1 = Time interval (s)

Due to the limited number of observations, the Hutchinson and Mosier (1981) solution is highly sensitive to measurement imprecision in the concentration data, although this can be partially overcome by using replicate observations at each measurement time. Even the non-linear approach does not include provision for objectively testing the predictive capability of the model. Livingston and Hutchinson (1995) illustrate an example where, despite the appearance of 'reasonable' linearity (R^2 = 0.96), the linear model underestimated the true exchange rate by 46%. However, the example considers only three concentration measurements to find the linearity. The magnitude of error in actual application may vary with each situation. Anthony et al. (1995) conclude that one of the limitations of Hutchinson and Mosier (1981) equation is that it is applicable to only a subset of chamber deployments and does not account for measurement variability.

According to Anthony et al. (1995), gas exchange across the soil-atmosphere boundary depends largely on the diffusivity and concentration gradient of each species between the soil surface and subsurface sites of production or consumption. Once a chamber is placed on the soil surface, the gradient of each species in underlying soil continually adjusts to the changing concentrations in the chamber headspace. The linear model is often used to approximate the relation between observed concentrations and time, under the assumption that for short deployment periods, the rate of change is nearly constant. Adopting a linear regression approach offers many advantages, including that it accommodates measurement

variability and facilitates testing both the model's goodness of fit to the observed concentration data and whether each observed exchange rate is significantly different from zero (Anthony et al., 1995).

More accurate and in-depth modeling has been done by Matthias et al. (1978), Jury et al. (1982), and Healy et al. (1996). Matthias et al. (1978) and Jury et al. (1982) modeled both the open and closed flux chambers and Healy et al. (1996) simulated closed flux chamber performance. Matthias et al. (1978) presented a mathematical simulation of N_2O flux from homogeneous soil when using both closed and open flux chambers. Their work involved a two-dimensional diffusion model under Cartesian coordinate system. Their results showed the closed chamber flux values might be under-estimated by as much as 55%. They showed that the smaller chambers (ie.small height) show a more rapid concentration increase and thus a more rapid feed back to the soil. Larger closed chambers minimize the non-linearity of concentration changes, though detectable concentration changes require longer time periods. However, larger volumes may require procedures to ensure uniform mixing within the chamber. Finally, they concluded that the use of open chambers might yield better flux estimates than closed chambers because of less disturbance to the natural gas concentration profile within the soil. Using Cartesian coordinates in place of cylindrical polar coordinates introduces some errors. Another limitation in their method is not considering the pressure variations inside the open flux chamber due to sweep air.

Matthias et al. (1978) examined the effect of closed chamber geometry on soil gas exchange rates through the use of a two-dimensional molecular diffusion model. They demonstrated that enclosures with a small ratio of volume to basal area (ie.V/A) exhibit more rapid concentration increases and thus more rapid feedback to the concentration gradient driving molecular diffusion across the surface, than with enclosures with large ratios. Enclosures with large V/A ratios also exhibit a more constant rate of concentration change within the enclosed air, but require longer sampling intervals to obtain a detectable concentration difference.

In general, a closed enclosure's V/A ratio should be small enough that a change in the enclosed trace gas concentration could be measured over as short a time as logically possible, yet large enough to minimize disturbance of the enclosed surface. For example, flux measurements on sites with large exchange rates are best served by chambers with large V/A ratios and short deployment periods, whereas smaller chambers and longer deployments are often more applicable to low-flux sites. Reported V/A ratios differ widely between studies, but are typically greater than 15 cm in field studies; overall measurement periods are generally in the range of 20-40 minutes. Livingston and Hutchinson (1995) state that, whenever possible, measurement periods should be chosen such that the rate of concentration change could be assumed constant and, therefore, modeled using linear regression.

Recently, Healy et al. (1996) employed one and three- dimensional models of gas diffusion to simulate the problem. Their study involved determining the errors in fluxes introduced by using a closed flux chamber. They treated diffusion as the sole mechanism for transport of gases within soils. In all model runs, the simulated flux measured by the chamber was smaller than the ambient rate of gas exchange between soil and atmosphere in the absence of a chamber. Healy et al. (1996) found that their one-dimensional results indicated under-estimations of flux rate in the range of 6-34%. However, three-dimensional results showed that the instantaneous measurement errors could be as large as 89%. They tried to incorporate air dispersion inside the chamber. All the earlier analyses of chamber performance (Matthias et al, 1978; Hutchinson and Mosier, 1981) assumed that the chamber headspace was perfectly mixed. Healy et al. (1996) concluded that linear regression model of simulated chamber concentration vs. time systematically under-estimates true flux rate, primarily due to the rapid rate of decrease in the instantaneous flux to the chamber. According to them quadratic and cubic regression, as well as the method of Hutchinson and Mosier (1981) offered substantial improvement over the linear estimation model, yet they did not completely correct the under-estimation. In addition, they propose minimizing duration of measurement, inserting chamber walls into the soil to retard radial

diffusion, and increasing chamber height to reduce the errors associated with the distortion of the concentration gradient. However, Healy et al. (1996) did not apply their model in the field.

CHAPTER THREE
EXPERIMENTAL SETUP AND METHODOLOGY

An experimental program was designed to evaluate the performance of flux chamber technique as a method of gas flux emissions measurement. The experimental program consisted of two components: Lysimeter field studies and laboratory studies.

3.1 Lysimeter Studies

Lysimeters are used by hydrologists to study infiltration and evaporation of water in soils. The same term is used, in solid waste management research too, to describe scaled-down controlled landfills (Rovers and Farquhar, 1973). Lysimeters with all the components of a landfill (bottom liner, drainage layer and leachate collection system, cover etc.) could be used to study many aspects of landfilling under controlled conditions.

A lysimeter was installed at the University of Calgary premises with the objective of studying the applicability of closed flux chamber in the field. With a waste of known composition, a uniform cover, and zero lateral migration lysimeter studies have the advantage of simplicity, to easily understand the processes occurring in a landfill. Some leachate generation studies were also carried out at the same time (Shroff, 1999).

3.1.1 Experimental Setup

The lysimeter was constructed from a corrugated steel pipe of 2.4 m diameter. Length of the pipe was 4 m. The lysimeter experimental setup is explained elsewhere (Shroff, 1999). Solid waste collected from the University of Calgary and the university residences were brought to the site. A detailed characterization was carried out before filling the lysimeter. The waste from the residences was similar to any domestic waste, and University waste

resembled institutional waste with high amount of paper and packaging. However, characterization was done on both types of wastes. 651 kg of residence waste and 261 kg of University waste were characterized.

Initial density of the waste was determined using the characterized waste. Initial density was found to be 110 kg/m^3 with moisture content of 29%. The waste was deposited in the lysimeter in layers using a front-end loader. It was compacted by a backhoe attached with a vibratory compactor. Thermocouples were installed to monitor the temperature variations inside the waste. This was done by attaching thermocouples onto a wooden pole at different levels and lowering the pole into the lysimeter. Because of the insufficient length of the backhoe arm the waste could not be compacted very well closer to the bottom. Subsequent layers were compacted well. However, because of this reason and the high content of paper and plastics the final density achieved was only 315 kg/m^3. Typically landfills in North America achieve a compaction density of 600-700 k/m^3.

Once the lysimeter was full, a layer of native soil was laid on the waste. A layer of clay having a thickness of one foot was placed on that and compacted well with a vibratory hand compactor. The clay was provided by the Solid Waste Services Department of the City of Calgary. Finally another one-foot layer of native soil and a layer of six inches of compost were used to cover the area. The top two meters of the lysimeter was insulated to prevent frost penetration into the waste.

Grain size distributions of the two soils were determined at the University's soils laboratory, and the resulted distributions are shown in the Figures 3.1 and 3.2.

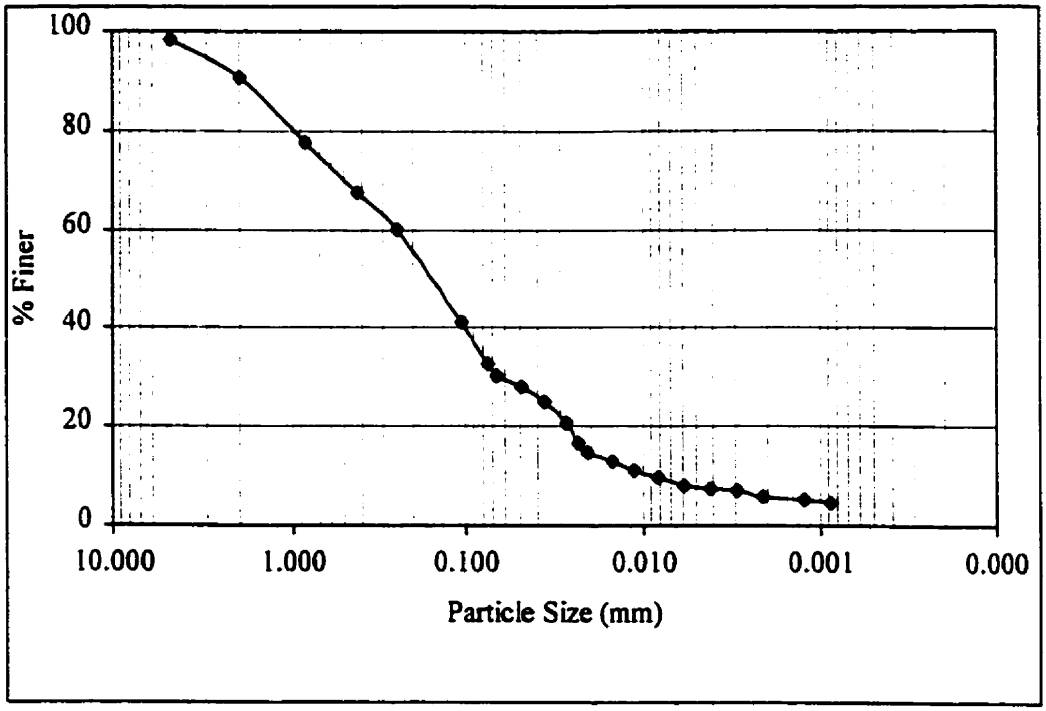

Figure 3.1: Grain Size Distribution for Sandy Loam Soil

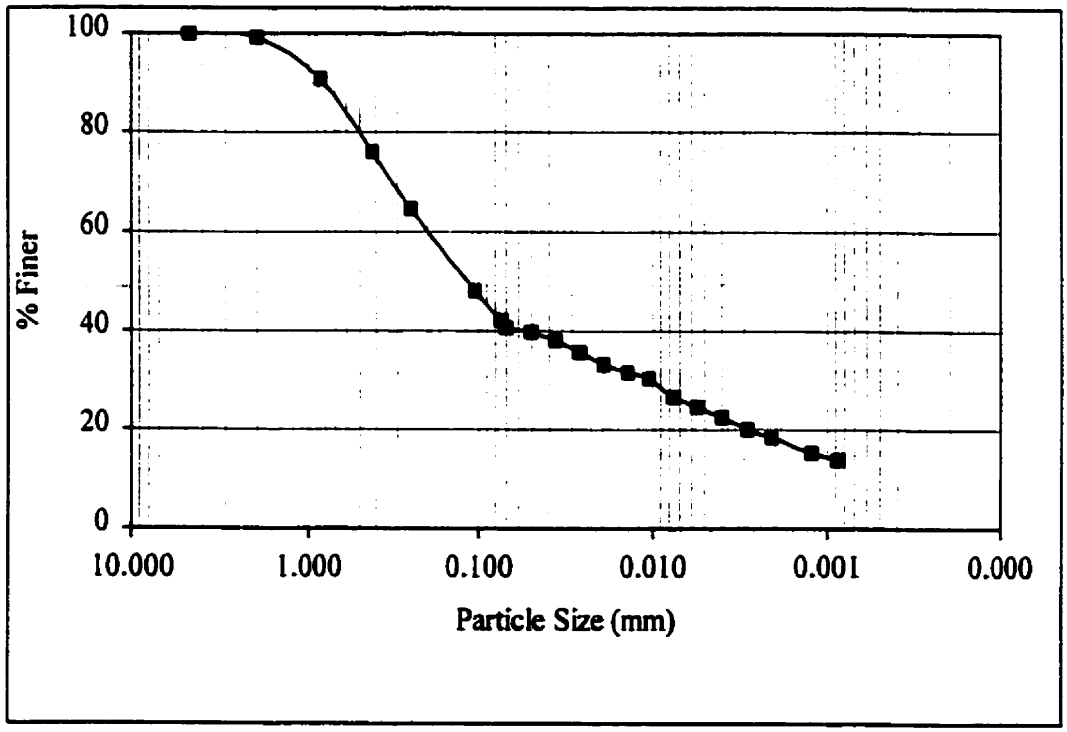

Figure 3.2: Grain Size Distribution for Sandy Clay Loam Soil

Some of the properties of these two soils are given in Table 3.1

Table 3.1: Properties of the soils used for the lysimeter cover

Properties	**Sandy Loam Soil**	**Sandy Clay Loam**
% Sand	63.0	39.0
% Silt	22.0	21.0
% Clay	6.0	20.0
Dry Density – Proctor (kg/m^3)	1905.0	1804.0
Optimum Moisture Content, %	10.6	12.25
Liquid Limit, %	19.5	28.6
Plastic Limit, %	14.9	15.0
Plasticity Index %	4.6	13.6

As per USDA classification, the two soils were identified as sandy loam soil (native soil) and sandy clay loam (hydraulic barrier).

However, during the 1998 summer, after some rain, the waste in lysimeter settled by more than six inches. This was caused to be mainly due to the water absorbence of cover soil. The increased weight compressed the waste underneath. After the settlement, the cover had to be restored. The whole cover was removed, and to raise the level, more waste was added. This time it was decided to add more organic waste and add water to the waste to assist gas generation. About 400 kg of garden waste and 500 kg of shredded paper were added. Some water infiltration studies were carried out while the lysimeter was open and that resulted in a fairly saturated waste after the experiments. It was assumed that there should have been CH_4 generation due to the high organic content of the new waste.

3.1.2 Instrumentation

Thermocouples were installed in the cover system. In addition, a few moisture probes and a few half-inch PVC pipes were installed to monitor the moisture and gas concentrations at different levels in the soil cover.

3.1.2.1 Thermocouples and Moisture Probes

Thermocouples were used to monitor the temperature inside the waste and the soil cover. As the atmospheric temperature variations during various seasons were significant, thermocouples gave important information on the response of the waste and the soil cover to ambient conditions. Aerobic and anaerobic processes occurring inside the waste generated heat and therefore thermocouples inside the waste provided information about the biological activities within the waste. Cole-Parmer 'T' type thermocouples were used for monitoring as their measurement range is –250 to 400 ^{0}C. They could measure temperatures with an accuracy of 0.1% of the full scale.

The soil moisture-temperature meter (Model MC 300B) manufactured by Soil Test Corporation could measure soil moisture and temperature by using a thermister soil cell buried in the soil. It measures temperature and resistance directly from the dual scale dial. Moisture content is determined by relating resistance readings to a calibration curve (i.e. resistance vs. moisture content) for any type of soil. The soil-moisture probes were buried in the soil cover at different depths to obtain the temperature and the moisture profile. However, they are not suitable for waste, as the thermister cells require a good contact with the medium to give reliable results.

3.1.2.2 Flux Chamber

The flux chamber used in the field experiments was fabricated at the University of Calgary. It constitutes of a stainless steel cylinder with a circular Plexiglas sheet as the top. Schematic diagram of the chamber is shown the Figure 3.3. The diameter of the chamber is 50 cm and the height is 25 cm.

The chamber was attached with ports to facilitate usage with both LEL meter and the Micro GC. When the LEL meter was used, two ports were used. When working with the GC, one port was closed and the other one was attached with a swagelok with a Teflon septum. In addition to sampling ports, there were two other openings to monitor the pressure and temperature inside the chamber.

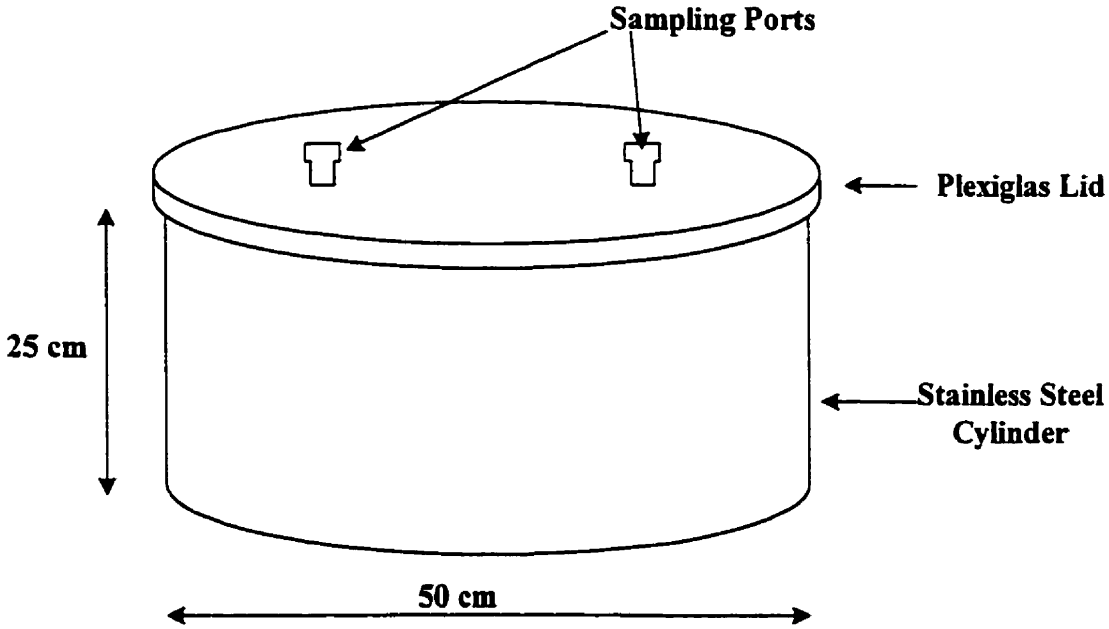

Figure 3.3: Dimensions of the Flux Chamber

3.1.3 Methodology

Although the objective of the field studies was to assess the applicability of flux chamber technique in the field, other background information was also gathered. Three PVC pipes were inserted into the lysimeter to measure gas concentrations at various depths. Gas concentrations provided the variation in concentration of different gases within the waste and also provided information on the processes occurring within the waste. Temperatures inside the lysimeter also provided similar information.

CH_4 and CO_2 emissions were measured using the flux chamber. The chamber was driven about 2-cm into the soil using the handles. To ensure that there was no short circuiting between the gases within the chamber and the atmosphere, the soil near the edge of the chamber was compacted well, sometimes adding a small amount of water. Gas concentrations inside the chamber were measured at five-minute intervals. This interval could be varied depending on the rate of increase in concentration. However, measurements were not carried out for more than 30 minutes.

When the LEL meter was used, gas was allowed to flow through the meter and recirculated into the chamber. Therefore two ports were used for this purpose. CO_2 analyzer was also connected to these ports parallel to the LEL meter. This was necessary as these meters pumped different gas amounts. Recirculation was necessary because the meters require a cumulative flow of 180 ml/min. With this amount of flow, pressure could have dropped drastically affecting the normal gas emissions unless gas was circulated. Simultaneously short-circuiting of the flow should have been prevented by separating the inlet and the outlet. When the GC was used to measure the concentrations, only one port was used. A syringe was used to obtain a sample and it was injected into the GC for analysis. A gas sample was taken through a swagelok with a Teflon septum connected to the port. Only 2 ml of gas sample was extracted to minimize the pressure drop inside the chamber. Before

taking the sample few syringe-volumes were taken and injected back for proper mixing. Pressure and the temperature variations were also monitored during the flux chamber measurements.

A glass-alcohol thermometer was used to measure temperature. Its range is –20 to 120 ^{0}C with the smallest graduation of 1^{0} C. Pressure was measured using a micro manometer (inclined manometer type). Literature indicates (Reinhart et al, 1992) that pressure increased inside the chambers up to 0.04 inches of water (10 Pa). The inclined manometer (Model Mark II 41-2) measures pressure up to 2.4 inches of water with minor gradations of 0.02 inches w.c. The accuracy of the instrument is ± 3% full range.

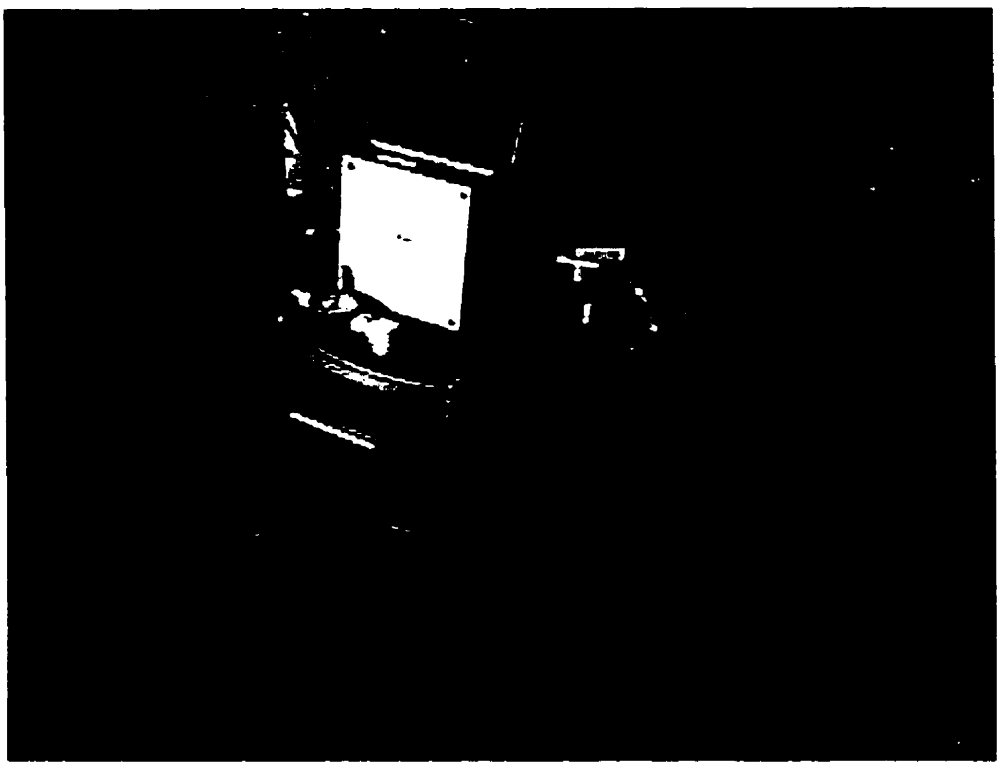

Figure 3.4: The flux chamber being used on the lysimeter

3.2 Laboratory Experiments

Main objective of the laboratory experiments was to determine the accuracy of the closed flux chamber technique under different flow rates using chambers of different sizes. Steady state gas concentration profiles were also monitored.

3.2.1 Experimental Setup

In addition to field experiments, laboratory experiments were also conducted under controlled conditions. A soil cell was constructed using a 35-gallon barrel filled with soil. It was designed to allow controlled amount of gas to be fed from the bottom of the barrel. This was achieved by using a perforated pipe kept closer to the bottom. It was desired to get a uniform gas flow throughout the cylinder. The perforated pipe was bent into a circle of diameter 25-cm so that equal distribution of flow was anticipated. This objective was further ensured by putting a layer of gravel at the bottom. A fine mesh (sieve size 30) was kept on the gravel and soil was laid on lop of that. The same soil used in the lysimeter cover (sandy loam soil) was used. Difference in pore sizes, therefore the contrast in permeabilities between soil and gravel cause the gases to diffuse in gravel and flow uniformly through the soil. The soil was laid in three layers and it was compacted with a hammer used for modified Proctor compaction test. The same compaction effort was needed to ensure similar densities in all three layers.

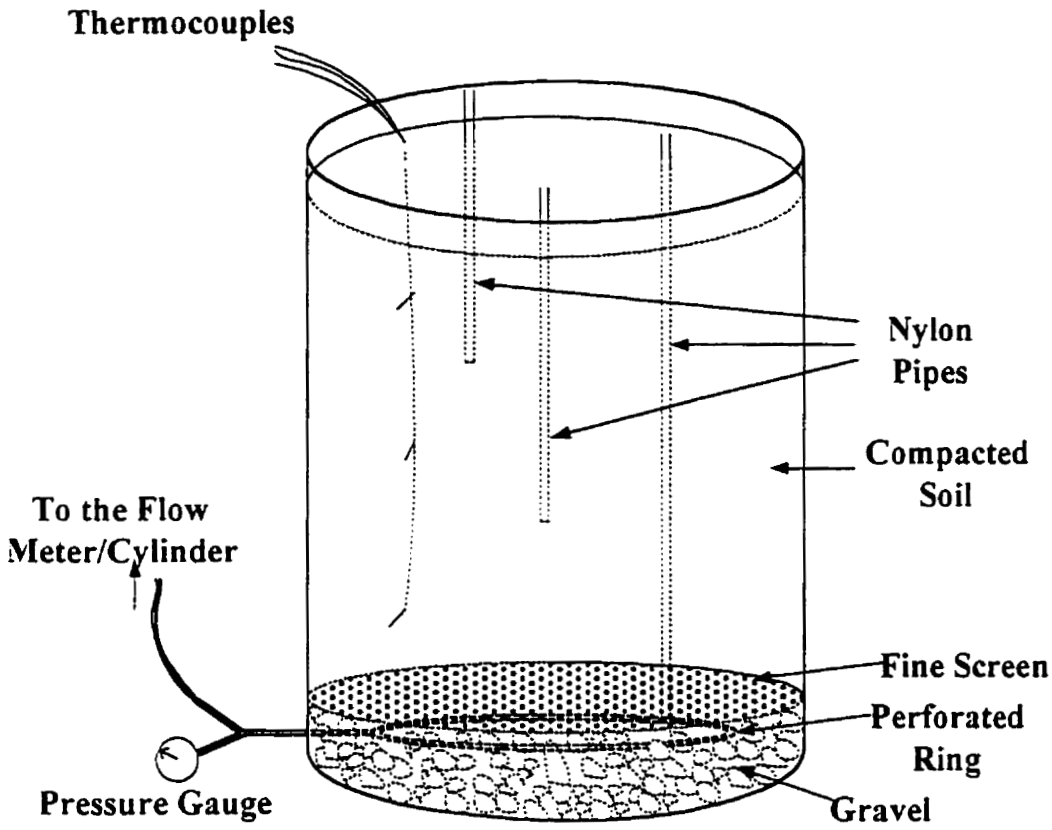

Figure 3.5: Laboratory experimental setup

3.2.2 Instrumentation

Only CO_2 was used as the test gas. Ultra high purity CO_2 cylinder (supplied by Praxair) with 800 psi pressure was used as feed gas. The gas was passed through a single stage regulator and a flow meter. Cole–Parmer 65 mm direct reading flow meter with a range of 0-100 ml/min of air was used (accuracy is ±5% full scale). After the flow meter, gas was sent through Tygon™ tubing to the bottom of the cylinder. Just before entering the cylinder, a pressure gauge was connected to measure the gas pressure inside the barrel using a 'Y' connector. The pressure gauge (Cole –Parmer) has a range of 0-15 inches of water (0 – 4

kPa) and its accuracy is ±3% of the full range. It measures low gauge pressures using a phosphor bronze diaphragm.

Three 3/8-inch nylon pipes were installed in the soil. They were used to obtain gas samples from different depths in the soil cell. The depths of the pipes were 16.5, 36, and 54 cm. The bottom of the pipes were perforated up to a height of one and a half inch and a fine steel mesh was wrapped around them to prevent soil particles entering the pipes. These pipes attached with swagelok fittings were used to measure the gas concentrations at three different levels. Three moisture probes with five feet long lead wires were also installed at three levels in the soil to monitor moisture content and the temperature. Pressure inside the chamber was measured using the inclined micro manometer.

3.2.3 Methodology

The laboratory experiments were carried out with two objectives:

- To evaluate the accuracy of closed flux chamber technique with different flux rates and different chambers
- To generate data for calibration of a model that can simulate gas migration in soils adjacent to a flux chamber

Both the objectives were accomplished using the same data sets. For the second objective, two types of data were collected, as the model consisted of two modules, namely steady state and transient cases. In the steady state, the gas flow was assumed to be one-dimensional. Therefore, gas concentrations were measured at various depths using nylon pipes inserted into the soil. Two milliliters of gas were taken into a syringe and analyzed using the Micro GC. Before taking the sample, gas was taken into the syringe and injected back several times to make sure a homogenized gas mixture was available for sampling. A maximum of 2 ml was taken to prevent any vacuum in the soil adjacent to the sampling point.

Flux chambers were used to generate transient case data. As the flux chamber used in the lysimeter studies was too large for the laboratory experiments, three smaller chambers were designed for this purpose. The largest one was with a 25cm diameter and 16.5 cm height and the smallest with a volume of 400 ml having a height of 5 cm, the medium size chamber was of 20 cm diameter and 12 cm height.

The laboratory set-up was used as a soil cell to be used with the flux chamber. The chamber was kept on the soil cell at the exact centre of the cell, to ensure axisymmetry. After the chamber was placed, the soil around the edge was pressed to achieve a good seal. Water was not used to make the seal tight, as it could have affected the gas flow near the chamber. Concentrations of gas components inside the chamber were monitored with time to develop the concentration vs. time graph.

Different options could be tested with the soil cell. Experiments could be conducted to generate data by varying the moisture content and gas flow rate, sending different gases, and using different soils. However, due to the time constraints and for purpose of simplicity at the preliminary stages, only CO_2 was used at a constant moisture content in sandy loam soil. For calibration purposes, experiments were conducted at different gas flow rates. The data generated consisted of gas concentrations at different depths of the soil column and the gas concentrations inside the chamber at different time intervals. In the calibration process of the model, these data were compared with the model results.

3.3 Analytical Methods

In the field and laboratory experiments, gas concentrations had to be measured with a high accuracy. Three types of equipment were used depending on the application. A portable micro gas chromatograph (GC), LEL (Lower Explosive Level) meter, and a CO_2 analyzer were used to measure various gases.

3.3.1 Gas Chromatograph

Model HP P 200 is a completely self-contained miniaturized gas chromatograph (GC) designed specifically for fast accurate analysis. The model contains two GC modules, an internal carrier gas cylinder, and a rechargeable battery pack. A single module consists of a micro-machined injection system, a micro-bore analytical and reference column, and a micro-machined solid state detector combined together. This is specifically made for portable use.

O_2, N_2, and CH_4 are separated in a molecular sieve column and CO_2 and CH_4 are separated in a PoraPlot column. The detector is a thermal conductivity detector (TCD). The detectors could be set to three different sensitivities, low medium and high. Helium (He) is used as the carrier gas for this study.

3.3.2 LEL Meter

Most of the initial CH_4 gas measurements were undertaken using a gas analyzer, G.M.I. Landsurveyor-I portable LEL (Lower Exposure Level) meter. It is capable of measuring methane concentrations as low as 50ppm. The LEL meter has three measuring ranges. They are, 0-100% volume CH4, 0-25% oxygen, and 0-100% LEL (Lower Exposure Level). Methane percentage is measured by a thermal conductivity sensor. Oxygen is measured by an electrochemical sensor. A catalyst reaction is utilized to measure the percentage LEL. Accuracy of the measurement is usually in the 2-3% range.

3.3.3 CO_2 Analyzer

CO_2 was measured using an EGM2 – CO_2 analyzer. It uses a non-dispersive infrared analyzer to measure CO_2. Measurement range is 0 – 50000 ppm by volume. The precision of the meter was 0.5% of full scale. This meter was used to measure CO_2 concentrations inside the flux chamber. It was not suitable for gas concentration measurements within the lysimeter as it could only measure up to 5% CO_2 by volume.

CHAPTER FOUR
EXPERIMENTAL RESULTS AND DISCUSSION

4.1 Lysimeter Results

4.1.1 Gas concentrations within the Waste

Gas samples were collected from the PVC pipe inserted into the waste and analyzed for various gases. Only CH_4 and O_2 were measured initially, as only the LEL meter was available at the beginning of the experiments. However, not much CH_4 was detected throughout the duration. That was anticipated, as initial stage of a landfill is aerobic. Low O_2 indicated the presence of significant amounts of CO_2. The CO_2 analyzer could measure up to 5 % of CO_2. Therefore, it could not provide much information on CO_2 concentrations. To solve this problem, gas samples were taken to the Chemical Engineering laboratory and analyzed with a GC from time to time. The Figure 4.1 shows the variation of CH_4 and O_2 concentrations against time. Due to the non-continuous nature of the CO_2 concentration measurements, these readings are given in Table 4.1.

Table 4.1: Concentrations of CH_4, CO_2, and O_2 inside the lysimeter

Date	CO_2 Concentration (%)	CH_4 Concentration (%)	O_2 Concentration (%)
10/05/1997	3.17	2.1	16.9
10/31/1997	1.23	0.2	18.7
11/28/1997	9.76	1.1	12.7
12/05/1997	13.63	0.6	6.78
10/20/1998	5.0	0.8	16.5
11/06/1998	1.08	0.031	21.5
02/02/1999	6.92	-	15.45
02/08/1999	6.38	-	15.91

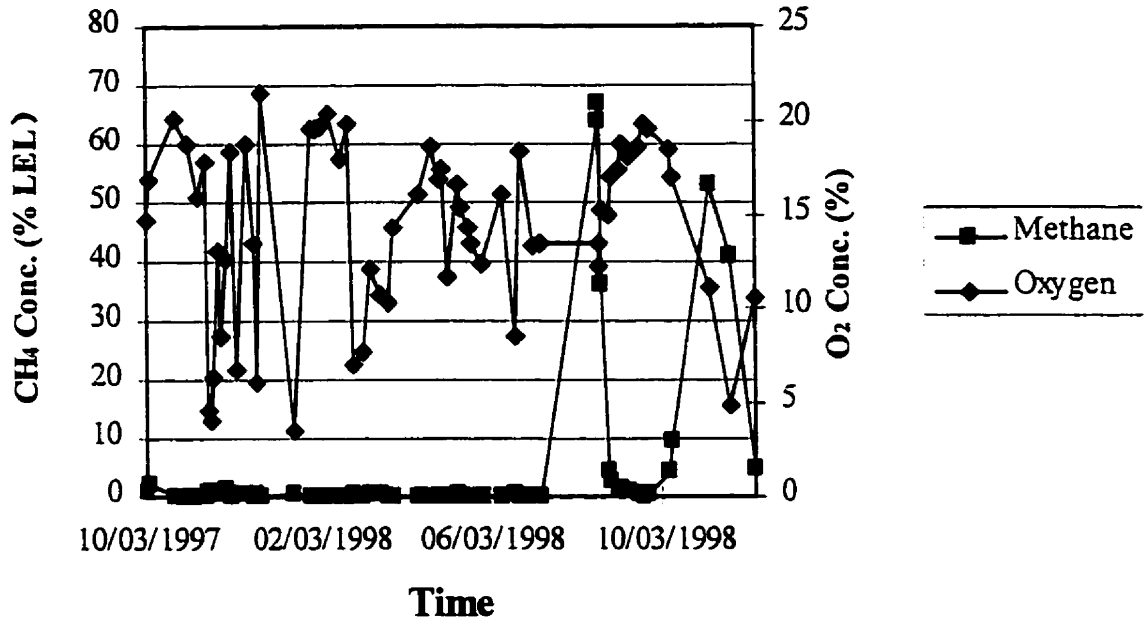

Figure 4.1: Concentrations of CH_4 and O_2 within the waste against time

At all times (except on two occasions), O_2 concentration within the top layer of the waste was above 5 %. This indicated the penetration of O_2 through the soil cover. Cracks due to the settlement of the cover also contributed for this O_2 penetration. Presence of O_2 within the waste implies that anaerobic conditions were not prevailing at least in the top layer of waste. On the other hand, that gives rise to a conclusion that CH_4 oxidation could have occurred even within the top layer of the waste.

Low concentrations of CH_4 and CO_2 indicate insignificant amount of biological activity inside the lysimeter. Temperature variations inside the lysimeter support that conclusion. As shown in the Figure 4.2 temperature inside the lysimeter follows the trends in the atmospheric temperature. As soon as the lysimeter was covered, the temperature inside shot up to 55 ^{o}C. However, during the winter, temperatures dipped down very fast. And it did not reach those high temperatures subsequently. Although the top portion of the lysimeter was insulated well to prevent frost penetration, the lower portion was without any insulation. That might have caused a loss of heat from lysimeter and it was apparent that the

biological activity could not have sustained due to heat loss. When the temperature goes down, microbes become less active. Another possible reason was unopened bags. Due to the nature of the compaction effort, it is possible that there were quite a few garbage bags containing organic matter, which did not open during the compaction. Lack of sufficient waste moisture also could have caused lower biological activity. The soil cover was constructed immediately after filling the lysimeter. Clay layer in the cover further reduced any rain water infiltration into the waste. Therefore, only initial moisture was available to facilitate CH_4 generation. It is important to note that there was no leachate production initially (Shroff, 1999).

Although it was expected that there would be CH_4 emissions after adding more organic waste in the summer of 1998, CH_4 production was very low. Although there was an increase in CH_4 concentration as shown in Figure 4.1 and a temperature increase (mainly due to atmospheric conditions) as shown in Figure 4.2, it was not sustained. This low activity was reflected in the gas flux and concentration measurements. The organic content inside the lysimeter had increased with the introduction of new waste. The pH of the leachate was measured to be closer to seven, therefore the hypothesis that the inhibition of methanogens due to low pH was also rejected. There were some emissions of CO_2, mainly due to aerobic microbial activity and possible CH_4 oxidation in the top layers of the cover soil.

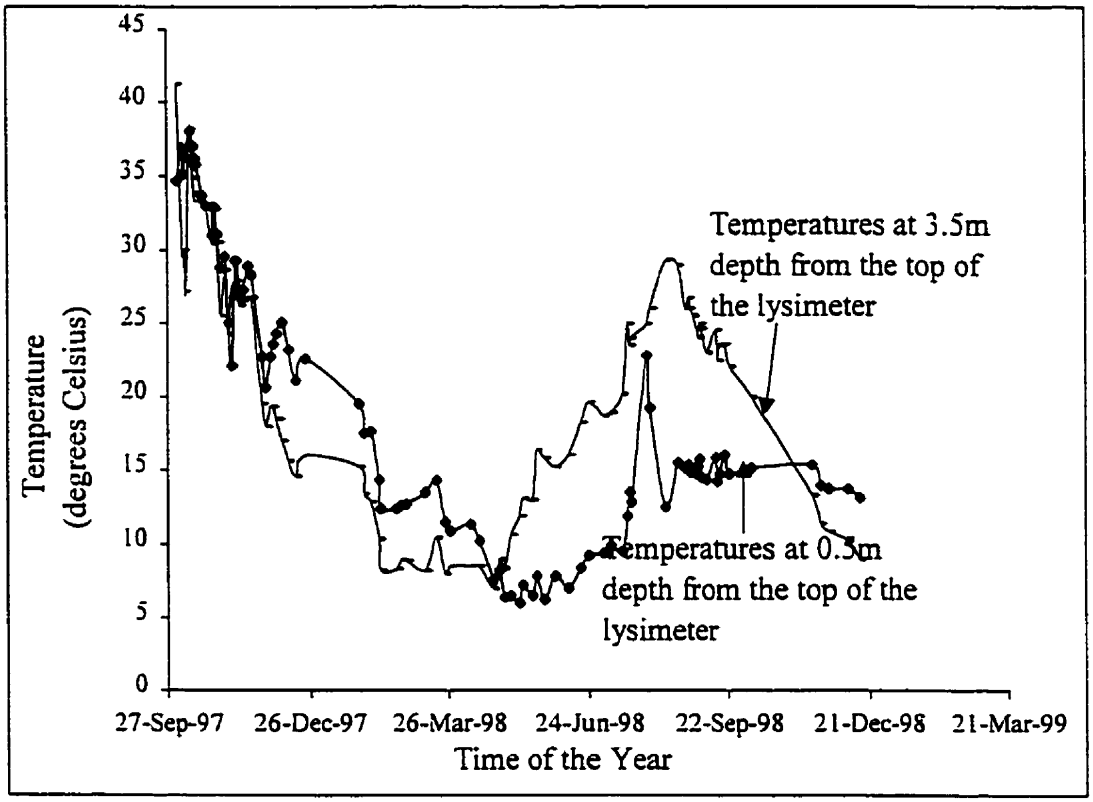

Figure 4.2: Temperature variation inside the lysimeter (after Shroff, 1999)

4.1.2 Flux Chamber Measurements

Flux chamber was used to monitor the gas flux rates emitted from waste inside the lysimeter. As explained earlier, CH_4 concentrations within the waste were very small, and the CH_4 flux rates were also negligible. Although the original objective was to measure CH_4 gas emissions, only CO_2 emissions could be measured.

Figure 4.3 shows the CO_2 gas emission rates measured within first few months after adding more waste to the lysimeter and redoing the cover. Initially it shows high fluxes due to higher activity. That was because adding more organic wastes as well as water. With time it was reduced to 3-4 $g.m^{-2}.day^{-1}$.

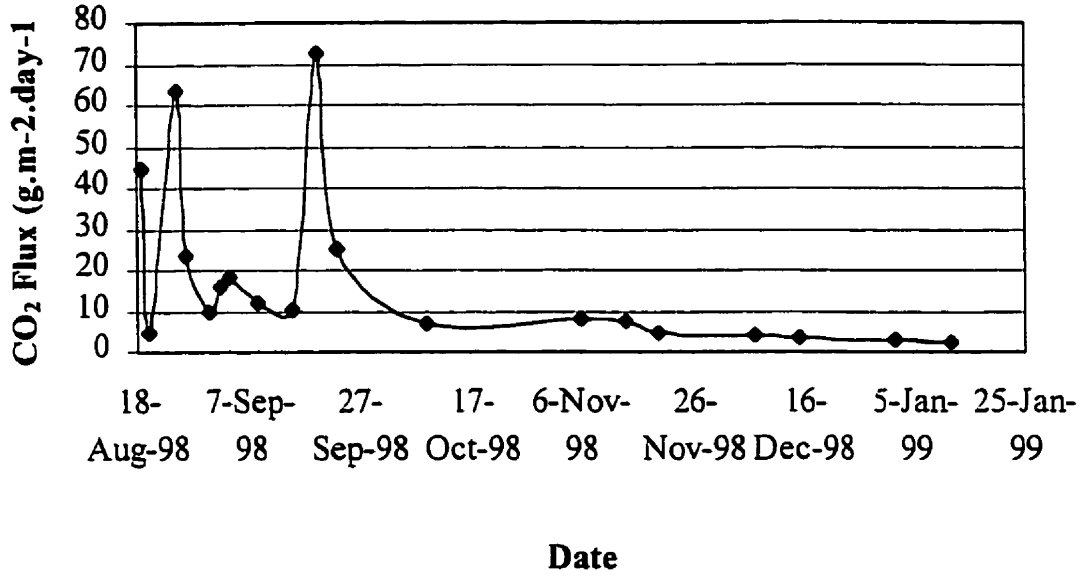

Figure 4.3: Variation of CO_2 emission rate from the lysimeter

4.1.3 Factors affecting Measurements

Gas generation rate within the landfills affects the emission rates. Depending on the consumption and the age of the waste, gas flux rates vary. Another factor influencing gas emission rates is CH_4 oxidation. The conditions of the soil also contribute for gas emission rates. Figure 4.4 and Figure 4.5 show gas flux rates variation from 73 to 25 $g.m^{-2}.day^{-1}$ within 3 days. The reason was a rainfall event occurred on September 22, 1998. This variation is caused by rainwater saturation of the soil after the rainfall event, which eventually decreases gas permeability. In addition to that observation it is clearly visible that the rate of change of CO_2 concentration inside the chamber reduced with time in both the cases. However, this decrease in rate was higher in Figure 4.5 because the flux is smaller in that case.

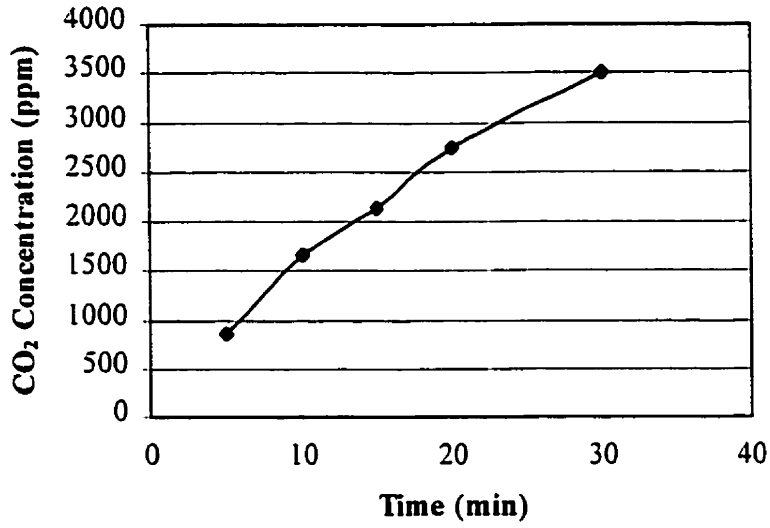

Figure 4.4: CO_2 Concentration variation inside the chamber – Sept. 20, 1998

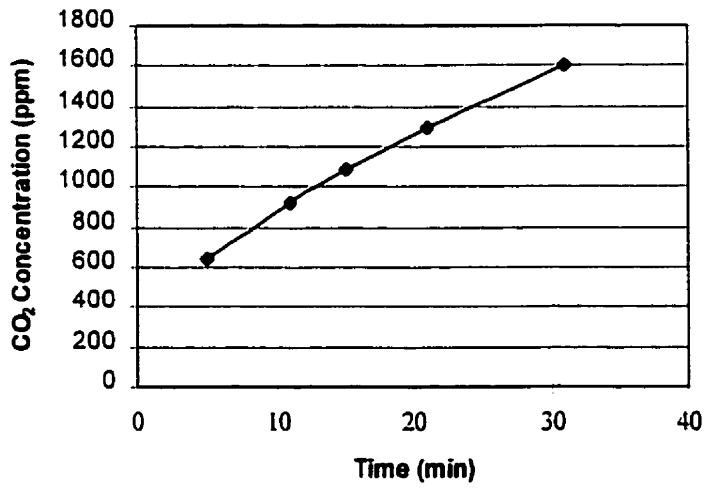

Figure 4.5: CO_2 Concentration variation inside the chamber – Sept. 23, 1998

4.2 Laboratory Experiments

4.2.1 Steady State Concentrations

Steady state CO_2 concentration profiles in the soil column under three different flux rates are given in the Figure 4.6. Non-linearity of the graphs emphasizes the inadequacy of explaining the gas migration in soils with only dispersion. In addition, it shows the difficulty of determining flux rates from the measured gas concentration gradient in the soils (see section 2.4.3).

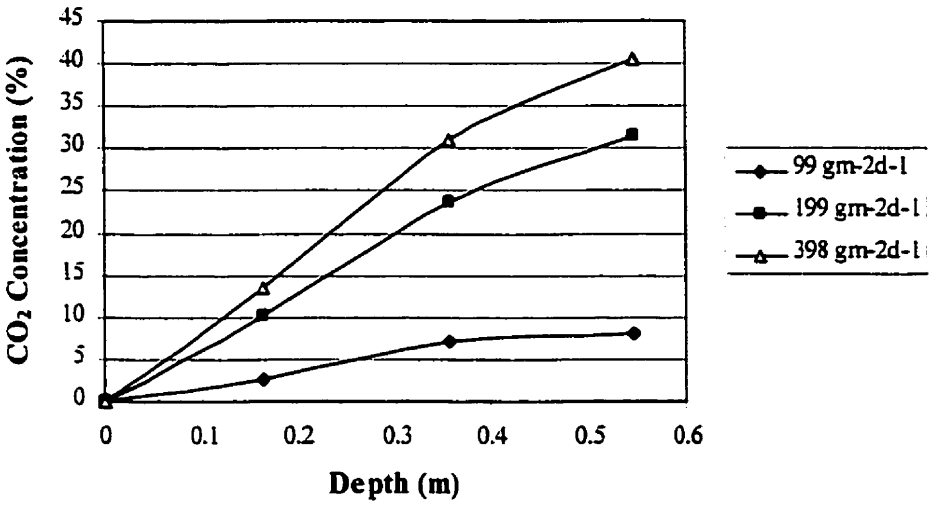

Figure 4.6: Steady state CO_2 gas concentration profile under different flow rates

4.2.2 Flux Chamber Measurements

The monitored CO_2 concentrations inside the chamber under different gas flow rates for small, medium, and large size flux chambers, are show in Figures 4.4, 4.5 and 4.6, respectively. The graphs clearly demonstrate the non-linearity of the rate of change of concentrations with the increase in flux rate. In addition, these figures show the effect of

chamber height on the flux rate calculation. With increase of chamber height, linearity of the rate of change of CO_2 concentration increases.

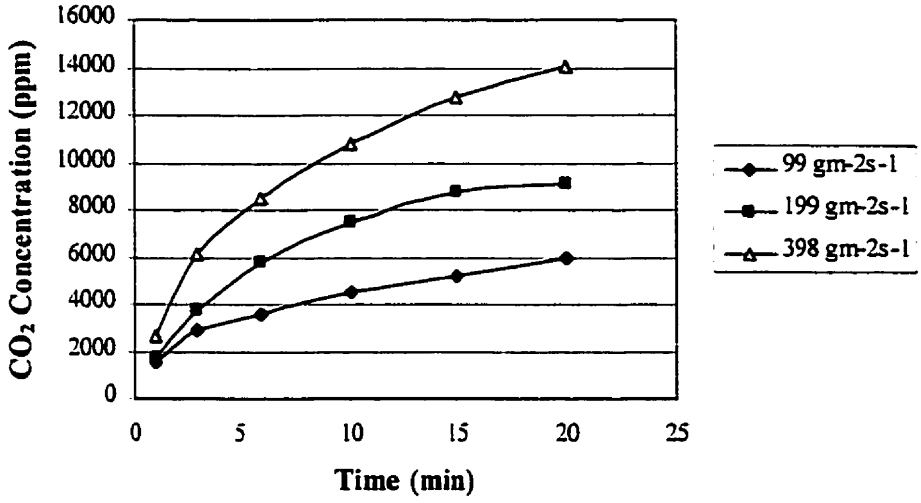

Figure 4.7: CO_2 concentrations inside the small chamber

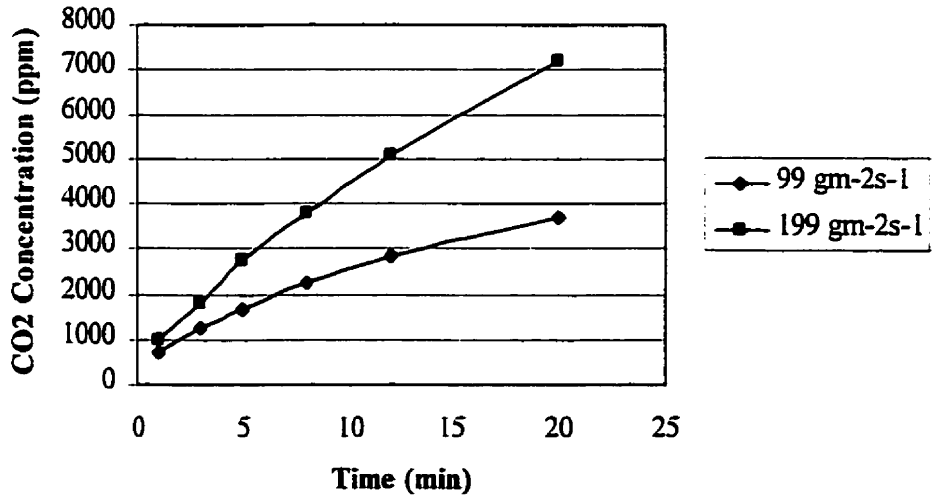

Figure 4.8: CO_2 concentration inside the medium size chamber

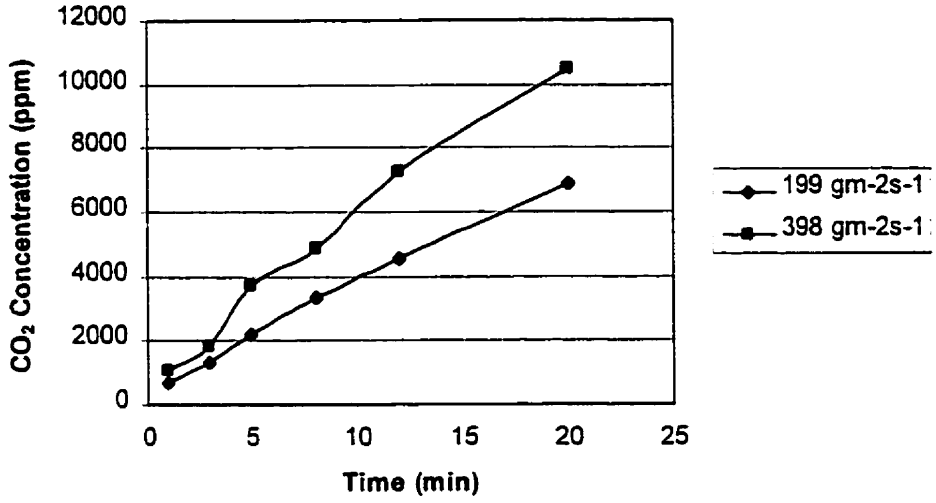

Figure 4.9: CO_2 concentrations inside the large chamber

These graphs suggest that measuring gas concentrations within first five minutes is sufficient to determine the flux rates because the linear portion of the graph occurs during this period. However, this is probably due to relatively higher gas flow rates used in the experiments.

4.2.3 Error Percentages in Chamber Measurements

Percentages of the flux rates determined by the closed flux chamber are presented in the Table 4.2. Flux rates were calculated using two methods. In the first option, gradient of the graph, CO_2 concentration inside the chamber versus time was determined by fitting a straight line to the first three observations (within first 5 minutes). The second option uses fitting a quadratic curve to the measured points and then obtaining the slope of the function at time = 0. In both methods, the correlation coefficient was above 0.98. Both methods gave similar results. Table 4.3 shows the effect of chamber height on accuracy of flux estimation. Taller chambers give more accurate results, as the impact of gas accumulation within the

chamber is the least in that case. However, with the increase of flux rate, the estimations become less accurate. The small chamber showed an error of about 70%. It was an extreme situation because the height of the chamber was very small (4 cm). Medium size and the large size chambers gave relatively satisfactory results. It was apparent with the proper selection of chamber height, more than 90% of the flux could be measured using a closed flux chamber.

Table 4.2: Flow rates measured by the flux chambers

Chamber	CO_2 Flow Rate ($g.m^{-2}.day^{-1}$)	% of the estimated flux	
		Linear fit	Quadratic fit
Small Chamber	99	34.5	34.3
	199	36	39.4
	398	29.3	28.9
Medium	99	80.6	86.3
	199	74.9	78.5
Large	199	85.1	93
	398	70.6	69

CHAPTER FIVE
THEORETICAL DEVELOPMENT

5.1 Derivation of Equations

Landfill cover systems are usually layered structures, with different layers to serve different purposes. For simplicity it is assumed here that a landfill cover consists of a single layer of soil. Gas migration in the soil cover is modeled assuming soil is a continuum. Soil cover adjacent to the flux chamber is considered for modeling. As the chambers are cylindrical, perturbations in the soil atmosphere are radial. Therefore, the modeling is done using a cylindrical polar co-ordinate system. However, it can still be simplified to an axisymmetric case assuming the soil properties are isotropic on the horizontal plane. Gas migration under a closed chamber is shown in Figure 5.1.

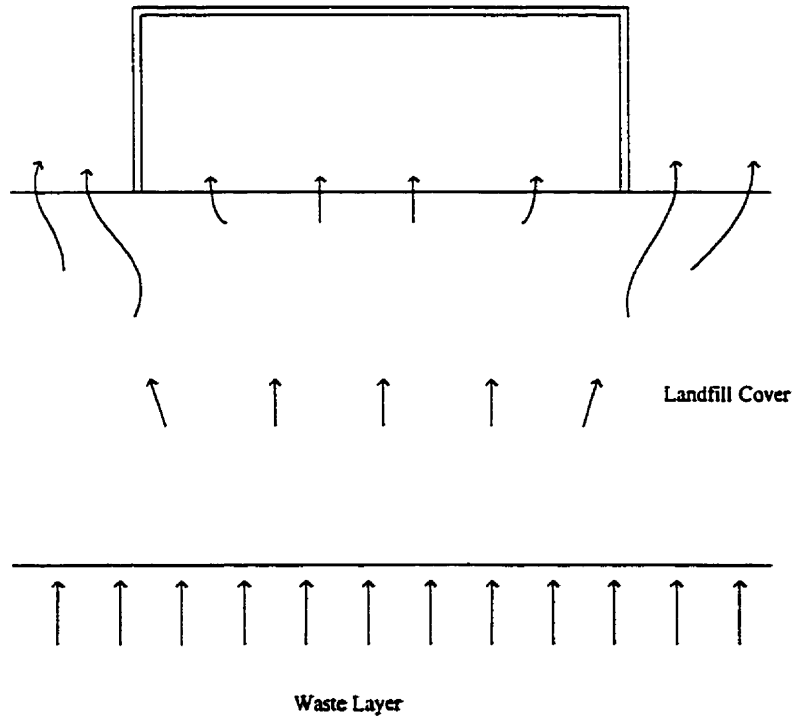

Figure 5.1: Gas flow adjacent to a flux chamber

5.1.1 Derivation of Differential Equations

Consider a point P (z, r, θ) surrounded by an element of δz, δr, and making an angle δθ at the axis of the flux chamber (As shown in Figure 5.2). Here r is the horizontal radial direction and z is in the vertically downward direction.

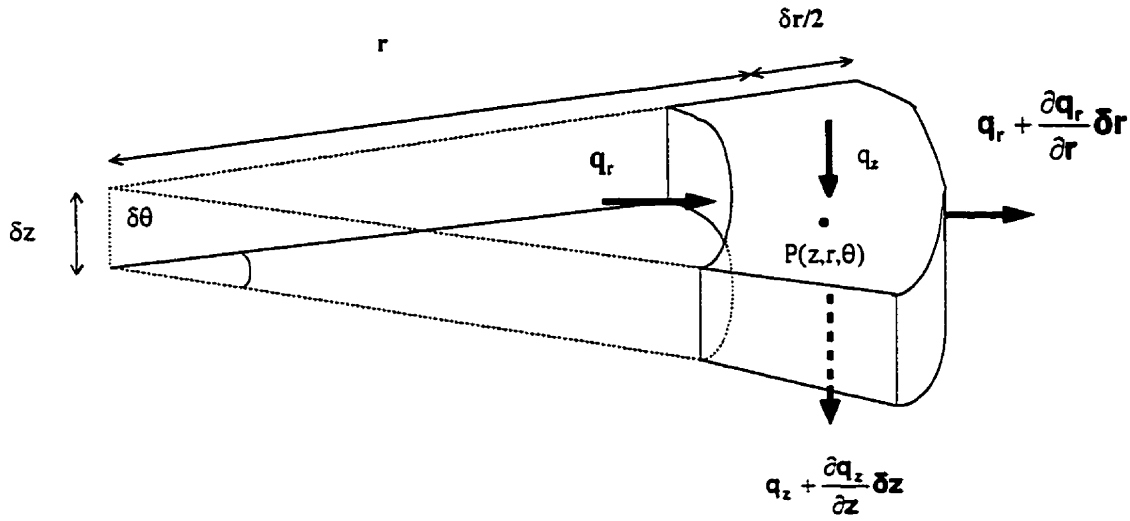

Figure 5.2: An element of soil

The general flow domain in a landfill cover is essentially multi-phase and multi-component consisting of a water phase and a gas phase with different gas components. However, objective of this model is to simulate gas migration within the landfill cover for a short time period (less than a half-hour). Therefore, water migration is neglected. However, effect of water in the pores is considered in gas porosity and gas permeabilities. Gas permeability is determined using relative permeability to account for the degree of saturation (Fredlund and Rahardjo, 1992). Therefore, this problem is simplified to an unsaturated, multi-component, single-phase (i.e. gas phase) transport problem.

Considering conservation of mass of component k in the gas phase;

Accumulation = Inflow - Outflow ± Reactions

$$\phi \frac{\partial C_k}{\partial t} \delta V = q_r \delta z \left(r - \frac{\delta r}{2} \right) \delta\theta - \left(q_r + \frac{\partial q_r}{\partial r} \delta r \right) \delta z \left(r + \frac{\delta r}{2} \right) \delta\theta + q_z \delta r \, r \delta\theta$$

$$- \left(q_z + \frac{\partial q_z}{\partial z} \delta z \right) \delta r \, r \delta\theta + R \delta V \quad \text{..... (5.1)}$$

where,

C_k = Concentration of gas component k ($mol.m^{-3}$)

ϕ = Air porosity

q_s = Flow rate of the gas in s direction; s = z, r ($mol.m^{-2}.s^{-1}$)

r = Radial distance to the point (m)

R = Reaction term ($mol.m^{-3}.s^{-1}$)

δV = Volume of the infinitesimal element (m^3)

$$\phi \frac{\partial C_k}{\partial t} \delta V = - \left(q_r + \frac{\partial q_r}{\partial r} + \frac{\partial q_r}{\partial r} \frac{\delta r}{2} \right) \delta z \delta r \delta\theta - \frac{\partial q_z}{\partial z} r \, \delta z \delta r \delta\theta + R \delta V$$

$$= \frac{1}{r} \left(q_r + \frac{r \partial q_r}{\partial r} \right) \delta V - \frac{\partial q_z}{\partial z} \delta V + R \delta V$$

$$\phi \frac{\partial C_k}{\partial t} = \frac{1}{r} \left(q_r + \frac{r \partial q_r}{\partial r} \right) - \frac{\partial q_z}{\partial z} + R \quad \text{..... (5.2)}$$

But q_s is due to advection and dispersion;

$$q_s = v_s C_k - D \frac{\partial C_k}{\partial s} \quad \text{..... (5.3)}$$

where;

D = Coefficient of Dispersion ($m^2.s^{-1}$)

v_s = Gas velocity in s direction; s = z, r ($m.s^{-1}$)

Substituting q_s in equation 5.2;

$$\phi\frac{\partial C_k}{\partial t} = -\frac{1}{r}\left(v_r C_k - D\frac{\partial C_k}{\partial r}\right) - \frac{\partial}{\partial r}\left(v_r C_k - D\frac{\partial C_k}{\partial r}\right) - \frac{\partial}{\partial z}\left(v_z C_k - D\frac{\partial C_k}{\partial z}\right) + R \ldots \quad (5.4)$$

Gas velocities can be determined using Darcy's law;

$$v_s = \frac{k_s k_{rel}}{\mu}\frac{\partial P^*}{\partial s} \quad (5.5)$$

where;

k_s = Intrinsic permeability in r or z direction (m^2)

k_{rel} = Relative permeability

μ = Gas viscosity (Pa.s)

P^* = Total potential (Pa)

Total potential is given as follows (in units of pressure, Pa):

$$P^* = P + \frac{v^2\rho}{2} + (z_0 - z)\rho g \quad (5.6)$$

where;

P^* = Total potential (energy)

z_0 = Elevation of the reference datum

ρ = Density of air

However, only pressure head and elevation head are considered in the Equation 5.6 due to the fact that the velocity head is negligible because of low gas velocities.

Viscosity of the gas mixture can be expressed as a function of the viscosities of the individual gases by (Reid et al., 1987);

$$\mu = \sum_{k=1}^{4} \frac{\mu_k}{1 + \sum_{\substack{l=1 \\ l \neq i}}^{4} \theta_{kl} \frac{y_k}{y_l}} \quad \text{..... (5.7)}$$

$$\text{in which } \theta_{kl} = \frac{\left[1 + \left(\frac{\mu_k}{\mu_l}\right)^{1/2} \left(\frac{M_l}{M_k}\right)^{1/4}\right]^2}{\sqrt{8}\left(1 + \frac{M_k}{M_l}\right)^{1/2}}$$

where,

y_k = Molar fraction of the component k (mol/mol)

M_k = Molecular weight of the component k

μ_k = Viscosity of the component k (Pa.s)

Equation 5.4 has two variables, concentration and velocity (or pressure when Darcy's law is used). Therefore, it cannot be solved directly. However, in gases, pressures can be derived from concentrations using the equation of state for gases. Considering all the partial pressures of component gases in the soil atmosphere, the total pressure could be given as the sum of the partial pressures.

The equation of state for gases is given by;

$$P_k V = n_k R T \quad \text{..... (5.8)}$$

where,

P_k = Partial pressure of gas component k (Pa)

n_k = No. of moles of gas k (mol)

R = Universal gas constant ($Pa.m^3mol^{-1}K^{-1}$)

T = Absolute temperature (K)

Arranging the terms, it is possible to write for a component gas i;

$P_k = C_k RT$

Now, the total pressure can be obtained from;

$$P = RT(C_1+C_2+C_3+C_4) \quad \text{.....} \quad (5.9)$$

where,

R = Universal gas constant ($Pa.K^{-1}.m^3.mol^{-1}$)

T = Absolute temperature (K)

C_1, C_2, C_3, C_4 = Concentrations of gas components CH_4, CO_2, O_2, and N_2, respectively ($mol.m^{-3}$)

The dispersion coefficient of an individual gas is calculated in a manner similar to the hydrodynamic dispersion in groundwater modeling. Hydrodynamic dispersion consists of molecular diffusion and mechanical dispersion. According to Bear (1972) mechanical dispersion is due to variation of local velocity, both in magnitude and direction, along the tortuous flow paths and between adjacent flow paths as a result of velocity distribution within each pore. Therefore;

$$D = D^* + \alpha|v| \quad \text{.....} \quad (5.10)$$

where,

D = Dispersion coefficient (m^2s^{-1})

D^* = Molecular diffusion (m^2s^{-1})

α = Dispersivity (m)

The gas diffusion coefficient in porous media is not easy to determine. However, values for atmospheric diffusion could be used with a modification for porosity and tortuosity. Among many available empirical relationships between diffusion coefficients in atmosphere and porous media, Millington and Quirks's (1961) equation is the most popular (Mendoza and

Frind, 1990, American Society of Agronomy, 1986). Dispersivity in mechanical dispersion is a scale dependent parameter. Values for α used in previous numerical modeling studies range from 0.01 to 1.0 m (Mendoza and Frind, 1990).

The reaction term R is due to CH_4 oxidation in the soil by methanotrophic bacteria. Biological reactions are difficult to represent by equations. There are many factors affecting methane oxidation; for example, moisture content, O_2 concentration, CH_4 concentration, temperature etc. However, Monod kinetics is generally used for this purpose. To account for the dependence of the reaction rate on concentrations of both CH_4 and O_2, a modified version of Monod kinetics is used (Cherry and Thompson, 1997);

$$R = V_{max} \frac{C_{CH4}}{K_{S-CH4} + C_{CH4}} \frac{C_{O2}}{K_{S-O2} + C_{O2}} X \quad \ldots\ldots\ldots\ldots\ldots\ldots\ldots\ldots\ldots\ldots \quad (5.11)$$

where,

V_{max} = Specific growth rate (s^{-1}.(mol. of CH_4/kg of microbial mass))

K_{s-i} = Half saturation constant for CH_4 or O_2 (mol/m^3)

X = Dry weight of biomass (kg of microbial mass/m^3)

R in Equation 5.11 is the reaction rate for methane. It is the oxidation rate for CH_4 as well as the generation rate for CO_2. Under steady state of oxidation (i.e. maintenance kinetics) cell growth is assumed to be zero. Considering the stoichiometry of methane oxidation.

$$CH_4 + 2O_2 \Rightarrow CO_2 + 2H_2O$$

According to the equation, for every mole of CH_4 that is oxidized, two moles of O_2 are consumed and one mole of CO_2 is generated. Therefore the rate of oxygen consumption is twice that of CH_4, and the rate of CO_2 generation is equal to that of CH_4 oxidized.

The governing Equation 5.4 could be written for all gases. Reaction term should be given as per stoicheometric reaction rates. Therefore the equations are functions of only concentrations. However, the equations become coupled and non-linear due to the velocity terms.

5.2 Model to Simulate Laboratory Experiments

Developing a model to solve the complete equation given in Equation 5.4 is complex and time consuming. In addition the reaction kinetics involved with CH_4 oxidation is not well understood. Monod parameters change with the soil depth, moisture content, temperature, and the historical gas concentrations the microbes are exposed to (Czepiel et al., 1996). Because of these factors, it was decided to develop the model without considering the reaction form. Therefore CO_2 was selected for the study. However, all the other physical processes encountered in landfill setting were simulated in the model. The omission of the reaction term is not a hindrance, as it is still possible to investigate the performance of the flux chambers under the influence of advection and dispersion.

When CO_2 is used, the reaction term of the governing equation vanishes, as well as the system consists of only two gases. All the other gases except CO_2 can be collectively considered as a single gas component. For convenience, this component is called 'air'. This makes the equations simple and only two equations are required to represent the system. The main equation is given as:

$$\phi \frac{\partial C_k}{\partial t} = -\frac{1}{r}\left(v_r C_k - D\frac{\partial C_k}{\partial r}\right) - \frac{\partial}{\partial r}\left(v_r C_k - D\frac{\partial C_k}{\partial r}\right) - \frac{\partial}{\partial z}\left(v_z C_k - D\frac{\partial C_k}{\partial z}\right) \quad \text{..... (5.12)}$$

Here k represents CO_2 or air. This equation can be written for both CO_2 and air.

5.3 Finite Difference Equations

A finite difference method is used to solve these equations numerically. The methodology is discussed in the next chapter.

The derivatives were determined using central difference. Pressures were taken explicitly to linearize the equations. Finite difference equation for a component gas is given below. The same equation is applicable to all the gases with appropriate parameter values.

5.3.1 Equations for Transient Case

From the Equation 5.14, let $v_r = u$ and $v_z = v$

$$\phi\frac{\partial C_k}{\partial t} = -\frac{1}{r}\left(uC_k - D\frac{\partial C_k}{\partial r}\right) - \frac{\partial}{\partial r}(uC_k) - \frac{\partial}{\partial z}(vC_k) + \frac{\partial}{\partial r}\left(D\frac{\partial C_k}{\partial r}\right) + \frac{\partial}{\partial z}\left(D\frac{\partial C_k}{\partial z}\right) \quad (5.13)$$

Consider the finite difference approach;

$$\phi\frac{C_{i,j}^{n+1} - C_{i,j}^{n}}{\Delta t} = (1-\omega)\left\{-\frac{1}{r}\left(u_{i,j}^{n}C_{i,j}^{n} - D_{i,j}\left(\frac{C_{i+1/2,j}^{n} - C_{i-1/2,j}^{n}}{(\Delta r_i + \Delta r_{i-1})/2}\right)\right)\right\}$$

$$+\omega\left\{-\frac{1}{r}\left(u_{i,j}^{n+1}C_{i,j}^{n+1} - D_{i,j}\left(\frac{C_{i+1/2,j}^{n+1} - C_{i-1/2,j}^{n+1}}{(\Delta r_i + \Delta r_{i-1})/2}\right)\right)\right\}$$

$$-(1-\omega)\left\{\frac{u_{i+1/2,j}^{n}C_{i+1/2,j}^{n} - u_{i-1/2,j}^{n}C_{i-1/2,j}^{n}}{(\Delta r_i + \Delta r_{i-1})/2}\right\} - \varpi\left\{\frac{u_{i+1/2,j}^{n+1}C_{i+1/2,j}^{n+1} - u_{i-1/2,j}^{n+1}C_{i-1/2,j}^{n+1}}{(\Delta r_i + \Delta r_{i-1})/2}\right\}$$

$$-(1-\omega)\left\{\frac{u_{i,j+1/2}^{n}C_{i,j+1/2}^{n} - u_{i,j-1/2}^{n}C_{i,j-1/2}^{n}}{(\Delta z_j + \Delta z_{j-1})/2}\right\} - \varpi\left\{\frac{u_{i,j+1/2}^{n+1}C_{i,j+1/2}^{n+1} - u_{i,j-1/2}^{n+1}C_{i,j-1/2}^{n+1}}{(\Delta z_j + \Delta z_{j-1})/2}\right\}$$

$$+(1-\omega)\left\{\frac{D_{i+1/2,j}\left(\frac{C^{n}_{i+1,j}-C^{n}_{i,j}}{\Delta r_i}\right)-D_{i-1/2,j}\left(\frac{C^{n}_{i,j}-C^{n}_{i-1,j}}{\Delta r_{i-1}}\right)}{\frac{(\Delta r_{i-1}+\Delta r_i)}{2}}\right\}$$

$$+\omega\left\{\frac{D_{i+1/2,j}\left(\frac{C^{n+1}_{i+1,j}-C^{n+1}_{i,j}}{\Delta r_i}\right)-D_{i-1/2,j}\left(\frac{C^{n+1}_{i,j}-C^{n+1}_{i-1,j}}{\Delta r_{i-1}}\right)}{\frac{(\Delta r_{i-1}+\Delta r_i)}{2}}\right\}$$

$$+(1-\omega)\left\{\frac{D_{i,j+1/2}\left(\frac{C^{n}_{i,j+1}-C^{n}_{i,j}}{\Delta z_j}\right)-D_{i,j-1/2}\left(\frac{C^{n}_{i,j}-C^{n}_{i,j-1}}{\Delta z_{j-1}}\right)}{(\Delta z_{j-1}+\Delta z_j)/2}\right\}$$

$$+\omega\left\{\frac{D_{i,j+1/2}\left(\frac{C^{n+1}_{i,j+1}-C^{n+1}_{i,j}}{\Delta z_j}\right)-D_{i,j-1/2}\left(\frac{C^{n+1}_{i,j}-C^{n+1}_{i,j-1}}{\Delta z_{j-1}}\right)}{(\Delta z_{j-1}+\Delta z_j)/2}\right\}\ldots\ldots \quad (5.14)$$

where

n represents the time and i and j represent spatial coordinates (r and z directions respectively)

Δr_i and Δz_j represent mesh size of i^{th} column and j^{th} row respectively

ω - Temporal weighting factor

Different ω values give different finite difference schemes. Outcome of $\omega = 0$ is a fully explicit scheme. Fully implicit finite difference scheme is generated with $\omega = 1$. If its value is 0.5 it gives the Crank-Nicholson scheme. Although Crank-Nicholson method is preferred due to its higher accuracy and stability, implicit scheme was used to reduce the amount of calculations. Implicit scheme is also stable.

$C_{i,j+1/2}$ is determined from a weighting function. The general equation is given by;

$$C_{i,j+1/2} = (1-\alpha)C_{i,j} + \alpha C_{i,j+1} \quad \text{.....} \quad (5.15)$$

where, α is the spatial weighting factor

The most obvious choice of α is 0.5; the resulting formulation is referred to as the central weighting scheme. With the central weighting scheme, the finite difference approximation of the advection term is accurate to the second order (Zheng and Bennett, 1995). However, the central weighting scheme tends to create artificial oscillations. An alternative spatial weighting scheme, upstream or upwind scheme, is frequently used to solve similar problem. Upstream weighting can be expressed as follows:

$$\alpha = \begin{cases} 0 & if \ v > 0 \\ 1 & if \ v < 0 \end{cases} \quad \text{.....} \quad (5.16)$$

However, central weighting was used because its accuracy is higher than upstream weighting scheme. Then the finite difference equation becomes;

$$\begin{aligned} \phi \frac{C_{i,j}^{n+1}}{\Delta t} = & \frac{1}{r}\left[u_{i,j} C_{i,j}^{n+1} - D_{i,j} \frac{C_{i+1,j}^{n+1} - C_{i-1,j}^{n+1}}{ADR} \right] \\ & - \frac{1}{ADR}\left[u_{i+1/2,j}\left(C_{i+1,j}^{n+1} + C_{i,j}^{n+1}\right) - u_{i-1/2,j}\left(C_{i,j}^{n+1} + C_{i-1,j}^{n+1}\right) \right. \\ & \left. - \frac{1}{ADZ}\left[v_{i,j+1/2}\left(C_{i,j+1}^{n+1} + C_{i,j}^{n+1}\right) - v_{i,j-1/2}\left(C_{i,j}^{n+1} + C_{i,j-1}^{n+1}\right) \right] \right. \\ & + \frac{D_{i+1/2,j}}{\Delta r_i * ADR}\left(C_{i+1,j}^{n+1} - C_{i,j}^{n+1}\right) - \frac{D_{i-1/2,j}}{\Delta r_{i-1} * ADR}\left(C_{i,j}^{n+1} - C_{i-1,j}^{n+1}\right) \\ & + \frac{D_{i,j+1/2}}{\Delta z_j * ADZ}\left(C_{i,j+1}^{n+1} - C_{i,j}^{n+1}\right) - \frac{D_{i,j-1/2}}{\Delta z_{j-1} * ADZ}\left(C_{i,j}^{n+1} - C_{i,j-1}^{n+1}\right) \quad \text{.....} \quad (5.17) \end{aligned}$$

where,

ADR $= \Delta r_i + \Delta r_{i+1}$

ADR $= \Delta z_j + \Delta z_{j+1}$

This is a finite difference equation of five variables. When all the equations are assembled, a penta-diagonal matrix is resulted. However, by using Alternating Direction Implicit (ADI) method, the matrices were simplified to tri-diagonal form. In ADI scheme, the equations are solved in two steps first solving in vertical direction and next in radial direction.
Finally, the form of equations in both directions is as follows;

In z-direction:

$$\left(\frac{v_{i,j-1/2}}{ADZ}+\frac{2*D_{i,j-1/2}}{\Delta z_{j-1}*ADZ}\right)C_{i,j-1}^{n+1/2}$$

$$+\left(-\frac{v_{i,j+1/2}}{ADZ}+\frac{v_{i,j-1/2}}{ADZ}-\frac{2*D_{i,j+1/2}}{\Delta z_j*ADZ}-\frac{2*D_{i,j-1/2}}{\Delta z_{j-1}*ADZ}-\frac{\phi}{\Delta t}\right)C_{i,j}^{n+1/2}$$

$$+\left(-\frac{v_{i,j+1/2}}{ADZ}+\frac{2*D_{i,j+1/2}}{\Delta z_j*ADZ}\right)C_{i,j+1}^{n+1/2}$$

$$=-\left(\frac{D_{i,j}}{r*ADR}+\frac{u_{i-1/2,j}}{ADR}+\frac{2*D_{i-1/2,j}}{\Delta r_{i-1}*ADR}\right)C_{i-1,j}^{n}$$

$$-\left(-\frac{1}{r}u_{i,j}-\frac{u_{i+1/2,j}}{ADR}+\frac{u_{i-1/2}}{ADR}-\frac{2*D_{i+1/2}}{\Delta r_i*ADR}-\frac{2*D_{i-1/2}}{\Delta r_{i-1}*ADR}-\frac{\phi}{\Delta t}\right)C_{i,j}^{n}$$

$$-\left(-\frac{D_{i,j}}{r*ADR}-\frac{u_{i+1/2}}{ADR}+\frac{2*D_{i+1/2}}{\Delta r_i*ADR}\right)C_{i+1,j}^{n} \quad \text{.....} \quad (5.18)$$

in the r-direction:

$$\left(\frac{D_{i,j}}{r*ADR}+\frac{u_{i-1/2,j}}{ADR}+\frac{2*D_{i-1/2,j}}{\Delta r_{i-1}*ADR}\right)C_{i-1,j}^{n+1}$$

$$+\left(-\frac{1}{r}u_{i,j}-\frac{u_{i+1/2,j}}{ADR}+\frac{u_{i-1/2}}{ADR}-\frac{2*D_{i+1/2}}{\Delta r_i*ADR}-\frac{2*D_{i-1/2}}{\Delta r_{i-1}*ADR}-\frac{\phi}{\Delta t}\right)C_{i,j}^{n+1}$$

$$+\left(-\frac{D_{i,j}}{r*ADR}-\frac{u_{i+1/2}}{ADR}+\frac{2*D_{i+1/2}}{\Delta r_i*ADR}\right)C_{i+1,j}^{n+1}$$

$$=-\left(\frac{v_{i,j-1/2}}{ADZ}+\frac{2*D_{i,j-1/2}}{\Delta z_{j-1}*ADZ}\right)C_{i,j-1}^{n+1/2}$$

$$+\left(-\frac{v_{i,j+1/2}}{ADZ}+\frac{v_{i,j-1/2}}{ADZ}-\frac{2*D_{i,j+1/2}}{\Delta z_j*ADZ}-\frac{2*D_{i,j-1/2}}{\Delta z_{j-1}*ADZ}-\frac{\phi}{\Delta t}\right)C_{i,j}^{n+1/2}$$

$$+\left(-\frac{v_{i,j+1/2}}{ADZ}+\frac{2*D_{i,j+1/2}}{\Delta z_j*ADZ}\right)C_{i,j+1}^{n+1/2} \quad \text{.....} \quad (5.19)$$

5.3.2 Boundary Conditions

Finite difference implementation of boundary conditions is discussed in this section. The boundary conditions are given for one gas to avoid repetition of the same equation. The equations are similar for all the gas components unless otherwise stated. Let the number of grid points in the flow domain be M and N, in the directions r and z, respectively. Because left, right and bottom boundaries have Newmann and mixed boundary conditions, additional imaginary grid points are required. Therefore, the final number of grid points will be (M+2) x (N+1). Let the number of grid points inside the chamber be M1. The boundary conditions are shown in the Figure 5.3. The following boundary conditions are the same for both the gases, CO_2 and air, except at the bottom boundary.

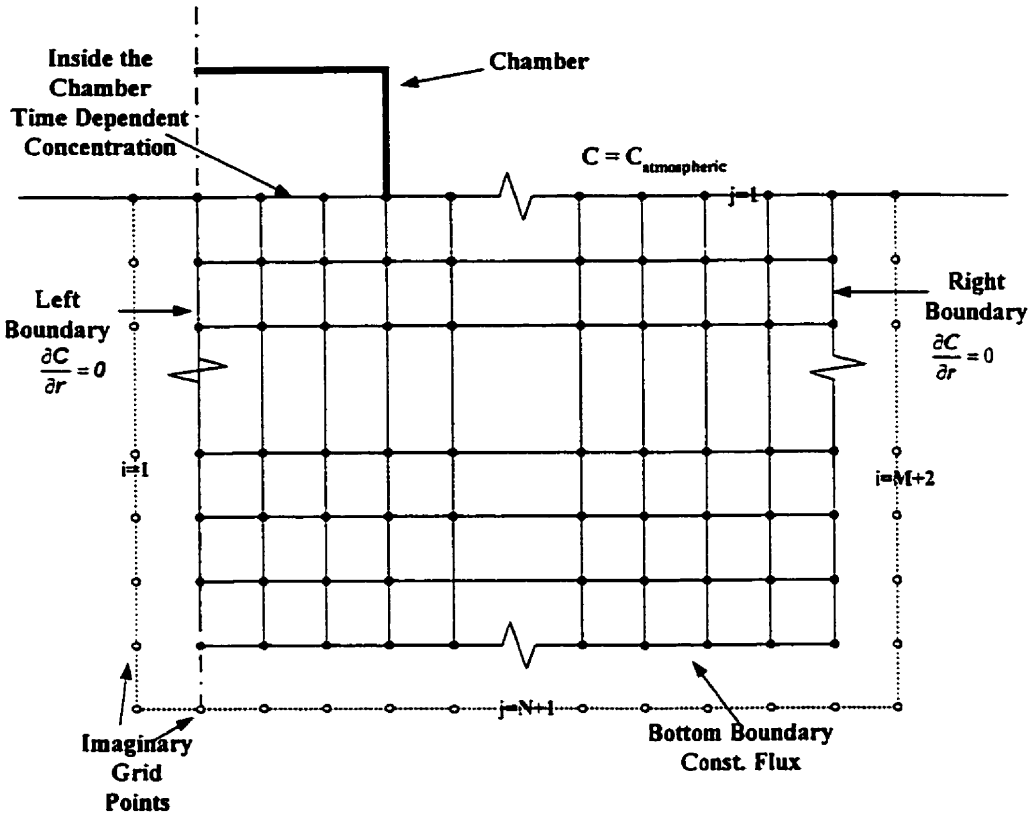

Figure 5.3: Boundary conditions for the model

5.3.2.1 Top Boundary

Outside the Chamber

$C_{i,1} = C_{atm}$ at any time

where, i = M1+1, M+2

This boundary condition will be common for both transient and steady state cases.

Inside the Chamber

Inside the chamber, gas concentrations are transient as gases accumulate with time. Therefore, this boundary condition is a time dependent one. This is calculated by

considering advective and diffusive flow into the chamber until a particular time. The flow is considered quasi-steady for this calculation.

$$C_{k,z=0,t=t} = C_{k,atm} + \frac{\iint q_k . dA . dt}{\pi R^2 H} \quad \text{..... (5.20)}$$

where,

q_i = Gas flux for component k ($mol.m^{-2}s^{-1}$)

R = Radius of the chamber (m)

H = Height of the chamber (m)

Finite difference form of this can be written as:

$$C_{i,1}^{n+1} = C_{i,1}^{n} + \sum \left\{ \left(D \frac{C_{i,2}^{n} - C_{i,1}^{n}}{\Delta z_1} + v_{1,1/2} C_{i,1}^{n+1} \right) * 2\pi r_i * \Delta t * \frac{ADR}{2} \right\} \Big/ \pi R^2 H \quad \text{..... (5.21)}$$

where, i = 2, M1

5.3.2.2 Left Boundary

Central axis of the chamber is characterized by the left boundary of the domain. Due to the symmetry, concentration gradient at this point should be zero.

$$\left[\frac{\partial C}{\partial r} \right]_{r=0} = 0 \quad \text{..... (5.22)}$$

$\therefore C_{1,j} = C_{3,j}$ at any time

where j = 1, N+1

5.3.2.3 Right Boundary

Right boundary is selected in such a manner there is no perturbation due to the chamber at that point. Then this boundary also could be defined as a zero concentration gradient.

$$\left[\frac{\partial C}{\partial r}\right]_{r=L} = 0 \quad \text{.....} \quad (5.23)$$

where L - distance to the right boundary from the chamber centre (m)

$\therefore C_{M+1,j} = C_{M,j}$ at any time

where j = 1, N+1

5.3.2.4 Bottom Boundary

The bottom of the soil cover is in contact with the waste layer. Therefore, this boundary condition should characterize the gas generation of the waste layer. To incorporate this fact the bottom boundary condition is given as a gas flux. The advective and diffusive flux at the bottom is set for constant values. In a landfill setting, fluxes for CH_4 and CO_2 are specified and fluxes for O_2 and N_2 are set for zero.

$$v_N C_N^{n+1} - D_N \frac{\partial C}{\partial z} = Q_{Bottom}$$

$$C_{N+1}^{n+1} = -\frac{Q_{Bottom}(\Delta z_N + \Delta z_{N-1})}{D_N} + C_{N-1}^{n+1} + \frac{v_N(\Delta z_N + \Delta z_{N-1})}{D_N} C_N^{n+1} \quad \text{.....} \quad (5.24)$$

Here, Q_{Bottom} is the gas flux rate at the bottom boundary. It will be a negative value ($mol.m^{-2}.s^{-1}$) for CO_2 and 0.0 for air component.

5.3.3 Initial Conditions

As this is a transient case, initial conditions are required. Initial condition is the concentrations at the steady state. Therefore, these concentrations are derived from steady state modeling. Assuming there is no spatial heterogeneity, the steady state is modeled as a one-dimensional situation. The top and the bottom boundaries are similar to the three-dimensional case outside the chamber. The governing equation for steady state is derived from Equation 5.4. It is the one-dimensional gas migration equation in z direction.

Removing the terms in radial direction,

$$0 = -\frac{\partial}{\partial z}\left(v_z C_i - D\frac{\partial C_i}{\partial z}\right) + S \qquad (5.25)$$

Similar equations could be written for all four gases and solved.

Finite difference equations for steady state could be derived from Equation 5.19. Here, the solution is derived from a transient 1-D model when there is a negligible difference between concentrations in two consecutive time steps. For higher accuracy Crank-Nicholson scheme was used in the steady state solution.

The steady state equation is as follows:

$$\left(\frac{v_{j-1/2}}{2*ADZ}+\frac{D_{j-1/2}}{\Delta z_{j-1}*ADZ}\right)C_{j-1}^{n+1}+\left(-\frac{v_{j+1/2}}{2*ADZ}+\frac{v_{j-1/2}}{2*ADZ}-\frac{D_{j+1/2}}{\Delta z_j*ADZ}-\frac{D_{j-1/2}}{\Delta z_{j-1}*ADZ}-\frac{\phi}{\Delta t}\right)C_j^{n+1}$$

$$+\left(-\frac{v_{j+1/2}}{2*ADZ}+\frac{D_{j+1/2}}{\Delta z_j*ADZ}\right)C_{j+1}^{n+1}=-\left(\frac{v_{j-1/2}}{2*ADZ}+\frac{D_{j-1/2}}{\Delta z_{j-1}*ADZ}\right)C_{j-1}^{n}$$

$$-\left(-\frac{v_{j+1/2}}{2*ADZ}+\frac{v_{j-1/2}}{2*ADZ}-\frac{D_{j+1/2}}{\Delta z_j*ADZ}-\frac{D_{j-1/2}}{\Delta z_{j-1}*ADZ}+\frac{\phi}{\Delta t}\right)C_j^{n}$$

$$-\left(-\frac{v_{j+1/2}}{2*ADZ}+\frac{D_{j+1/2}}{\Delta z_j*ADZ}\right)C_{j+1}^{n} \qquad (5.26)$$

CHAPTER SIX
MODEL DEVELOPMENT

6.1 Conceptual Model

One of the first steps in developing a model to simulate gas migration in a landfill is to define the boundaries in such a manner that all the perturbations in the environment due to the processes involved are adequately considered. The major difficulty in this regard is the heterogeneity of various parameters involved. Although physical processes are well established, biological reactions are yet to be satisfactorily understood and modeled. Waste is heterogeneous, which makes its modeling very complex. Some researchers (Findikakis and Leckie, 1979; El-Fadel et al, 1996) have modeled the whole landfill, including the waste layer as well as the cover system. However, for simplicity, the model presented here considers only the soil cover. Avoiding the waste layer for modeling is advantageous for two reasons. First, it helps to avoid modeling highly heterogeneous waste layer. Second, it prevents considering the very complex gas generation process in the model. Due to many parameters involved in gas generation, there is no acceptable equation to represent this phenomenon. As the permeability of the cover is a few orders of magnitude lower than that of the waste layer below, it is realistic to assume that gas accumulates below the cover and enters it uniformly. Hence, it is possible to represent the gas generation with a constant gas flux at the bottom of the cover. On the other hand, as the time involved does not exceed 30 minutes the perturbations occurring in the waste due to the application of a flux chamber is minimal. This further justifies not considering the waste layer. The lateral boundaries of the model should be considered at a sufficient distance to capture all the perturbations in the vicinity of the chamber.

6.2 Finite Difference Approach

The partial differential equations governing the gas transport through landfill covers are continuous in space and time. In the finite difference approach, instead of trying to find a continuous and sufficiently smooth function which satisfies the governing equation, approximate values of the solution are sought on a finite set of discrete points (Ames, 1992). The partial differential equations are replaced by a set of algebraic equations related to the values of the variable (i.e. concentrations in this situation) for all points. These equations are called finite difference equations and the differential equations are then reduced to an algebraic problem.

Finite difference method was utilized in this model to discretize the flow domain and solve for concentrations. As the flow domain is of a regular shape, finite difference method was suitable for this purpose. Finite difference method uses two different approaches for grid construction. They are block centered and mesh centered grid systems (Anderson and Woessner, 1992). In the block-centered method, grid blocks are defined first and points are assigned at the centers of the blocks. Therefore, points do not fall on the boundaries. The mesh centered method distributes points in the domain and then defines blocks by centering these points. In this method, grid points are placed along the boundaries too. This model uses mesh centered grid system. Therefore, boundary conditions could be defined more realistically.

As the flux chamber is cylindrical, the effect on the gas migration is assumed to be axisymmetric. In other words, variables change in the same way radially in the horizontal plane. By considering axisymmetric case, the three-dimensional effects could be simulated. Therefore, the domain is discretized only in vertical and radial direction. Variable size grid system is preferred to represent the physics properly and for efficiency of the solution. It is desirable to have finer grids where there are large variations or large gradients occur. In the

radial direction, smaller grids were used closer to the chamber wall as there is a significant difference in concentrations at the two sides of the wall. The top layer of the domain is represented better using a thin layer. However, very small time steps determined by stability constraints prevented using smaller grids, and therefore variable grids were not used. Both the vertical and radial directions were discretized with 2 cm grids.

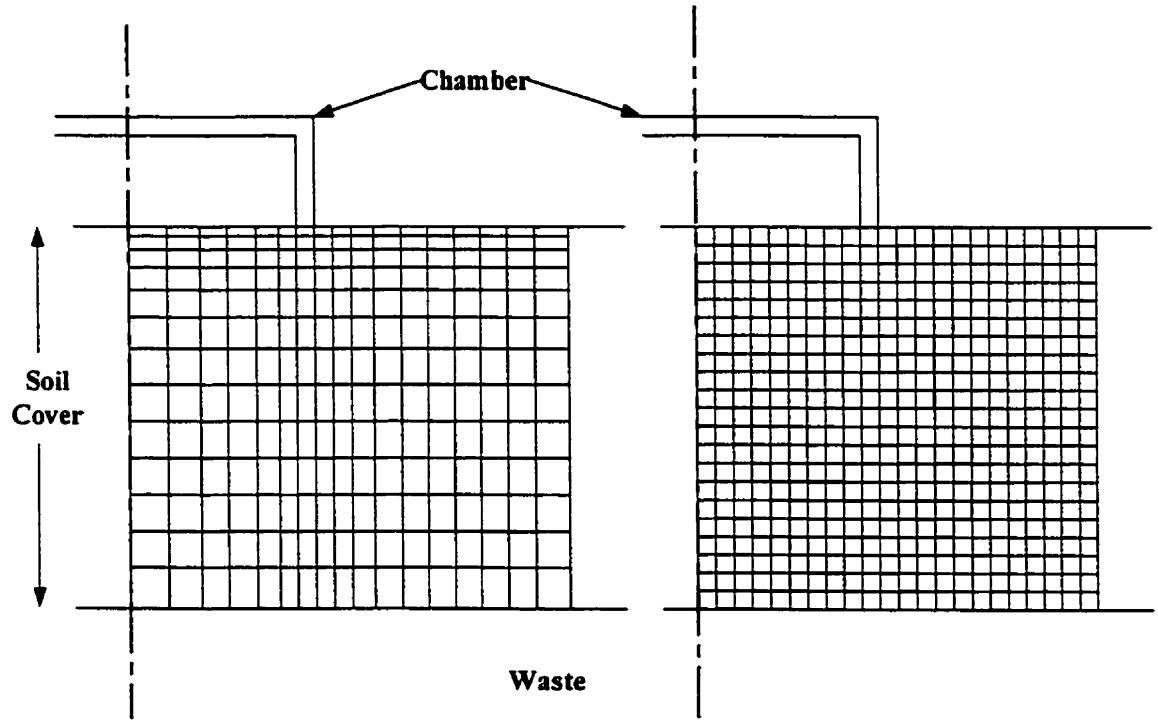

Figure 6.1: Variable and equal size grid system

6.3 Solution Scheme

The finite difference equations were derived in Chapter 5. The complete equations are essentially non-linear and coupled. These equations can be solved only by non-linear methods such as Newton-Raphson method (Chapra and Canale, 1998). However, they are locally convergent, and therefore a good estimation of the solution is required as the initial input. For simplification, the equations were linearized taking pressures explicitly. All the

other parameters that depend on gas concentrations (e.g. permeability, dispersion coefficient etc.) were also determined explicitly. This approach was advantageous because the finite difference equations become de-coupled. A separate set of equations was generated for each gas component in the system. Therefore, equations for each gas component could be solved independently.

However, finite difference equations for each gas depend on coordinates z and r, and time t. Resulting coefficient matrix is a penta-diagonal one, which unfortunately involves a great amount of floating point operations for the solution. Therefore, these equations were further reduced by considering the Alternating Direction Implicit (ADI) technique.

6.3.1 ADI method

Two-dimensional problems could be solved by introducing ADI methods that are two-step methods involving the solution of tri-diagonal sets of equations along each direction (ie. z and r directions in this case) at the first and second steps (Mitchell and Griffiths, 1980). These steps could be represented as follows:

$$f_1\left(C_{i,j-1}^{n+1/2}, C_{i,j}^{n+1/2}, C_{i,j+1}^{n+1/2}\right) = g_1\left(C_{i-1,j}^{n}, C_{i,j}^{n}, C_{i+1,j}^{n}\right)$$

$$f_2\left(C_{i-1,j}^{n+1}, C_{i,j}^{n+1}, C_{i+1,j}^{n+1}\right) = g_2\left(C_{i,j-1}^{n+1/2}, C_{i,j}^{n+1/2}, C_{i,j+1}^{n+1/2}\right) \quad \text{.....} \quad (6.1)$$

This scheme is represented graphically in Figure 6.1 (From Huyakorn and Pinder, 1983). The known values are given as hollow dots and the values from the next time step are given as solid dots. During each row or column calculation, a tri-diagonal matrix is generated. This tri-diagonal scheme could be solved efficiently by using the Thomas algorithm which is discussed below.

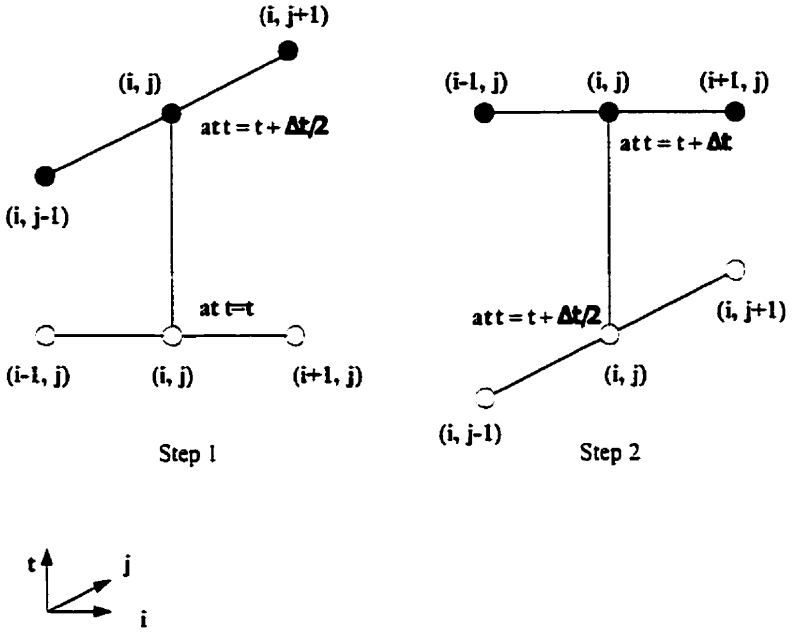

Figure 6.2: Representation of ADI method

6.3.2 Thomas Algorithm

Thomas algorithm is particularly efficient for a system of linear equations with non-zero elements only along three diagonals. This method is similar to LU factorization, which consists of three steps.

1. Decomposition
2. Forward substitution
3. Back substitution

This technique requires only five multiplications and three subtractions per grid point (Huyakorn and Pinder, 1983). Therefore, it is very efficient.

6.4 Computer Code

Once the finite difference equations were derived, a computer code was developed to solve them. Two separate codes were developed to solve steady state and transient case. The steady state case also solved using transient equations until the concentrations at consecutive time steps are differ only by a very small tolerance. The flow charts for both the computer codes are given in Figures 6.3 and 6.4. The language used was Fortran 90. A subroutine called DGTSV from LAPACK (SIAM, 1999) was modified for solving the tri diagonal matrices.

All the real variables were assigned double precision. The convergence criterion for steady state was set as a maximum tolerance of $1x10^{-12}$ for concentrations at every grid point.

The computer codes are given in the appendices.

6.5 Numerical Considerations

When numerical techniques are used to solve continuous differential equations, various approximations introduce errors and other numerical problems. Minimization of effects of these factors is very important for accuracy and the efficiency of the solution. Some of them are discussed below.

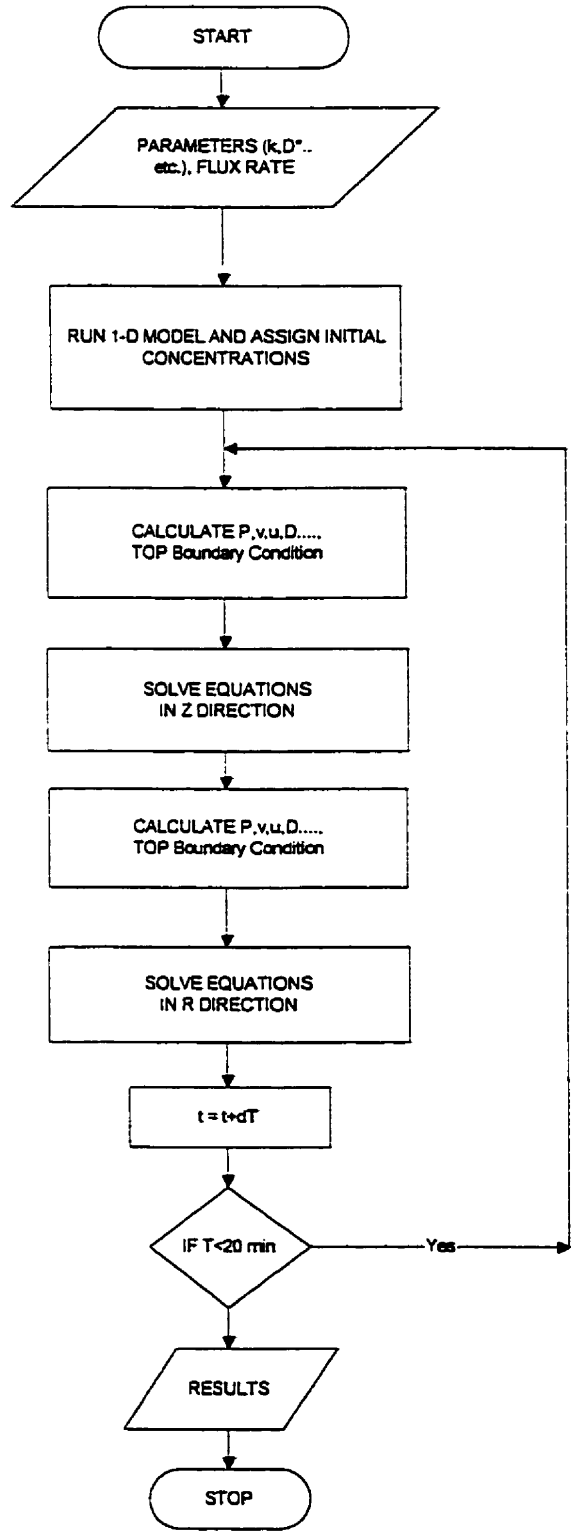

Figure 6.3: Flow-chart for transient case

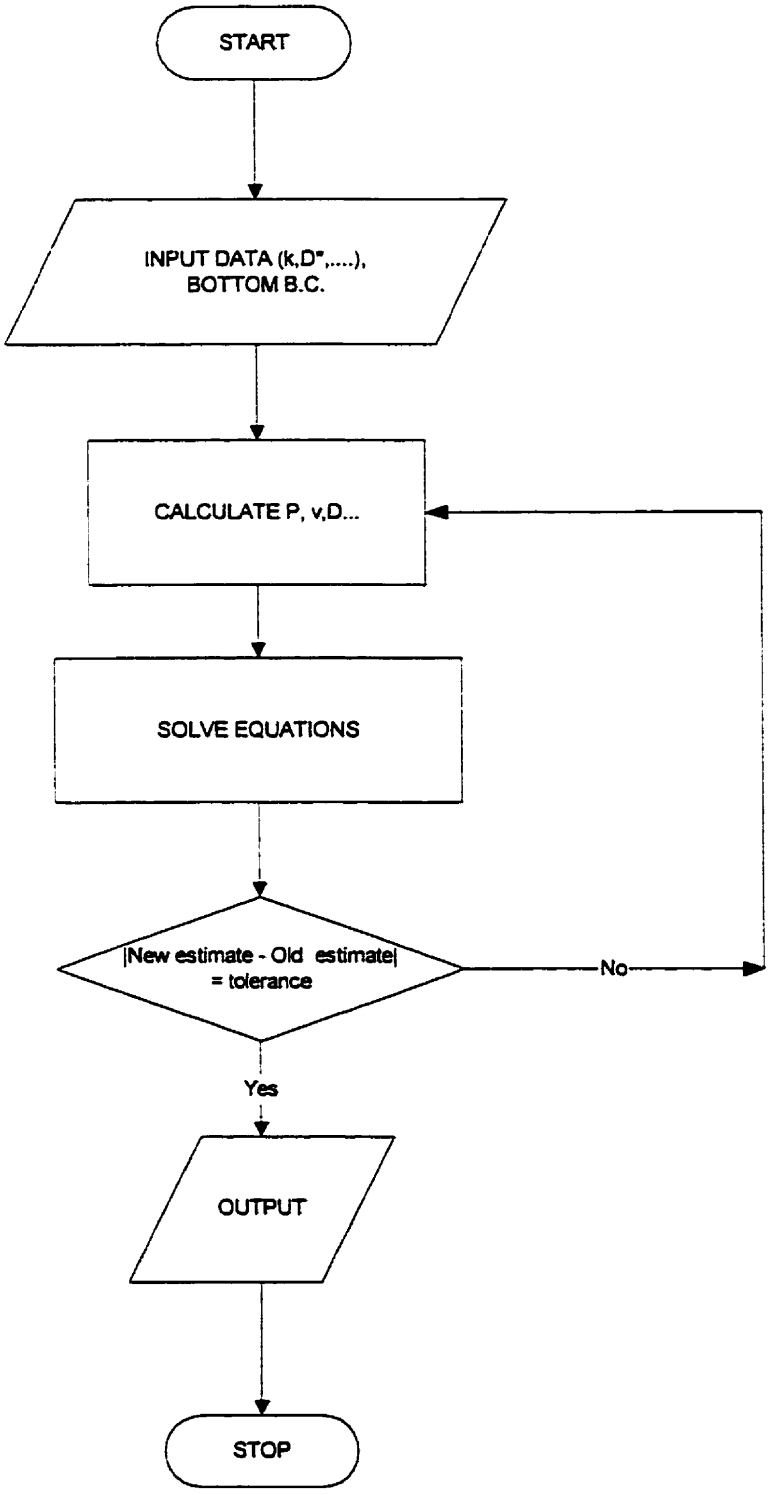

Figure 6.4: Flow-chart for steady state case

6.5.1 Accuracy

Accuracy of the solution depends on many factors. Deriving correct equations, proper discretization of time and space, and the accuracy of the solvers are of prime importance to ensure that the results are accurate. In addition, accurate estimations of the parameters are also required for accuracy.

Correct representation of the physics involved, by the governing equations, is crucial for accurate results. Both advection and dispersion processes were considered in deriving the equations. The time step was very small because it was even less than one millionth of the total prediction time. Therefore, it could be assumed that all the temporal variations were captured by the model. The Courant number for any time step was less than 10^{-5}.

6.5.2 Stability

Numerical stability is an important issue in modeling. Stability is ensured if the errors at any stage of the computations are not amplified but attenuated as the computation progresses (Smith, 1985). Presence of round-off errors or any other computational errors may lead to numerical instability. Stability requires small time steps resulting in increased model run time. It varies depending on the finite difference scheme. The fully implicit and Crank-Nicholson schemes are always stable. The fully explicit case is conditionally stable. Depending on the problem, stability requires very small time steps for fully explicit schemes.

Due to the complexity involved, it is difficult to derive the stability constraints analytically. Stability criterion can be derived using Fourier stability method and matrix stability method (Ames, 1992).

Although concentrations were considered implicitly in this model, velocities and other parameters were taken explicitly. Therefore, the model has some stability issues. The most critical parameter contributed for instability was found to be the gas intrinsic permeability value. Calibration process required high permeability value in the range 10^{-10} m^2. Therefore, time step for the model was taken as 10^{-4} s.

6.5.3 Numerical Dispersion

A term similar to dispersive flux could be introduced to the finite difference equation when derivatives are approximated by Taylor's series expansion. This term introduces dispersion into the solution that is not a physical phenomenon but completely of numerical origin. This numerical dispersion could originate from approximation of both the spatial and temporal derivatives. Peaceman (1977) presented a general formula for the ratio of the numerical dispersion coefficient to physical dispersion coefficient for one-dimensional advective-dispersive flow as follows:

$$\frac{D_{numerical}}{D_{physical}} = Pe\left[\left(\frac{1}{2}-\alpha\right)+Cr\left(\omega-\frac{1}{2}\right)\right] \quad \text{.....} \quad (6.2)$$

where, α and ω are the spatial and temporal weighting factors respectively. This expression shows that both the Courant number (Cr) and the Peclet number (Pe) affect numerical dispersion, but effect of Pe is more significant. Crank-Nicholson approximation with centered weighting in space diminishes the numerical dispersion.

Numerical dispersion is an issue when solving transport equations. This occurs due to truncation errors in the derivatives. Both finite difference and finite element schemes generate numerical dispersion. However, by reducing space and time discretization, it is possible to reduce this effect.

In one-dimensional case, Peclet No. (Pe) is defined as;

$$Pe = \frac{v.\Delta z}{D} \qquad \text{.....(6.3)}$$

The accepted criterion is to keep Pe below 1.0 to minimize the numerical dispersion. In all the model runs carried out Pe was found to be below 0.1, thereby numerical dispersion was minimized.

6.5.4 Mass Conservation

One advantage of finite difference method is that it ensures mass conservation. Therefore checking conservation of mass, considering flows between cells, provides a means of determining accuracy of the solution. For accuracy, mass conservation was checked for all the grid points in the steady state case. As the bottom of the domain has a constant flux boundary condition, in steady state the same flux should pass through any node. Both CO_2 (specified) and air (which is zero) fluxes at all the grid points were checked for any larger discrepancy. With tolerance value used (10^{-12}) it was found the discrepancy in the flow was less than 0.1 % of the specified value.

CHAPTER SEVEN
MODEL CALIBRATION, VERIFICATION, AND RESULTS

A major portion of this research includes developing a model to simulate gas migration in landfill covers in a flux chamber measurement scenario. Calibration and verification are integral components of the model development. Because of the complexities in the field experiments, laboratory data was used for these purposes.

7.1 Model Calibration

Calibration is a process in which model input parameters are adjusted until model output variables (or dependent variables) match field or experimental observed values to a reasonable degree. Model input parameters include permeabilities, dispersion coefficients, porosity etc. The model output variables for this research are concentrations or pressures at various points at various times.

Model parameters such as gas permeability, molecular diffusion, and dispersivity etc. are difficult to determine accurately. As a result, one can seldom reproduce the field-observed (or experimental) conditions to a satisfactory degree using initially assigned model input parameters. Calibration thus provides a primary means for obtaining optimal values of model input parameters. In this sense, model calibration is synonymous with parameter estimation. Model calibration can be performed either by adjusting the input parameters assigned for a simulation model repeatedly in a manual trial and error manner, or by using a computer code that has been designed specifically for parameter estimation.

Parameter estimation is a non-unique process (Zheng et al., 1995). In other words, a large number of parameter combinations, which may differ significantly, can provide equally reasonable matches between model results and field observations. However, a sensitivity

analysis provides more comprehensive framework for dealing with non-uniqueness problem.

When a model is intended to predict the transient behaviour of a system, calibration of the model against steady state data is not adequate, and calibration against transient data also should be considered.

7.1.1 Calibration for Steady State

Calibration for steady state was achieved by changing all the parameters until there was an acceptable match between the simulated and experimental results. Some of the parameters were determined from the information available from the laboratory experiments. Other parameters were decided ensuring they are within the range reported in literature.

After sending gas through the soil column for several weeks, the soil was almost dry and therefore, the volumetric air content (gas porosity) of the soil was roughly equal to total porosity. Gas porosity was determined using the estimated dry density of the soil at the time it was compacted. Using the following equation (American Society of Agronomy);

$$\phi_t = 1 - \frac{\rho_d}{\rho_s} \qquad \text{.....} \qquad (7.1)$$

where,

ϕ_t = Total porosity

ρ_d = Dry density of the soil (kg/m^3)

ρ_s = Density of particles (kg/m^3)

Assuming a density of 2650 kg/m^3 for solid particles of soil, and using the measured dry density of 1634 kg/m^3, the total porosity can be calculated as 0.383. Therefore, gas porosity is assumed as 0.35. (volumetric water content = 3-4%)

Most of the gas diffusion coefficient values given in the literature are for gas diffusion in air (Reid et al., 1987). Values for gas diffusion coefficient in porous media are rare. Therefore, the coefficient of molecular diffusion was determined from measured values in air. The diffusion coefficients in porous media differ from values in air because of the effects of porosity and tortuosity. This factor was taken into consideration by using an empirical equation proposed by Millington and Quirk (1961). Their equation is given as follows:

$$D_{soil} = D_{air} \frac{\phi_a^{10/3}}{\phi_t^2} \qquad \text{.....} \qquad (7.2)$$

where,

D_{soil} = Diffusion coefficient in soil (m^2s^{-1})

D_{air} = Diffusion coefficient in air (m^2s^{-1})

ϕ_a, ϕ_t = Air porosity and total porosity, respectively

Using binary diffusion coefficient of CO_2 in air as 1.8×10^{-5} m^2s^{-1} (Reid et al., 1987), the soil gas diffusion coefficient was determined to be 4.6×10^{-6} m^2s^{-1}.

When parameter values were changed for calibration process, sensitivity of the parameters to the results was also considered. When the uncertainty of a parameter was low, an attempt was made to keep it unchanged. That was the case with the gas porosity and the coefficient of molecular diffusion. Other parameters were varied within the ranges reported in literature until the simulated concentrations match the experimental values.

Laboratory results showed a higher dispersion of air into the system. The molecular diffusion was too small to account for this dispersion. However, when the gas velocities are

comparatively large, in the range of $1 m.day^{-1}$, mechanical dispersion becomes important. Therefore, the dispersivity value was changed until the simulated results match the experimental CO_2 concentration values. The value for calibrated dispersivity was found to be 0.5 m which lies on the higher side of the dispersivity range reported in literature. According to Mendoza and Frind (1990) dispersivity values range from 0.01 to 1.0m. Lateral (horizontal) dispersivity was assumed to be 0.05 m.

Gas permeability did not affect concentration profile significantly. However, it affected the flux rates due to advection and gas pressure within the soil. Very low pressures (5 –10 Pa) were monitored at the bottom of the soil cell. This shows that the soil has a high intrinsic permeability. The intrinsic permeability for calibration was decided to be 10^{-10} m^2. This is equivalent to a gas permeability of $2x10^{-4}$ ms^{-1}. This value is acceptable for sandy loam soil (Zheng and Bennett, 1995). Horizontal permeability was assumed to be five times that of vertical value (Mendoza and Frind, 1990). The values used for calibration are given in the Table 7.1 Experimental and simulated concentration profiles are given in the Figure 7.1. Results from one-dimensional model with a CO_2 flow rate of 199 $gm^{-2}d^{-1}$ were used for the calibration.

Table 7.1: Parameters used to calibrate the model

Parameter	Value
Intrinsic Permeability - vertical	1×10^{-10} m^2
Intrinsic Permeability – horizontal	5×10^{-10} m^2
Molecular Diffusion Coefficient	5.46×10^{-5} m^2s^{-1}
Dispersivity – vertical	0.5 m
Dispersivity – horizontal	0.05 m
Volumetric Air Content	0.35

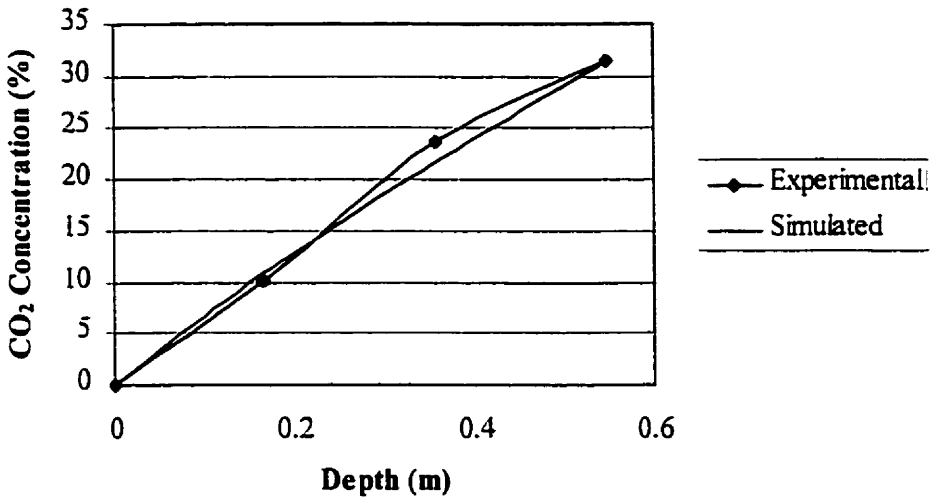

Figure 7.1: Steady state CO_2 concentration profiles from experimental and model results

7.1.2 Calibration for Transient State

Calibration for transient state is also done using different parameter values. However, all the parameters used for calibration in both the states should be the same. Therefore, a trial and error method used to determine these parameter values. The final set of parameters presented in Table 7.1 provided a somewhat satisfactory result. For transient state calibration, medium size flux chamber with a 199 $gm^{-2}day^{-1}$ CO_2 flow was selected. The graphs for simulated and experimental results are given in Figure 7.2. However, The model cannot simulate the latter part of the experimental curve accurately. Therefore, if the model is used to correct the flux chamber measurement, it is required to consider measurements within first 10 minutes.

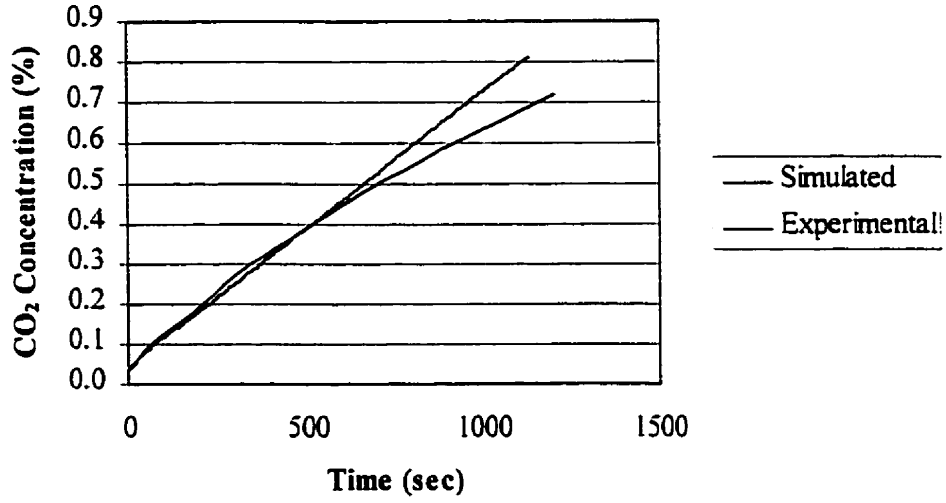

Figure 7.2: CO_2 concentrations over time in the medium size flux chamber

7.2 Sensitivity Analysis

The purpose of a sensitivity analysis is to quantify the uncertainty in the calibrated model caused by uncertainties in the estimation of aquifer parameters and boundary conditions (Anderson and Woessner, 1992). A sensitivity analysis is an essential step in all modeling applications.

During a sensitivity analysis, calibrated values of all the parameters (eg. permeability, dispersion coefficients, porosity etc.) and boundary conditions are systematically changed within a previously established plausible range. The magnitude of change in concentration or pressure (or head in a flow model) from the calibrated solution is a measure of the sensitivity of the solution to that particular parameter. Sensitivity analysis is typically performed by changing one parameter value at a time.

Sensitivity analysis in the model is carried out using 1-D steady state solution. As the transient model takes a long time to run this was the preferred option. Gas concentration profiles with changed parameter values were compared with the calibrated model results.

7.2.1 Sensitivity Analysis on Grid Size

Sensitivity of steady state gas concentrations on grid size of the model was found to be small. The results of the analysis considering grid sizes of 1 cm, 2 cm, and 6 cm are given in the Figure 7.5. This less sensitivity has a great advantage of decreasing the number of grids in the model and thereby effectively reducing the model run time. However, as these results have to be imported for 2-D transient model, a larger grid size was not preferred. Since the flux chamber wall has to be simulated in r direction, large grid sizes were not appropriate. The grid size used for the model was 2 cm.

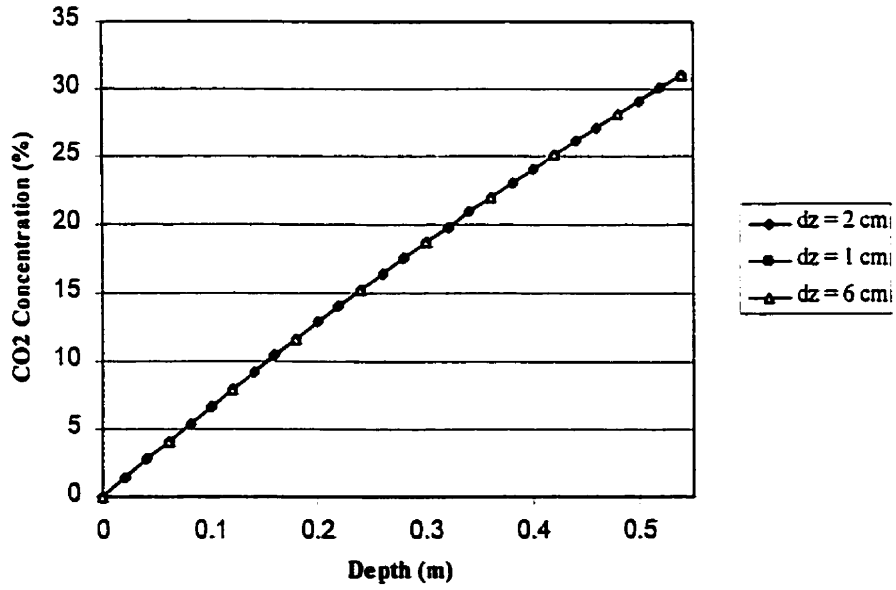

Figure 7.3: Sensitivity on grid size

7.2.2 Sensitivity Analysis on Intrinsic Permeability

Sensitivity on the intrinsic permeability was found to be very small. Intrinsic permeability values of one order of magnitude higher and lower than calibrated value were considered and the resulted concentration profiles were very similar. However, it had an impact on the gas pressure within the system. Therefore, when the target dependent variable was selected as pressure, permeability had a high sensitivity.

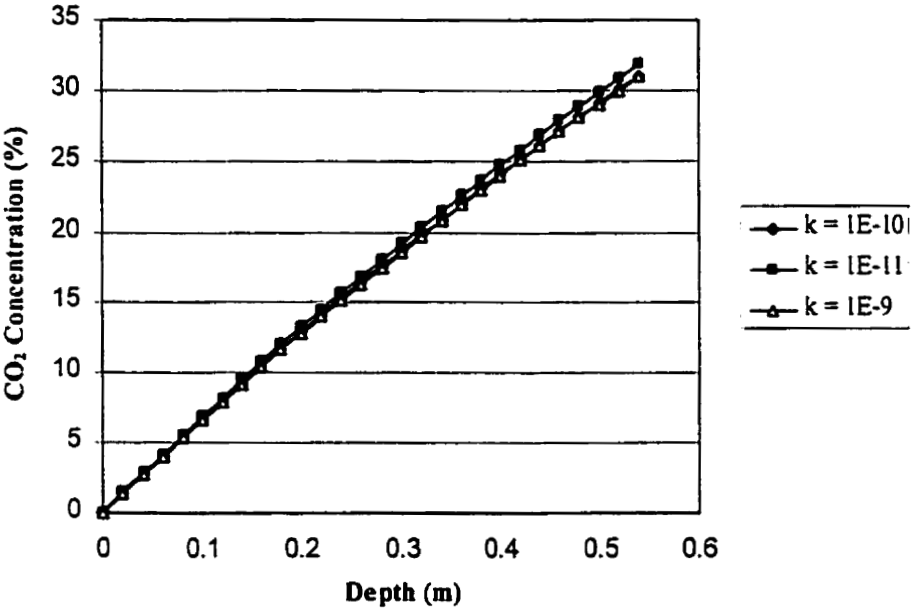

Figure 7.4: Sensitivity on intrinsic permeability

7.2.3 Sensitivity on Molecular Dispersion

Sensitivity of steady state gas concentration profiles on molecular diffusion coefficient (D) was found to be negligible. When a D value of 10 times higher that the calibrated value was used, the model showed some sensitivity. However, that value was even larger than reported D in air.

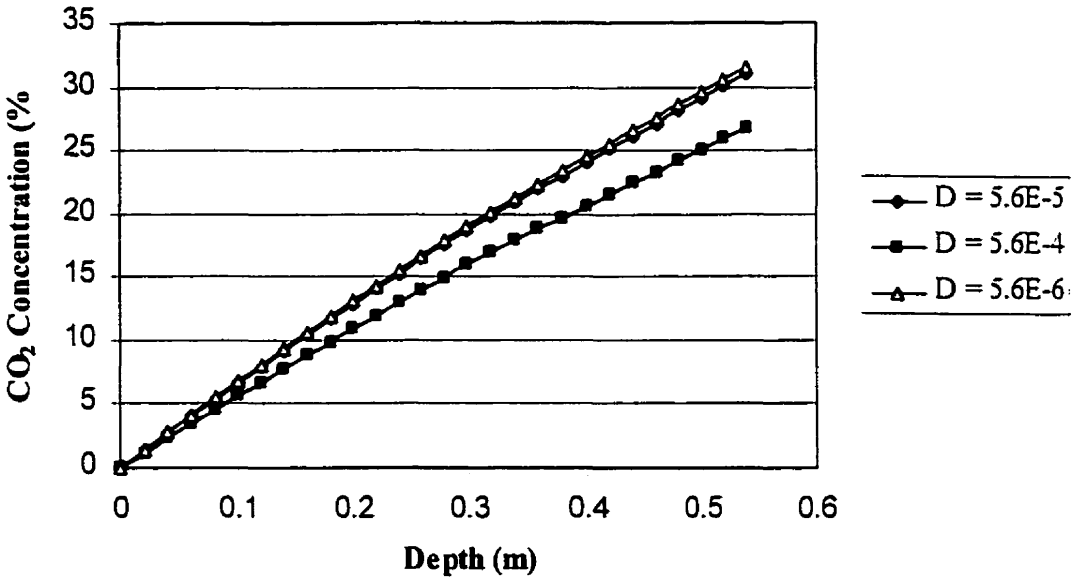

Figure 7.5: Sensitivity on molecular dispersion

7.2.4 Sensitivity on gas porosity

Gas porosity has a considerable impact on steady state gas concentration profile. However, as the porosity for laboratory experiments was determined based on actual dry density of the soil its uncertainty was low. However, under variable moisture content scenarios this is a very critical parameter.

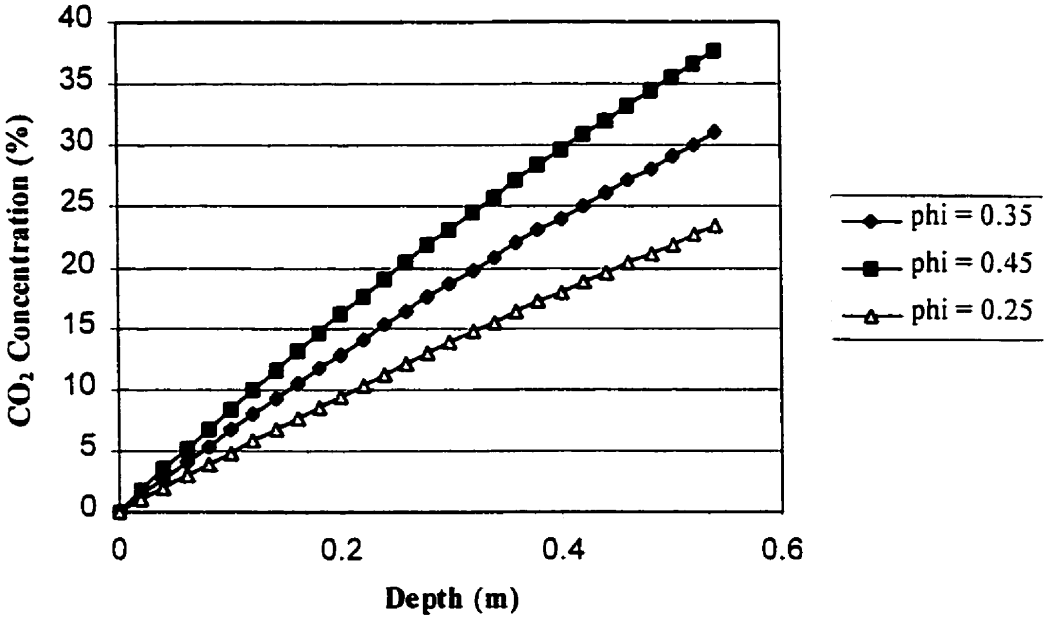

Figure 7.6: Sensitivity on gas porosity

7.2.5 Sensitivity on Dispersivity

Sensitivity on dispersivity was significant. That was because the major portion of the dispersion was due to mechanical dispersion. This is the most critical parameter for calibration.

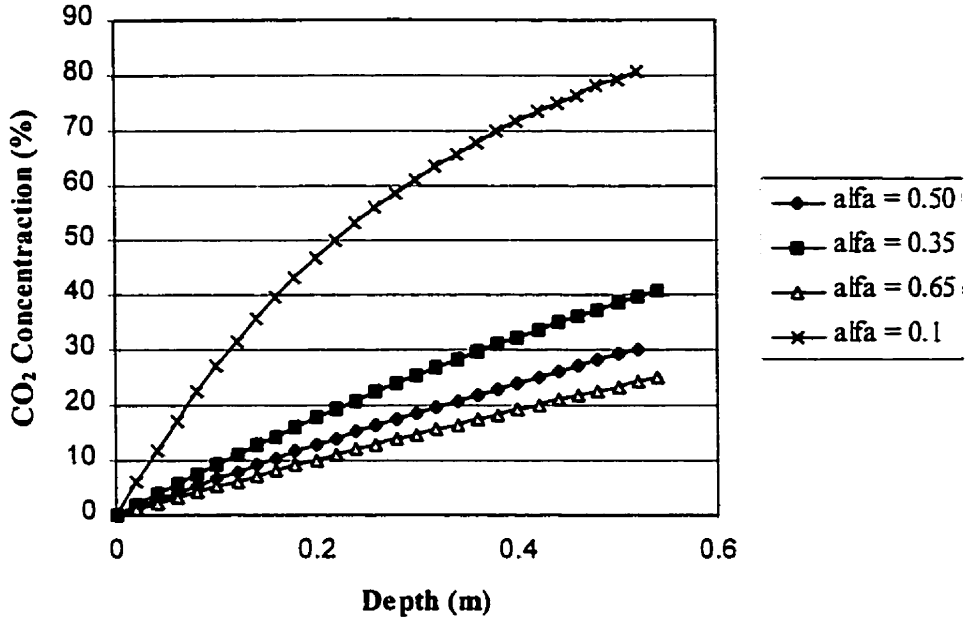

Figure 7.7: Sensitivity on dispersivity

7.3 Model Verification

Model verification is defined as the process in which the calibrated model is shown to be capable of reproducing a set of field observations independent of that used in model calibration (Zheng and Bennett, 1995). Verification of this model was done by considering a different data set using the large chamber. The simulated and experimental results for that scenario are presented in Figure 7.3. According to that graph, The results of the model were in agreement with the experimental data. In addition, a data set obtained using the small chamber was also compared with the model results. The Figure 7.4 presents those results. In this case the model over-estimates the chamber concentration after about 10 minutes. However, this result was also obtained using a grid size of 1 cm. Therefore, it could be

assumed that the accuracy of the model prediction will be high if smaller grids are used. Doing that is restricted by the unacceptably small time steps.

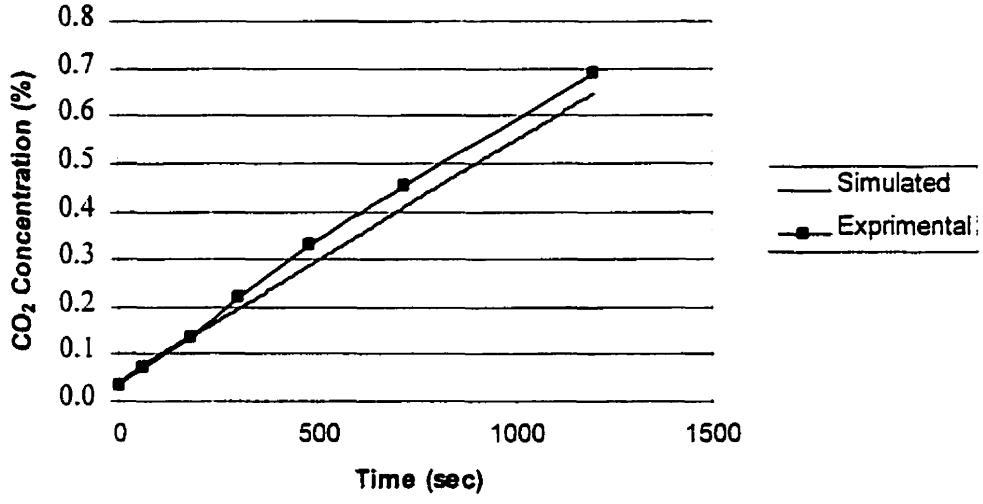

Figure 7.8: CO_2 concentrations over time in the large flux chamber

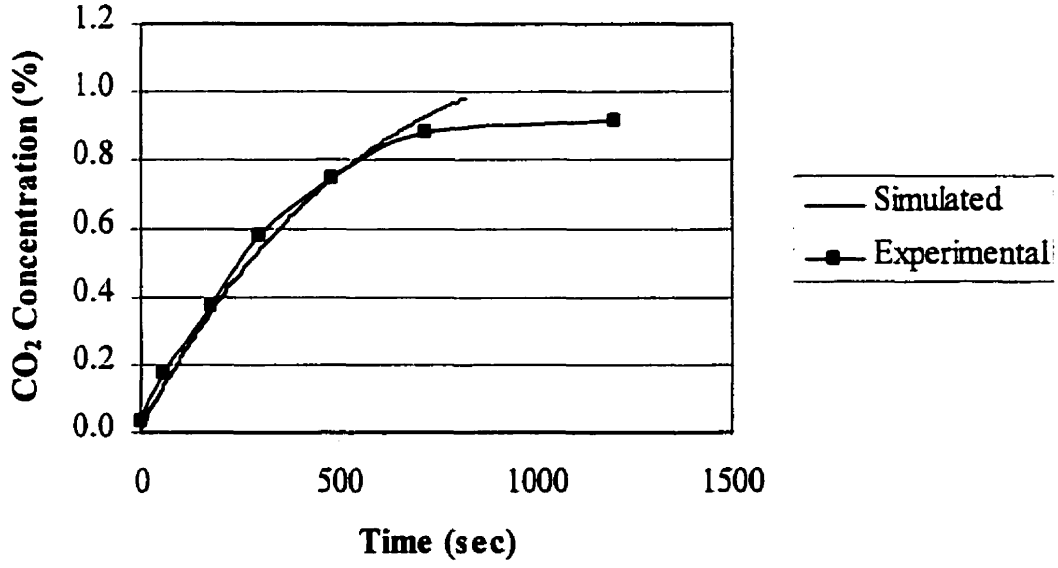

Figure 7.9: CO_2 concentrations over time in the small flux chamber

7.4 Model Results

Both experimental and model results give linear plots for Concentration vs. time curves in case of medium size or large size chambers. Only in the small chamber, this is different. Although those graphs are almost straight lines with coefficients of determination (r^2) closer to unity, they also under-estimate the gas emissions. The reason for this is the reduction of slope of the curve in very early stage of the measurement. If the model results were observed very closely it is possible to notice that the rate of change of concentration inside the chamber decreases very fast. Figures 7.10 and 7.11 demonstrate this observation. These figures are for the experiment with a flux rate of 199 $gm^{-2}day^{-1}$ using the medium size chamber.

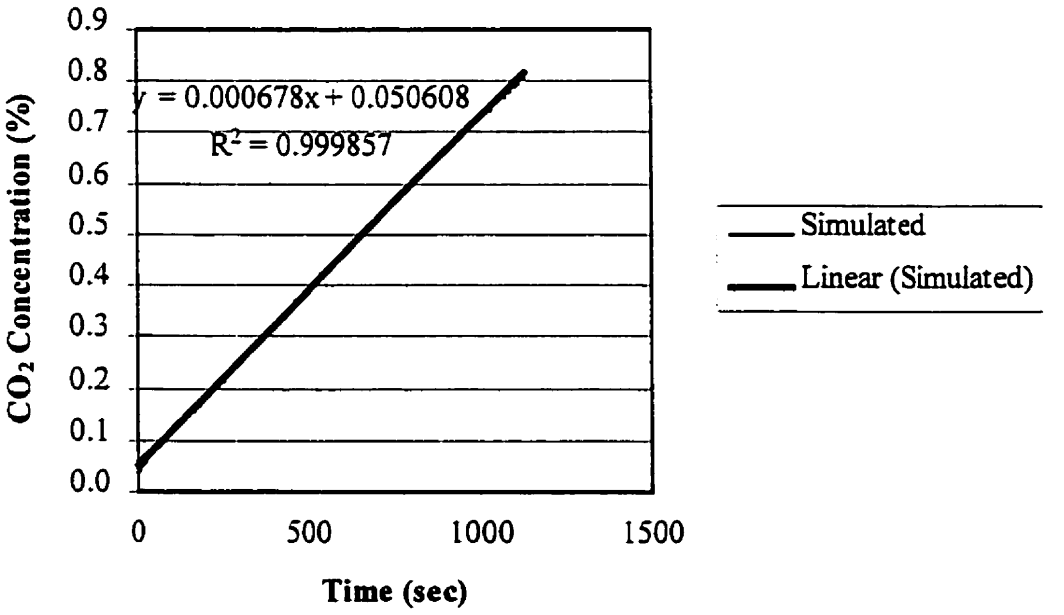

Figure 7.10: Concentration variation for 20 minutes

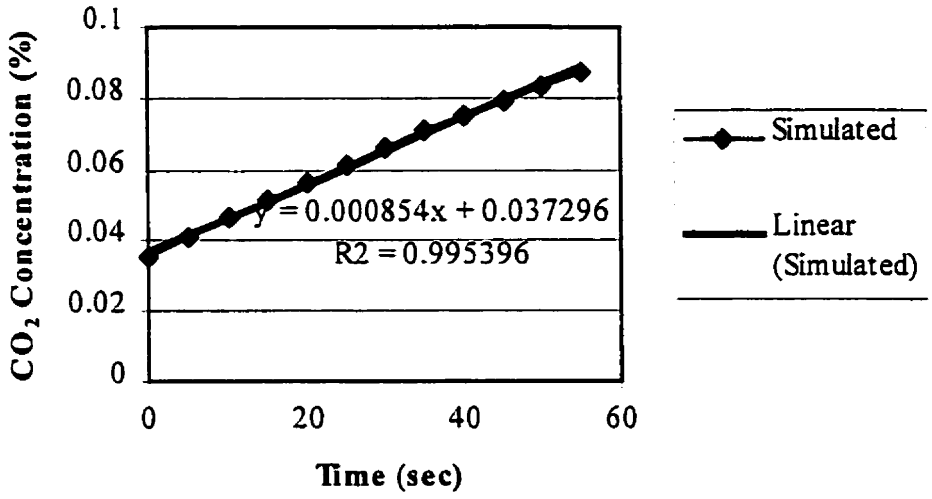

Figure 7.11: Concentration variation for first one minute

Although both the coefficient of determination are satisfactory slope of the curve within first minute is 25% more than the overall slope. This gives an error of 25% for the emission rates. Therefore, under-estimation in closed flux chamber occurs even within first minute. This is not noticed in field measurements unless high frequency gas analyzers are used for measurements. CO_2 concentration contours and velocity vectors also show the same phenomenon.

The Figure 7.12 shows how the CO2 concentration contours change with time during a flux chamber measurement. There is a large variation even within first minute. It shows that concentration gradient has been reduced under the chamber and increased away from the chamber. Figure 7.13 shows the gas velocities within the study area.

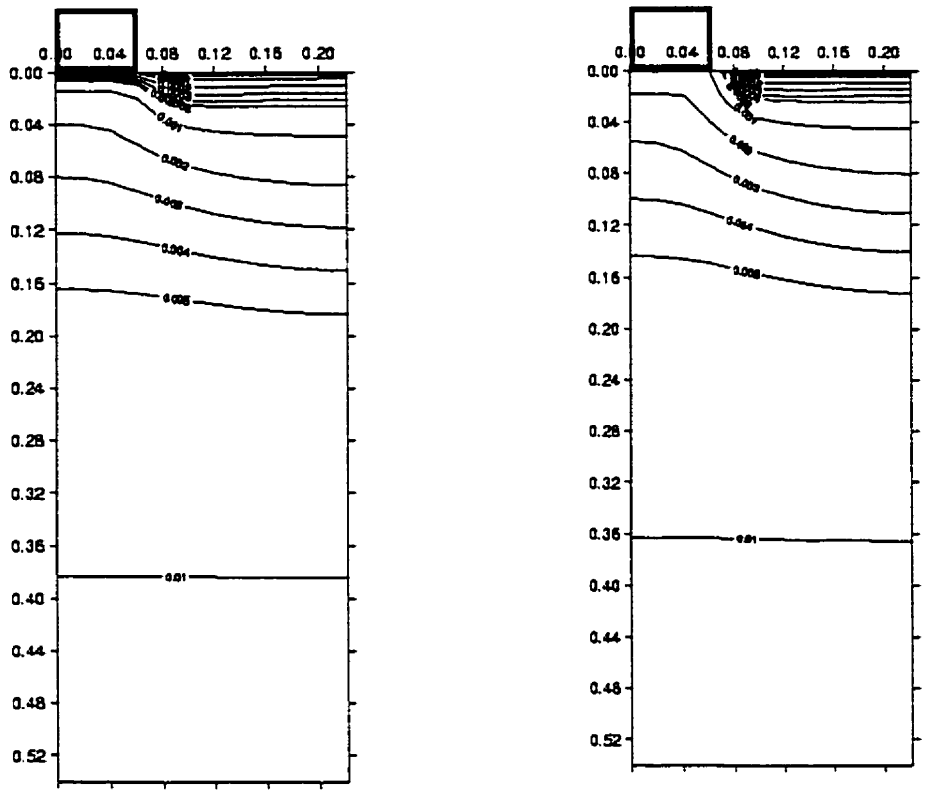

Figure 7.12: CO_2 concentration contours after 1 min. and 20 min. (values are in mol/l)

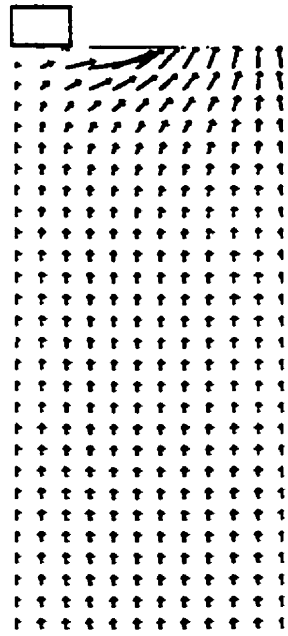

Figure 7.13: Velocity vectors in the soil after 20 minute

CHAPTER EIGHT

CONCLUSIONS AND RECOMMENDATIONS FOR FURTHER RESEARCH

Field estimation of CH_4 emissions from landfills is important to determine the global warming implications of waste landfilling. Furthermore, quantification of CH_4 emissions is required to assess the effectiveness of gas management practices at landfills. Economical and convenient techniques to measure gas emissions are therefore needed. Closed flux chamber method easily qualifies for this task, provided the errors encountered are accounted for.

The following conclusions were drawn from the field and laboratory experiments, and the mathematical model simulations:

- Closed flux chamber technique alters the concentration gradient in the soil and therefore, measured flux rates are lower than the actual emission rates.
- Similar flux rates were obtained by calculating the initial rate of change of concentration within the chamber, by both linear regression and second order polynomial regression.
- Size of the chamber, mainly height of the chamber, and the flow rate determine the magnitude of error involved with flux measurements.
- Lab experiments showed that by selecting a chamber of suitable size (either by laboratory trials or by model simulations), as much as 90% of the flux could be measured.
- The 2-D model is capable of simulating the reduction of gas flow into the chamber over time.
- Initial flow into the chamber is mainly caused by dispersion. But advection takes over quickly as the concentration inside the chamber increases. Ultimately, both advection and dispersion decrease rapidly due to very small concentration gradient.

- Under-estimation of the flux rate occurs even within the first minute after commencement of field measurement.

Recommendations for further Research

Findings of this research suggest several directions for future studies:

- The model should be verified for different types of soils, under different moisture contents etc. More laboratory experiments should be conducted to generate data for model verification.
- The model should be modified to incorporate different soil layers found in landfill cover systems.
- CH_4 oxidation kinetics should be incorporated into the model before it is used in the field to simulate landfill gas emissions. Therefore, more research has to be done to understand and model CH_4 oxidation.

- A calibrated and verified model including all processes, advection, dispersion, and reactions could increase the accuracy of the closed flux chamber measurements. The model could be used to determine the actual gas emission rate using the flux chamber measurement as an input to the model. In addition to gas emission measurement rates, the model could be developed to determine source strength of the landfill and the amount of CH_4 oxidized within the soil cover. This information is very useful for landfill gas utilization projects, as gas generation rates could be determined economically without going for intrusive methods.

REFERENCES

Alzaydi, A.A., C.A. Moore, and I.S. Rai. 1978. Combined Pressure and Diffusional Transition Region Flow of Gases in Porous Media. Journal of American Institute of Chemical Engineers. 24(1): 35-43

American Society of Agronomy. 1982. Methods of Soil Analysis: Part I – Physical and Mineralogical Methods – 2nd Edition. Ed. A.Klute. Soil Science Society of America.

Ames, W.F. 1992. Numerical Methods for Partial Differential Equations. Third Edition. Academic Press Inc., San Diego

Anderson, M.P. and Woessner. 1992. Applied groundwater modeling: simulation of flow and advective transport. Academic Press, SanDiego

Anthony, W.H., G.L. Hutchinson, and G.P. Livingston. 1995. Chamber measurement of soil-atmosphere gas exchange: Linear vs. diffusion-based flux models. Journal of Soil Science Society of America. 59: 1308-1310

Arigala, S.G., T.T. Tsotsis, I.A. Webster, Y.C. Yovstsos, J.J. Kattapuram. 1995. Gas generation, transport and extraction in landfills. Journal of Environmental Engineering. ASCE. 121(1): 33-44

Aziz, K. and A. Settari. 1979. Petroleum Reservoir Simulation. Elsevier Science Publishers, Essex, England. pp. 476

Barlaz, M.A., R.K. Ham, and D.M. Schaefer. 1989. Mass-balance analysis of anaerobically decomposed refuse. Journal of Environmental Engineering, ASCE. 115(6): 1088-1102

Barlaz, M.A., R.K. Ham, and D.M. Schaefer. 1990. Methane production from municipal refuse: A review of enhancement techniques and microbial dynamics. Critical Reviews in Environmental Control. 19(6): 557-584

Barlaz, M.A. 1996. Microbiology of solid waste landfills. In Microbiology of Solid Waste. Eds. A.C. Palmisano and M.A. Barlaz. 31-70

Bear, J. 1972. Dynamics of Fluids in Porous Media. American Elsevier, New York.

Bingemer, H.G. and P.J. Crutzen. 1987. The production of methane from solid wastes. Journal of Geophysical Research. 92(D2): 2181-2187

Bogner, J.E., K.A. Spokas, E.A. Burton, R. Sweeney, and V. Corona. 1995. Landfills as atmospheric methane sources and sinks. Chemosphere. 31(9): 4119-1130

Bogner, J.E., M. Meadows, and P. Czepiel. 1997. Fluxes of methane between landfills and the atmosphere: Natural and engineering controls. Soil Use and Management. 13: 268-277

Bogner, J.E., Meadows, M., and E. Repa. 1998. A new perspective: Measuring and modeling of landfill methane emissions. Waste Age. 1998(June): 118-130

Bogner, J.E., K.A. Spokas, and E.A. Burton. 1999. Temporal variations in Greenhouse gas emissions at a Midlatitude landfill. Journal of Environmental Quality. 28: 278-288

Chan, A.S.K., J.H. Prueger, and T.B. Parkin. 1998. Comparison of closed chamber and Bowen ration methods for determining methane flux from peatland surfaces. Journal of Environmental Quality. 27: 232-239

Chapra, S.C. and R.P. Canale. 1998. Numerical Methods for Engineers, 3rd Edition. McGraw-Hill, New York

Clement, R.J., S.B. Verma, and E.S. Verry. 1995. Relating chamber measurements to eddy correlation measurements of methane flux. Journal of Geophysical Research. 100(D10): 21047-21056

Conen, F. and K.A. Smith. 1998. A re-examination of closed flux chamber methods for the measurement of trace gas emissions from soils to the atmosphere. European Journal of Soil Science. 49: 701-707

Corapcioglu, M.Y. and A.L. Baehr. 1987. A compositional multiphase model for groundwater contamination by petroleum products: 1. Theoretical considerations. Water Resources Research. 23(1): 191-200

Czepiel, P.M., B.Mosher, R.C. Harriss, J.H. Shorter, J.B. McManus, C.E. Kolb, E.Allwine, and B.K. Lamb. 1996a. Landfill methane emissions measured by enclosure and atmospheric tracer methods. Journal of Geophysical Research. 101(D11): 16711-16719

Czepiel, P.M., B. Mosher, P.M. Crill, and R.C. Harriss. 1996b. Quantifying the effect of oxidation on landfill methane emissions. Journal of Geophysical Research. 101(D11): 16721-16729

Dabberdt, W.F., D.H. Lenschow, T.W. Horst, P.R. Zimmerman, S.P. Oncley, and A.C. Delany. 1993. Atmosphere-surface exchange measurements. Science. 260:1472-1481

Denmead, O.T. 1979. Chamber systems for measuring nitrous oxide emission from soils in the field. Journal of Soil Science Society of America. 43: 89-95

Doorn, M. and M. Barlaz. 1995. Estimate of Global Methane emissions from Landfills and Open Dumps. Report EPA-600/R-95-019. U.S. EPA, Washington D.C.

Dubey, S.K., A.K. Kashyap, and J.S. Singh. 1996. Methanotrophic acteria, methanotrophy, and methane oxidation in soil and rhizosphere. Tropical Ecology. 37(2): 167-182

Eklund, B.M., W.D. Balfour, and C.E. Schmidt. 1985. Measurement of fugitive volatile organic emission rates. Environmental Progress. 4(3): 199-202

El-Fadel, M., A.N. Findikakis, and J.O. Leckie. 1989. A numerical model for methane production in managed sanitary landfills. Waste Management and Research. 7: 31-42

El-Fadel, M., A.N. Findikakis, and J.O. Leckie. 1996. Numerical modeling of generation and transport of gas and heat in landfills 1. Model formulation. Waste Management and Research. 14(5): 483-504

Emcon Associates. 1980. Methane Generation and Recovery from Landfills. Ann Arbor Science Publishers, Ann Arbor, Michigan

Environment Canada. 1996. An assessment of the physical, economic and energy dimensions of waste management in Canada. Waste Treatment Division, Hazardous Waste Branch, Environment Canada. 136 pp

Erno, B. and R. Schmitz. 1996. Measurements of soil gas migration around oil and gas wells in the Lloydminster area. Journal of Canadian Petroleum Technology. 35(7): 37-46

Findikakis, A.N. and J.O. Leckie. 1979. Numerical simulation of gas flow in sanitary landfills. Journal of Environmental Engineering Division, ASCE. 105(5): 927-945

Findikakis, A.N., C. Papelis, C.P. Halvadakis, and J.O. Leckie. 1988. Modeling gas production in managed sanitary landfills. Waste Management and Research. 6: 115-123

Fowler, D. and J.H. Duyzer. 1989. Micrometeorological Techniques for the measurement of trace gas exchange. In Exchange of Trace Gases between Terrestrial Ecosystems and the Atmosphere. Eds. M.O. Andreae and D.S. Shimel. 189-207

Fredhend, D.G. and H. Rahardjo. 1993 Soil mechanics for unsaturated soils. John Wiley & Sons, N.Y.

Frind, E.O. 1982. Simulation of long-term transient density-dependent transport in groundwater. Advances in Groundwater. 5: 73-88

Hartless, R. 1995. Measuring pressures and flow of landfill gas. Proceedings of Sardinia 95, 5th International Landfill Symposium, Cagliary. Vol. III: 517-531

Healy, R.W., R.G. Striegl, T.F. Russel, G.P. Hutchinson, and G.P. Livingston. 1996. Numerical evaluation of static-chamber measurements of soil-atmosphere gas exchange: Identification of physical processes. Journal of Soil Science Society of America. 60: 740-747

Hogan, K.B. and D.W. Kruger. 1992. Methane reductions are a cost-effective approach for reducing emissions of greenhouse gases. Proceedings of Greenhouse Gas Emissions and Mitigation Research Symposium. 1.25-1.34

Hutchinson, G.L. and A.R. Mosier. 1979. Nitrous oxide emissions from an irrigated cornfield. Science. 205:1125-1127

Hutchinson, G.L. and A.R. Mosier. 1981. Improved soil cover method for field measurement of nitrous oxide fluxes. Journal of Soil Science Society of America. 45: 311-316

Huyakorn, P.S. and G.F. Pinder. 1983. Computational Methods in Subsurface Flow. Academic Press, New York

Jensen, L.S., T. Mueller, K.R. Tate, D.J. Ross, J.Magid, and N.E. Nielsen. 1996. Soil surface CO2 flux as an index of soil respiration in situ: A comparison of two chamber methods. Soil Biology and Biochemistry. 28(10/11): 1297-1306

Jones, H.A. and D.B. Nedwell. 1990. Soil atmosphere concentration profiles and methane emission rates in the restoration covers above landfill sites: Equipment and preliminary results. Waste Management and Research. 8: 21-31

Jury, W.A., J. Letey, and T. Collins. Analysis of chamber methods used for measuring nitrous oxide production in the field. Journal of Soil Science Society of America. 46: 250-256

Kanemasu, E.T., W.L. Powers, and J.W. Sij. 1974. Field chamber measurements of CO2 flux from soil surface. Soil Science. 118(4): 233-237

Khalil, M.A.K., R.A. Rasmussen, and M.J. Shearer. 1992. Glogal atmospheric methane: Trends of sources, sinks, and concentrations. Proceedings of Greenhouse Gas Emissions and Mitigation Research Symposium. Durham, North Carolina. 4.1 – 4.10

Kightley, D., D.B. Nedwell, and M. Cooper. 1995. Capacity of methane oxidation in landfill cover soils measured in laboratory-scale soil microcosm. Applied and Environmental Microbiology. 61(2): 592-601

King, G.M. 1992. Ecological aspects of methane oxidation, a key determinant of global methane dynamics. Advances in Microbial Ecology. 12: 431-468

Klenbusch, M.R. 1986. Measurement of gaseous emission rates from land surfaces using an emission isolation flux chamber: User's guide. Environmental Monitoring Systems Laboratory, U.S. Environmental Protection Agency. Report No. EPA/600/8-86/008

Lenschow, D.H. 1995. Micrometerological techniques for measuring biosphere-atmosphere trace gas exchange. In Biogenic Trace Gases: Measuring Emissions from Soil and Water. Eds. P.A. Matson and R.C. Harris. 126-163

Livingston, G.P. and G.L. Hutchinson. 1995. Enclosure-based measurement of trace gas exchange: applications and sources of error. In Biogenic Trace Gases: Measuring Emissions from Soil and Water. Eds. P.A. Matson and R.C. Harris. 14-51

Matthias, A.D., D.N. Yarger, and R.S. Weinbeck. 1978. A numerical evaluation of chamber methods for determining gas fluxes. Geophysical Research Letters. 5(9): 765-768

Mendoza, C.A. and E.O. Frind. 1990. Advective-dispersive transport of dense organic vapors in the unsaturated zone 1. Model development. Water Resources Research. 26(3): 379-387

Mendoza, C.A. and T.A. McAlary. 1990. Modeling of groundwater contamination caused by organic solvent vapors. Ground Water. 28(2): 199-206

Metcalfe, D.E. and G.J. Farquhar. 1987. Modeling gas migration through unsaturated soils from waste disposal sites. Water, Air, and soil Pollution. 32: 247-259

Millington, R.J. and J.P. Quirk. 1961. Permeability of porous solids. Transactions, Faraday Society. 57: 1200-1207

Mitchell, A.R. and D.F. Griffiths. 1980. The Finite Difference Methods in Partial Differential Equations. Wiley-Interscience Publication, New York

Mohsen, M.F.N., G.J. Frquhar, and N. Kouwen. 1980. Gas migration and vent design at landfill sites. Water, Air, and Soil Pollution. 13: 79-97

Moore, C.A., I.S. Rai, and A.A. Alzaydi. 1979. Methane migration around sanitary landfills. Journal of the Geotechnical Engineering Division, ASCE, 105(2): 131-144

Mosier, A.R. 1989. Chamber and isotope techniques. In Exchange of Trace Gases between Terrestrial Ecosystems and the Atmosphere. Eds. M.O. Andreae and D.S. Shimel. 175-187

Mosier, A.R. 1990. Gas flux measurement techniques with special reference to techniques suitable for measurements over large ecologically uniform areas. In Soils and Greenhouse Effect. Ed. A.F. Bouwman. 289-301

Palmisano, A.C. and M.A. Barlaz. 1996. Introduction to solid waste decomposition. In microbiology of Solid Waste. Eds. A.C. Palmisano and M.A. Barlaz. 122 pp

Princiotta, F.T. 1992. Greenhouse warming: The mitigation challenge. Proceedings of Greenhouse Gas Emissions and Mitigation Research Symposium. Durham, North Carolina. 1.1-1.24

Rasmussen, R.A. and M.A.K. Khalil. 1984. Atospheric methane in the recent and ancient atmospheres: Concentrations, trends, and interhemispheric gradient. Journal of Geophysical Research. 89(D7): 11599-11605

Rasmussen, R.A. and M.A.K. Khalil. 1986. Atmospheric trace gases:trends and distributions over the last decade. Science. 232:1623-1624

Reid, R.C., J.M. Prausnitz, and B.E. Poling. 1987. The Properties of Gases and Liquids. McGraw-Hill Inc., New York

Reinhart, D.R., D.C. Cooper, and B.L. Walker. 1992. Flux chamber design and operation for the measurement of municipal solid waste landfill gas. Journal of Air and Waste Management Association. 42(8): 1067-1070

Rolston, D.E., D.L. Hoffman, and D.W. Toy. 1978. Field measurement of denitrification: I. Flux of N_2 and N_2O. Journal of Soil Science Society of America. 41:863-869

Rovers, F.A. and G.J. Farquhar. 1973. Effect of Season on Landfill Leachate and Gas Production, Final Report: Part II. University of Waterloo Research Institute

Schutz, H., W. Seiler, and H. Rennenberg. 1990. Soil and land use related sources and sinks of methane in the context of the global methane budget. In Soils and Greenhouse Effect. Ed. A.F. Bouwman. 269-285

Shroff, V.S. 1999. An Investigation of Leachate Production from MSW Landfills in Semi-Arid Climates. MSc Thesis, University of Calgary, Calgary, Alberta

Smith, G.D. 1985. Numerical Solution of Partial Differential Equations: Finite Difference Methods. Third Edition. Oxford University Press, Oxford.

SIAM (Society for Industrial and Applied Mathematics). 1999. LAPACK User's Guide. 3rd Edition. Authors: E. Anderson, Z. Bai, C. Bischof, S. Blackford, J.Demmel, J. Du Croz, A. Greenbaum, S. Hammarling, A. McKenny, D. Sorensen

Tchobanoglous, G., H. Thiesen, and S. Vigil. 1993. Integrated Solid Waste Management - Engineering Principles and Management Issues. McGraw-Hill, New York.

Tregoures, A., M.A. Gonze, and P. Berne. 1997. Measurement of methane emissions using tracer-gas: method improvement. Proceedings of Sardinia 97, Sixth International Landfill Symposium, Cagliary. Vol. IV: 95-102

US EPA. 1998a. Characterization of municipal solid waste in the United States: 1997 update. Municipal and Industrial Solid Waste Division, Office of Solid Waste. Report no. EPA530-R-98_007

US EPA. 1998b. Methods for estimating greenhouse gas emissions from municipal waste disposal. Emission Inventory Improvement Program, US EPA

Whalen, S.C., W.S. Reeburgh, and K.A. Sandbeck. 1990. Rapid methane oxidation in a landfill cover soil. Applied and Environmental Microbiology. 56(11): 3405-3411

Young, A. 1989a. Mathematical modeling of landfill degradation. Journal of Chemical Technology and Biotechnology. 46: 189-208

Young, A. 1989b. Mathematical modeling of landfill gas extraction. Journal of Environmental Engineering, ASCE. 115(6): 1073-1087

Zheng, C. and G.D. Bennett. 1995. Applied Contaminant Transport Modeling: Theory and Practice. Van Nostrand Reinhold, New York

APPENDIX A – TRANSIENT TWO-DIMENSIONAL MODEL

```
      Program Transient Flux Chamber

c     ++++++++++++++++++++++++++++++++++++++++++++++++++++++++++++++++++++++++
c
c     Transient axisymmetric finite difference model to simulate gas migration
c     in a landfill cover when a closed flux chamber is used. Only two gases were
c     considered CO2 and air. Advection and dispersion were considered. Use Steady
c     state solutionsas the initial conditions. ADI scheme was used and the tri
c     diagonal matrices were solved using modified DGSTV subroutines taken from LAPACK.
c
c     Developed by M.D.N. Perera, Department of Civil Engineering, U. of Calgary
c      1999
c
c     ++++++++++++++++++++++++++++++++++++++++++++++++++++++++++++++++++++++++

      DOUBLE PRECISION X1(80),X2(80),Y1(80,50),Y2(80,50),DPZ(80,50),
     * Z(80),DPR(80,50),A1(80,50),B1(80,50),C1(80,50),D1(80,50),
     * A2(80,50),B2(80,50),C2(80,50),D2(80,50),
     * P(80,50),R(50),DZ(80),DR(50),DT,CKK1,CKK2,CK1(80,50),CK2(80,50),
     * CK1I,CK2I,DEPTH,DIA,H,ADZ(80),ADR(50),CFC1,CFC2,VZ(80,50),
     * VR(80,50),VCN,VRC(80,50),DDRC(80,50),QBOT,U1,U2,WM1,WM2,THETA1,
     * THETA2,PN,CN,DDZ(80,50),DDR(80,50),DDZC,V1,V2,V3,V4,
     * V5,RDT,RALFA1,RALFA2,R1ADZ(80),R2ADZ(80),R1ADR(50),R2ADR(50),
     * RADZ(80),RADR(50)

      INTEGER N,M,IC,IR,NM
      CHARACTER Filename1*20, Filename2*20

      WRITE (*,*) 'Give the Filename1:  '
      READ (*,*) Filename1
      OPEN (unit =8,access= 'APPEND',file =Filename1, status ='UNKNOWN')

      WRITE (*,*) 'Give the Filename2:  '
      READ (*,*) Filename2
      OPEN (unit =9, access='APPEND',file = Filename2, status='UNKNOWN')

      OPEN (UNIT = 10, FILE = 'k1.txt', STATUS = 'OLD')

c     Initial values

      QBOT = 6.135D-5

      DEPTH = 0.54D0
```

```
      DIA = 0.254D0
      H = 0.160D0
      PHI = 0.35D0
      CKK1 = 1D-10
      CKK2 = 5D-10
      DD = 4.60D-5
      ALFA1 = 0.50D0
      ALFA2 = 0.05D0
      DT = 1.0D-5
      RT = 24.0427D0
      N = 28
      M = 23
      N1 = 13
      CFC1 = 1.46D-5
      CFC2 = 0.0415781D0
      WM1 = 44D0
      WM2 = 28.94D0
      U1 = 1.519D-10
      U2 = 1.755D-10
      T = 0.0D0


      RDT = PHI/DT
      RALFA1 = ALFA1/PHI
      RALFA2 = ALFA2/PHI

c     Disretization in z and r directions

      Z(1) = 0.0D0
      DO IR = 1,N
        DZ(IR) = 2D-2
      END DO

      DO IR = 2,N
        Z(IR) = Z(IR-1) + DZ(IR-1)
        ADZ(IR) = DZ(IR-1)+DZ(IR)
      END DO
      Z(N+1) = Z(N)+DZ(N)

      DO J=1,M+1
        DR(J) = 1D-2
      END DO


      R(1) = DR(1)
      R(2) = 1D-1*DR(2)
      R(3) = DR(2)
```

```
      ADR(2) = DR(1)+DR(2)
      ADR(3) = DR(2)+DR(3)
      DO J = 4,M+1
       R(J) = R(J-1)+DR(J-1)
       ADR(J) = DR(J-1)+DR(J)
      END DO

      DO IR = 2,N
       RADZ(IR) = 1D0/ADZ(IR)
       R1ADZ(IR) = 1D0/(DZ(IR-1)*ADZ(IR))
       R2ADZ(IR) = 1D0/(DZ(IR)*ADZ(IR))
      END DO

      DO IC = 2,M+1
       RADR(IC) = 1D0/ADR(IC)
       R1ADR(IC) = 1D0/(DR(IC-1)*ADR(IC))
       R2ADR(IC) = 1D0/(DR(IC)*ADR(IC))
      END DO

c     Read steady sate values and assign for initial values

      DO IR = 1,N+1
       READ (10,*) X1(IR),X2(IR)
      END DO



      DO IC = 1, M+2
       DO IR = 2,N+1
         Y1(IR,IC) = X1(IR)
         Y2(IR,IC) = X2(IR)
       END DO
      END DO

      DO IC = 1,M+2
       Y1(1,IC) = 1.46D-5
       Y2(1,IC) = 0.0415781D0
      END DO

c     Calculation for viscosity


      THETA1 = (1+DSQRT(U1/U2)*((WM2/WM1)**0.25D0))**2D0/
     *          (DSQRT(8D0*(1+WM1/WM2)))
      THETA2 = (1+DSQRT(U2/U1)*((WM1/WM2)**0.25D0))**2D0/
     *          (DSQRT(8D0*(1+WM2/WM1)))
```

```
c       Beginning of Z-direction equations

        PN = 0.0D0
        CN = 0.0D0
        NM = 1
        NT = 1

 100    CALL GRAD(Y1,Y2,N,M,P,DPZ,DPR,DR,DZ,Z)

c       Calculate velocities and dispersion coefficients

        WRITE (*,*) P(28,5), P(15,5),P(1,5)
        IF ((NM.EQ.1).OR.(NM/100.EQ.NM/100.0)) THEN
         DO IC = 1,M+2
          DO IR = 1,N+1
           IF (Y1(IR,IC).EQ.0) THEN
            VIS = U2
           ELSE IF (Y2(IR,IC).EQ.0) THEN
            VIS = U1
           ELSE
            VIS = U1/(1D0+THETA1*Y2(IR,IC)/Y1(IR,IC))+U2/(1D0+THETA2*
     *       Y1(IR,IC)/Y2(IR,IC))
           END IF
          CK1(IR,IC) = CKK1/VIS
          CK2(IR,IC) = CKK2/VIS

          IF ((IR.GT.1).AND.(IR.LT.N+1).AND.(IC.GT.1).AND.(IC.LT.M+2))THEN
           V = DABS(CK1(IR,IC)*DPZ(IR,IC))
           DDZC = DD+RALFA1*V
           PE = V*DZ(IR)/DDZC
           CO = V*DT/DZ(IR)
          END IF

       IF (PE.GT.PN)      PN = PE
          IF (CO.GT.CN)  CN = CO


       END DO
          CK1(1,IC) = 1D3*CK1(2,IC)
          END DO

      END IF


          DO IC = 1,M+1
```

```
          DO IR = 1,N
           CK1I = 2D0/(1D0/CK1(IR+1,IC)+1D0/CK1(IR,IC))
           CK2I = 2D0/(1D0/CK2(IR,IC+1)+1D0/CK2(IR,IC))
           VZ(IR,IC) = -CK1I*DPZ(IR,IC)
           VR(IR,IC) = -CK2I*DPR(IR,IC)
           DDZ(IR,IC) = DD+RALFA1*DABS(VZ(IR,IC))
           DDR(IR,IC) = DD+RALFA2*DABS(VZ(IR,IC))
          END DO
         END DO


        DO IC = 2,M+1
         DO IR = 2,N
          VRC(IR,IC) = -CK2(IR,IC)*0.5D0*(DPR(IR,IC)+DPR(IR,IC-1))
          DDRC(IR,IC) = DD+RALFA2*DABS(VZ(IR,IC))
         END DO
        END DO



        CALL BC(Y1,Y2,N1,CFC1,CFC2,DDZ,DZ,DR,R,DT,VZ)

      DO IC = 1, N1
       Y1(1,IC) = CFC1
       Y2(1,IC) = CFC2
      END DO

c     Diagonals of the coefficient matrix

        DO IC = 2,M+1
         DO IR = 3,N-1

          V1 = 2D0*DDZ(IR-1,IC)*R1ADZ(IR)
          V2 = 2D0*DDZ(IR,IC)*R2ADZ(IR)
          V3 = 2D0*DDR(IR,IC-1)*R1ADR(IC)
          V4 = 2D0*DDR(IR,IC)*R2ADR(IC)
          V5 = DDRC(IR,IC)/(R(IC)*ADR(IC))

          A1(IR-1,IC) = VZ(IR-1,IC)*RADZ(IR)+V1
          B1(IR,IC) = -VZ(IR,IC)*RADZ(IR)+VZ(IR-1,IC)*RADZ(IR)-V1-V2-RDT
          C1(IR,IC) = -VZ(IR,IC)*RADZ(IR)+V2
          D1(IR,IC) = -(VRC(IR,IC)/R(IC)-VR(IR,IC)*RADR(IC)+VR(IR,IC-1)*
     *                RADR(IC)-V3-V4+RDT)*Y1(IR,IC)-(V5+VR(IR,IC-1)*RADR(IC)
     *          +V3)*Y1(IR,IC-1)-(-VR(IR,IC)*RADR(IC)-V5+V4)*Y1(IR,IC+1)
```

```
          A2(IR-1,IC) = A1(IR-1,IC)
          B2(IR,IC) = B1(IR,IC)
          C2(IR,IC) = C1(IR,IC)
          D2(IR,IC) = -(VRC(IR,IC)/R(IC)+VR(IR,IC-1)*RADR(IC)-VR(IR,IC)*
     *                    RADR(IC)-V4-V3+RDT)*Y2(IR,IC)-(V5+VR(IR,IC-1)*RADR(IC)
     *              +V3)*Y2(IR,IC-1)-(-VR(IR,IC)*RADR(IC)-V5+V4)*Y2(IR,IC+1)
        END DO
        END DO


c       Top boundary condition (inside/outside chamber)

          DO IC = 2, M+1

          V1 = 2D0*DDZ(1,IC)*R1ADZ(2)
          V2 = 2D0*DDZ(2,IC)*R2ADZ(2)
          V3 = 2D0*DDR(2,IC-1)*R1ADR(IC)
          V4 = 2D0*DDR(2,IC)*R2ADR(IC)
          V5 = DDRC(2,IC)/(R(IC)*ADR(IC))

          B1(2,IC) = VZ(1,IC)*RADZ(2)-VZ(2,IC)*RADZ(2)-V2-V1-RDT
          C1(2,IC) = -VZ(2,IC)*RADZ(2)+V2
          D1(2,IC) = -(V1+VZ(1,IC)*RADZ(2))*Y1(1,IC)-(VRC(2,IC)/R(IC)
     *                    +VR(2,IC-1)*RADR(IC)-VR(2,IC)*RADR(IC)-V3-V4+RDT)*
     *                    Y1(2,IC)-(V5+VR(2,IC-1)*RADR(IC)+V3)*Y1(2,IC-1)-
     *                    (-VR(2,IC)*RADR(IC)-V5+V4)*Y1(2,IC+1)


          B2(2,IC) = B1(2,IC)
          C2(2,IC) = C1(2,IC)
          D2(2,IC) = -(V1+VZ(1,IC)*RADZ(2))*Y2(1,IC)-(VRC(2,IC)/R(IC)
     *                    +VR(2,IC-1)*RADR(IC)-VR(2,IC)*RADR(IC)-V3-V4+RDT)*
     *                    Y2(2,IC)-(V5+VR(2,IC-1)*RADR(IC)+V3)*Y2(2,IC-1)-
     *                    (-VR(2,IC)*RADR(IC)-V5+V4)*Y2(2,IC+1)
        END DO


c       Bottom boundary condition

          DO IC = 2,M+1

          VCN = -CK1(N,IC)*(P(N+1,IC)-P(N-1,IC))*RADZ(N)
```

```
      V1 = 2D0*DDZ(N-1,IC)*R1ADZ(N)
      V2 = 2D0*DDZ(N,IC)*R2ADZ(N)
      V3 = 2D0*DDR(N,IC-1)*R1ADR(IC)
      V4 = 2D0*DDR(N,IC)*R2ADR(IC)
      V5 = DDRC(N,IC)/(R(IC)*ADR(IC))

      A1(N-1,IC) = VZ(N-1,IC)*RADZ(N)-VZ(N,IC)*RADZ(N)+V1+V2
      B1(N,IC) = VZ(N-1,IC)*RADZ(N)-VZ(N,IC)*RADZ(N)-V1-V2+(-VZ(N,IC)
     *                  +V2*ADZ(N))*VCN/(DD+DABS(VCN)*RALFA1)-RDT
      D1(N,IC) = -(-VZ(N,IC)+V2*ADZ(N))*QBOT/(DD+DABS(VCN)*
     *                  RALFA1)-(VRC(N,IC)/R(IC)+VR(N,IC-1)*RADR(IC)-VR(N,IC)
     *                  *RADR(IC)-V3-V4+RDT)*Y1(N,IC)-(V5+VR(N,IC-1)*RADR(IC)
     *                  +V3)*Y1(N,IC-1)-(-VR(N,IC)*RADR(IC)-V5+V4)*Y1(N,IC+1)


      A2(N-1,IC) = A1(N-1,IC)
      B2(N,IC) = B1(N,IC)
      D2(N,IC) = -(VRC(N,IC)/R(IC)+VR(N,IC-1)*RADR(IC)-VR(N,IC)*
     *                  RADR(IC)-V3-V4+RDT)*Y2(N,IC)-(V5+VR(N,IC-1)*RADR(IC)+
     *                  V3)*Y2(N,IC-1)-(-VR(N,IC)*RADR(IC)-V5+V4)*Y2(N,IC+1)

      END DO

c     Solve for z direction

      DO IC = 2,M+1
       CALL DGTSV1(N,IC,A1,B1,C1,D1)
       CALL DGTSV1(N,IC,A2,B2,C2,D2)
    END DO

c     update y values


      DO IC = 2, M+1
       DO IR = 2,N
        Y1(IR,IC) = D1(IR,IC)
        Y2(IR,IC) = D2(IR,IC)
       END DO
      END DO

      DO IC = 2,M+1
       Y1(N+1,IC) = Y1(N,IC)+(Y1(N,IC)-Y1(N-1,IC))
       Y2(N+1,IC) = Y2(N,IC)+(Y2(N,IC)-Y2(N-1,IC))
      END DO

      DO IR = 1, N+1
       Y1(IR,1) = Y1(IR,3)
```

```
          Y2(IR,1) = Y2(IR,3)
          Y1(IR,M+2) = Y1(IR,M)
          Y2(IR,M+2) = Y2(IR,M)
        END DO

c       End of Z direction

        T = T+DT


c       Beginning of r-direction

        CALL GRAD(Y1,Y2,N,M,P,DPZ,DPR,DR,DZ,Z)

c       IF ((NM.EQ.1).OR.(NM/1000.EQ.NM/1000.0)) THEN
c
c       DO IC = 1,M+2
c         DO IR = 1,N+1
c           IF (Y1(IR,IC).EQ.0) THEN
c             VIS = U2
c           ELSE IF (Y2(IR,IC).EQ.0) THEN
c             VIS = U1
c           ELSE
c             VIS = U1/(1D0+THETA1*Y2(IR,IC)/Y1(IR,IC))+U2/(1D0+THETA2*
c     *       Y1(IR,IC)/Y2(IR,IC))
c           END IF
c         CK1(IR,IC) = CKK1/VIS
c         CK2(IR,IC) = CKK2/VIS
c
c         IF (((IR.GT.1).AND.(IR.LT.N+1)).AND.((IC.GT.1).AND.(IC.LT.M+2)))
c     *  THEN
c           V = DABS(CK1(IR,IC)*DPZ(IR,IC))
c           DDZC = DD+RALFA1*V
c           PE = V*DZ(IR)/DDZC
c           CO = V*DT/DZ(IR)
c
c           IF (PE.GT.PN) PN = PE
c           IF (CO.GT.CN)  CN = CO
c
c         END IF
c
c         END DO
c       END DO
c
c       END IF

        DO IC = 1,M+1
```

```
      DO IR = 1,N
       CK1I = 2D0/(1D0/CK1(IR+1,IC)+1D0/CK1(IR,IC))
       CK2I = 2D0/(1D0/CK2(IR,IC+1)+1D0/CK2(IR,IC))
       VZ(IR,IC) = -CK1I*DPZ(IR,IC)
       VR(IR,IC) = -CK2I*DPR(IR,IC)
       DDZ(IR,IC) = DD+RALFA1*DABS(VZ(IR,IC))
       DDR(IR,IC) = DD+RALFA2*DABS(VZ(IR,IC))
      END DO
     END DO

     DO IC = 2,M+1
      DO IR = 2,N
       VRC(IR,IC) = -CK2(IR,IC)*0.5D0*(DPR(IR,IC)+DPR(IR,IC-1))
       DDRC(IR,IC) = DD+RALFA2*DABS(VZ(IR,IC))
      END DO
     END DO


  CALL BC(Y1,Y2,N1,CFC1,CFC2,DDZ,DZ,DR,R,DT,VZ)

  DO IC = 1, N1
   Y1(1,IC) = CFC1
   Y2(1,IC) = CFC2
     END DO


c       Diagonals of coefficient matrix


      DO IC = 3,M
       DO IR = 2,N-1

        V1 = 2D0*DDZ(IR-1,IC)*R1ADZ(IR)
        V2 = 2D0*DDZ(IR,IC)*R2ADZ(IR)
        V3 = 2D0*DDR(IR,IC-1)*R1ADR(IC)
        V4 = 2D0*DDR(IR,IC)*R2ADR(IC)
        V5 = DDRC(IR,IC)/(R(IC)*ADR(IC))

        A1(IR,IC-1) = V5+VR(IR,IC-1)*RADR(IC)+V3
        B1(IR,IC) = VRC(IR,IC)/R(IC)+VR(IR,IC-1)*RADR(IC)-VR(IR,IC)*
     *                  RADR(IC)-V4-V3-RDT
        C1(IR,IC) = -V5-VR(IR,IC)*RADR(IC)+V4
        D1(IR,IC) = -((VZ(IR-1,IC)-VZ(IR,IC))*RADZ(IR)-V2-V1+RDT)*
     *                  Y1(IR,IC)-(VZ(IR-1,IC)*RADZ(IR)+V1)*Y1(IR-1,IC)-
     *            (-VZ(IR,IC)*RADZ(IR)+V2)*Y1(IR+1,IC)
```

```
          A2(IR,IC-1) = A1(IR,IC-1)
          B2(IR,IC) = B1(IR,IC)
          C2(IR,IC) = C1(IR,IC)
          D2(IR,IC) = -((VZ(IR-1,IC)-VZ(IR,IC))*RADZ(IR)-V1-V2+RDT)*
     *                    Y2(IR,IC)-(V1+VZ(IR-1,IC)*RADZ(IR))*Y2(IR-1,IC)-
     *               (-VZ(IR,IC)*RADZ(IR)+V2)*Y2(IR+1,IC)

         END DO
        END DO

c       Bottom layer

        DO IC = 3,M
         VCN = -CK1(N,IC)*(P(N+1,IC)-P(N-1,IC))*RADZ(N)

         V1 = 2D0*DDZ(N-1,IC)*R1ADZ(N)
         V2 = 2D0*DDZ(N,IC)*R2ADZ(N)
         V3 = 2D0*DDR(N,IC-1)*R1ADR(IC)
         V4 = 2D0*DDR(N,IC)*R2ADR(IC)
         V5 = DDRC(N,IC)/(R(IC)*ADR(IC))

         A1(N,IC-1) = V5+VR(N,IC-1)*RADR(IC)+V3
         B1(N,IC) = VRC(N,IC)/R(IC)-VR(N,IC)*RADR(IC)+VR(N,IC-1)*RADR(IC)
     *                  -V3-V4-RDT
         C1(N,IC) = -VR(N,IC)*RADR(IC)-V5+V4
         D1(N,IC) = -(-VZ(N,IC)+V2*ADZ(N))*QBOT/(DD+DABS(VCN)*RALFA1)
     *                  -(-V1-V2-VZ(N,IC)*RADZ(N)+VZ(N-1,IC)*RADZ(N)+
     *                  (-VZ(N,IC)+V2*ADZ(N))*VCN/(DD+DABS(VCN)*RALFA1)+RDT)
     *                  *Y1(N,IC)-(V1-VZ(N,IC)*RADZ(N)+VZ(N-1,IC)*RADZ(N)+V2)
     *                  *Y1(N-1,IC)


         A2(N,IC-1) = A1(N,IC-1)
         B2(N,IC) = B1(N,IC)
         C2(N,IC) = C1(N,IC)
         D2(N,IC) = -(VZ(N-1,IC)*RADZ(N)-VZ(N,IC)*RADZ(N)-V2-V1+
     *                  (-VZ(N,IC)+V2*ADZ(N))*VCN/(DD+DABS(VCN)*RALFA1)+
     *                  RDT)*Y2(N,IC)-(V1-VZ(N,IC)*RADZ(N)+VZ(N-1,IC)*
     *                  RADZ(N)+V2)*Y2(N-1,IC)
        END DO

C       Left boundary condition

        DO IR = 2,N-1

         V1 = 2D0*DDZ(IR-1,2)*R1ADZ(IR)
         V2 = 2D0*DDZ(IR,2)*R2ADZ(IR)
```

```
      V3 = 2D0*DDR(IR,1)*R1ADR(2)
      V4 = 2D0*DDR(IR,2)*R2ADR(2)

      B1(IR,2) = VRC(IR,2)/R(2)-VR(IR,2)*RADR(2)+VR(IR,1)*RADR(2)
     *                -V3-V4-RDT
      C1(IR,2) = V4+V3+VR(IR,1)*RADR(2)-VR(IR,2)*RADR(2)
      D1(IR,2) = -(VZ(IR-1,2)*RADZ(IR)-VZ(IR,2)*RADZ(IR)-V1-V2+RDT)*
     *                Y1(IR,2)-(V1+VZ(IR-1,2)*RADZ(IR))*Y1(IR-1,2)-
     *           (-VZ(IR,2)*RADZ(IR)+V2)*Y1(IR+1,2)

      B2(IR,2) = B1(IR,2)
      C2(IR,2) = C1(IR,2)
      D2(IR,2) = -(VZ(IR-1,2)*RADZ(IR)-VZ(IR,2)*RADZ(IR)-V1-V2+RDT)*
     *                Y2(IR,2)-(V1+VZ(IR-1,2)*RADZ(IR))*Y2(IR-1,2)-
     *           (-VZ(IR,2)*RADZ(IR)+V2)*Y2(IR+1,2)

   END DO

C     Bottom layer

      VCN = -CK1(N,2)*(P(N+1,2)-P(N-1,2))*RADZ(N)

      V1 = 2D0*DDZ(N-1,2)*R1ADZ(N)
      V2 = 2D0*DDZ(N,2)*R2ADZ(N)
      V3 = 2D0*DDR(N,1)*R1ADR(2)
      V4 = 2D0*DDR(N,2)*R2ADR(2)

      B1(N,2) = VRC(N,2)/R(2)+VR(N,1)*RADR(2)-VR(N,2)*RADR(2)
     *                -V4-V3-RDT
      C1(N,2) = VR(N,1)*RADR(2)-VR(N,2)*RADR(2)+V3+V4
    D1(N,2) = -(-VZ(N,2)+V2*ADZ(N))*QBOT/(DD+DABS(VCN)*RALFA1)
     *       -(VZ(N-1,2)*RADZ(N)-VZ(N,2)*RADZ(N)-V1-V2+(-VZ(N,2)+V2
     *            *ADZ(N))*VCN/(DD+DABS(VCN)*RALFA1)+RDT)*Y1(N,2)-(
     *                 V1-VZ(N,2)*RADZ(N)+VZ(N-1,2)*RADZ(N)+V2)*Y1(N-1,2)

      B2(N,2) = B1(N,2)
      C2(N,2) = C1(N,2)
      D2(N,2) = -(VZ(N-1,2)*RADZ(N)-VZ(N,2)*RADZ(N)-V1-V2+(-VZ(N,2)
     *           +V2*ADZ(N))*VCN/(DD+DABS(VCN)*RALFA1)+RDT)*Y2(N,2)
     *                -(V1-VZ(N,2)*RADZ(N)+VZ(N-1,2)*RADZ(N)+V2)*Y2(N-1,2)


c     Right boundary condition

      DO IR = 2,N-1

      V1 = 2D0*DDZ(IR-1,M+1)*R1ADZ(IR)
```

```
      V2 = 2D0*DDZ(IR,M+1)*R2ADZ(IR)
      V3 = 2D0*DDR(IR,M)*R1ADR(M+1)
      V4 = 2D0*DDR(IR,M+1)*R2ADR(M+1)

      A1(IR,M) = V3+V4-VR(IR,M+1)*RADR(M+1)+VR(IR,M)*RADR(M+1)
      B1(IR,M+1) = VRC(IR,M+1)/R(M+1)-VR(IR,M+1)*RADR(M+1)+VR(IR,M)*
     *                  RADR(M+1)-V3-V4-RDT
      D1(IR,M+1) = -(VZ(IR-1,M+1)*RADZ(IR)-VZ(IR,M+1)*RADZ(IR)-V1-V2+
     *                  RDT)*Y1(IR,M+1)-(V1+VZ(IR-1,M+1)*RADZ(IR))*
     *             Y1(IR-1,M+1)-(-VZ(IR,M+1)*RADZ(IR)+V2)*Y1(IR+1,M+1)

      A2(IR,M) = A1(IR,M)
      B2(IR,M+1) = B1(IR,M+1)
      D2(IR,M+1) = -(VZ(IR-1,M+1)*RADZ(IR)-VZ(IR,M+1)*RADZ(IR)-V1-V2+
     *                  RDT)*Y2(IR,M+1)-(V1+VZ(IR-1,M+1)*RADZ(IR))*
     *             Y2(IR-1,M+1)-(-VZ(IR,M+1)*RADZ(IR)+V2)*Y2(IR+1,M+1)
      END DO

C     Bottom layer

      VCN = -CK1(N,M+1)*(P(N+1,M+1)-P(N-1,M+1))*RADZ(N)

      V1 = 2D0*DDZ(N-1,M+1)*R1ADZ(N)
      V2 = 2D0*DDZ(N,M+1)*R2ADZ(N)
      V3 = 2D0*DDR(N,M)*R1ADR(M+1)
      V4 = 2D0*DDR(N,M+1)*R2ADR(M+1)

      A1(N,M) = V3+V4+VR(N,M)*RADR(M+1)-VR(N,M+1)*RADR(M+1)
      B1(N,M+1) = VRC(N,M+1)/R(M+1)-VR(N,M+1)*RADR(M+1)+VR(N,M)*
     *                  RADR(M+1)-V3-V4-RDT
      D1(N,M+1) = -(-VZ(N,M+1)+V2*ADZ(N))*QBOT/(DD+DABS(VCN)*RALFA1)
     *                  -(VZ(N-1,M+1)*RADZ(N)-VZ(N,M+1)*RADZ(N)-V1-V2+
     *                  VZ(N,M+1)+V2*ADZ(N))*VCN/(DD+DABS(VCN)*RALFA1)+RDT)
     *            *Y1(N,M+1)-(V1+V2-VZ(N,M+1)*RADZ(N)+VZ(N-1,M+1)*
     *            RADZ(N))*Y1(N-1,M+1)

      A2(N,M) = A1(N,M)
      B2(N,M+1) = B1(N,M+1)
      D2(N,M+1) = -(VZ(N-1,M+1)*RADZ(N)-VZ(N,M+1)*RADZ(N)-V1-V2+(-
     *          VZ(N,M+1)+V2*ADZ(N))*VCN/(DD+DABS(VCN)*RALFA1)+RDT)*
     *            Y2(N,M+1)-(V1+V2-VZ(N,M+1)*RADZ(N)+VZ(N-1,M+1)*
     *                  RADZ(N))*Y2(N-1,M+1)

    DO IR = 2,N
      CALL DGTSV2(M+1,IR,A1,B1,C1,D1)
      CALL DGTSV2(M+1,IR,A2,B2,C2,D2)
    END DO
```

```
      DO IC = 2,M+1
       DO IR = 2,N
        Y1(IR,IC) = D1(IR,IC)
        Y2(IR,IC) = D2(IR,IC)
       END DO
      END DO

      DO IR = 2,N
       Y1(IR,1) = Y1(IR,3)
       Y1(IR,M+2) = Y1(IR,M)
       Y2(IR,1) = Y2(IR,3)
       Y2(IR,M+2) = Y2(IR,M)
      END DO

      DO IC = 2,M+1
       Y1(N+1,IC) = Y1(N,IC)+(Y1(N,IC)-Y1(N-1,IC))
       Y2(N+1,IC) = Y2(N,IC)+(Y2(N,IC)-Y2(N-1,IC))
      END DO


      T = T+DT
      NM = NM+1

c     End of r- direction

      IF (T.LT.59) THEN
       IF (MOD(T,0.1).LT.0.00025) THEN
       OPEN (unit =8,access= 'APPEND',file =Filename1)
       WRITE (8,*) T,Y1(1,5),Y2(1,5)
       CLOSE(8)
       END IF
      ELSE IF (MOD(T,60.0).LT.0.00025) THEN
          OPEN (unit =8,access= 'APPEND',file =Filename1)
      WRITE (8,*) T,Y1(1,5),Y2(1,5)
          CLOSE(8)
         END IF
        IF (MOD(T,300.0).LT.0.00025) THEN
         OPEN (unit =9, access='APPEND',file = Filename2)
         WRITE(9,*) T
         DO IC = 2,M+1
          DO IR = 1,N
           WRITE (9,225) R(IC),Z(IR),Y1(IR,IC), Y2(IR,IC)
225        FORMAT (4F13.10)
          END DO
         END DO
         WRITE (9,*) PN, CN
```

```
          CLOSE (9)
        END IF

        IF (T.LT.1) GOTO 100


300   CONTINUE


          OPEN (unit =9, access='APPEND',file = Filename2)
          WRITE(9,*) T
          DO IC = 2,M+1
           DO IR = 1,N
            WRITE (9,225) R(IC),Z(IR),Y1(IR,IC), Y2(IR,IC)
           END DO
          END DO
          WRITE (9,*) PN, CN
          CLOSE (9)
        OPEN (unit =8,access= 'APPEND',file =Filename1)
        WRITE (8,*) PN,CN
        WRITE (8,*) TIME1
        CLOSE(8)
      END


        SUBROUTINE GRAD(Y1,Y2,N,M,P,DPZ,DPR,DR,DZ,Z)

        DOUBLE PRECISION Y1(80,50),Y2(80,50),DPZ(80,50),Z(80),
     *    DPR(80,50),DR(50),P(80,50),DZ(80)
        INTEGER N,M,IR,IC

c     Calculate pressures
        DO IC = 1,M+2
         DO IR = 1,N+1
          P(IR,IC) = 24.0427D0*(Y1(IR,IC)+Y2(IR,IC))+(0.56D0-Z(IR))*
     *       1.204D0*9.81D0/1.014D5
         END DO
        END DO



C       Calculate gradients
        DO IC = 1,M+1
         DO IR = 1,N
          DPZ(IR,IC) = (P(IR+1,IC)-P(IR,IC))/DZ(IR)
          DPR(IR,IC) = (P(IR,IC+1)-P(IR,IC))/DR(IC)
         END DO
```

```
      END DO

      RETURN
      END


      SUBROUTINE BC(Y1,Y2,N1,CFC1,CFC2,DDZ,DZ,DR,R,DT,VZ)
      DOUBLE PRECISION Y1(80,50),Y2(80,50),DR(50),R(50),DT,VZ(80,50),
     *   CFC1,CFC2,DDZ(80,50),DZ(80),RAREA
      INTEGER N1

      RAREA = 1D-3/(0.03D0*0.111D0*0.111D0)
c     Flux chamber concentration for the next time step
      DO IC = 3,N1-1
       CFC1 = CFC1+(DDZ(1,IC)*(Y1(2,IC)-Y1(1,IC))/DZ(1)
     *      -0.5D0*(Y1(1,IC)+Y1(2,IC))*VZ(1,IC))*R(IC)*(DR(IC)+
     *      DR(IC-1))*4*DT*RAREA
       CFC2 = CFC2+(DDZ(1,IC)*(Y2(2,IC)-Y2(1,IC))/DZ(1)
     *      -0.5D0*(Y2(1,IC)+Y2(2,IC))*VZ(1,IC))*R(IC)*(DR(IC)+
     *      DR(IC-1))*4*DT*RAREA
      END DO

       CFC1 = CFC1+(DDZ(1,2)*(Y1(2,2)-Y1(1,2))/DZ(1)-0.5D0*(Y1(1,2)
     *      +Y1(2,2))*VZ(1,2))*DR(1)*DR(1)*DT*RAREA
     *      +(DDZ(1,N1)*(Y1(2,N1)-Y1(1,N1))/DZ(1)-0.5D0*(Y1(1,N1)+
     *      Y1(2,N1))*VZ(1,N1))*R(N1-1)*DR(N1-1)*4*DT*RAREA
       CFC2 = CFC2+(DDZ(1,2)*(Y2(2,2)-Y2(1,2))/DZ(1)-0.5D0*(Y2(1,2)+
     *      Y2(2,2))*VZ(1,2))*DR(1)*DR(1)*DT*RAREA
     *      +(DDZ(1,N1)*(Y2(2,N1)-Y2(1,N1))/DZ(1)-0.5D0*(Y2(1,N1)+
     *      Y2(2,N1))*VZ(1,N1))*R(N1-1)*DR(N1-1)*4*DT*RAREA


      RETURN
      END


      SUBROUTINE DGTSV1( NN, I, DL, D, DU, B )
*
* -- LAPACK routine (version 2.0) --
*    Univ. of Tennessee, Univ. of California Berkeley, NAG Ltd.,
*    Courant Institute, Argonne National Lab, and Rice University
*    September 30, 1994
*
*    .. Scalar Arguments ..
      INTEGER          NN, I
*    ..
*    .. Array Arguments ..
```

```
      DOUBLE PRECISION  B( 80,50 ), D( 80,50 ), DL( 80,50 ),
     *                  DU( 80,50 )
     *  ..
     *
     * Purpose
     * =======
     *
     * DGTSV  solves the equation
     *
     *    A*X = B,
     *
     * where A is an N-by-N tridiagonal matrix, by Gaussian elimination with
     * partial pivoting.
     *
     * Note that the equation  A'*X = B  may be solved by interchanging the
     * order of the arguments DU and DL.
     *
     * Arguments
     * =========
     *
     * N      (input) INTEGER
     *        The order of the matrix A.  N >= 0.
     *
     * NRHS   (input) INTEGER
     *        The number of right hand sides, i.e., the number of columns
     *        of the matrix B.  NRHS >= 0.
     *
     * DL     (input/output) DOUBLE PRECISION array, dimension (N-1)
     *        On entry, DL must contain the (n-1) subdiagonal elements of
     *        A.
     *        On exit, DL is overwritten by the (n-2) elements of the
     *        second superdiagonal of the upper triangular matrix U from
     *        the LU factorization of A, in DL(1), ..., DL(n-2).
     *
     * D      (input/output) DOUBLE PRECISION array, dimension (N)
     *        On entry, D must contain the diagonal elements of A.
     *        On exit, D is overwritten by the n diagonal elements of U.
     *
     * DU     (input/output) DOUBLE PRECISION array, dimension (N-1)
     *        On entry, DU must contain the (n-1) superdiagonal elements
     *        of A.
     *        On exit, DU is overwritten by the (n-1) elements of the first
     *        superdiagonal of U.
     *
     * B      (input/output) DOUBLE PRECISION array, dimension (LDB,NRHS)
     *        On entry, the N-by-NRHS right hand side matrix B.
     *        On exit, if INFO = 0, the N-by-NRHS solution matrix X.
```

```
*
* LDB    (input) INTEGER
*        The leading dimension of the array B.  LDB >= max(1,N).
*
* INFO   (output) INTEGER
*        = 0:  successful exit
*        < 0:  if INFO = -i, the i-th argument had an illegal value
*        > 0:  if INFO = i, U(i,i) is exactly zero, and the solution
*              has not been computed.  The factorization has not been
*              completed unless i = N.
*
* ===================================================================
*
*    .. Parameters ..
     DOUBLE PRECISION   ZERO
     PARAMETER        ( ZERO = 0.0D+0 )
*    ..
*    .. Local Scalars ..
     INTEGER          K
     DOUBLE PRECISION   MULT, TEMP
*    ..
*    .. Intrinsic Functions ..
     INTRINSIC        ABS, MAX

     DO 30 K = 2, NN - 1
*       IF( DL( K,I ).EQ.ZERO ) THEN
*
*          Subdiagonal is zero, no elimination is required.
*
*          IF( D( K,I ).EQ.ZERO ) THEN
*
*             Diagonal is zero: set INFO = K and return; a unique
*             solution can not be found.
*

C             INFO = K
*             RETURN
*          END IF
        IF( ABS( D( K,I ) ).GE.ABS( DL( K,I ) ) ) THEN
*
*          No row interchange required
*
           MULT = DL( K,I ) / D( K,I )
           D( K+1,I ) = D( K+1,I ) - MULT*DU( K,I )

           B( K+1,I ) = B( K+1,I ) - MULT*B( K,I )
```

```
            IF( K.LT.( NN-1 ) )
     $         DL( K,I ) = ZERO
          ELSE
*
*           Interchange rows K and K+1
*
            MULT = D( K,I ) / DL( K,I )
            D( K,I ) = DL( K,I )
            TEMP = D( K+1,I )
            D( K+1,I ) = DU( K,I ) - MULT*TEMP
            IF( K.LT.( NN-1 ) ) THEN
              DL( K,I ) = DU( K+1,I )
              DU( K+1,I ) = -MULT*DL( K,I )
            END IF
            DU( K,I ) = TEMP

              TEMP = B( K,I )
              B( K,I ) = B( K+1,I )
              B( K+1,I ) = TEMP - MULT*B( K+1,I )

          END IF
   30   CONTINUE

*
*     Back solve with the matrix U from the factorization.
*

          B( NN,I ) = B( NN,I ) / D( NN,I )
          IF( NN.GT.1 )
     $      B( NN-1,I ) = ( B( NN-1,I )-DU( NN-1,I )*B( NN,I ) )/
     $                D( NN-1,I )
          DO 40 K = NN - 2, 2, -1
            B( K,I ) = ( B( K,I )-DU( K,I )*B( K+1,I )-DL( K,I )*
     $                B( K+2,I ) ) / D( K,I )
   40     CONTINUE

*
      RETURN
*
*     End of DGTSV1
*
      END


      SUBROUTINE DGTSV2( NN, I, DL, D, DU, B)
*
*  -- LAPACK routine (version 2.0) --
```

```
*    Univ. of Tennessee, Univ. of California Berkeley, NAG Ltd.,
*    Courant Institute, Argonne National Lab, and Rice University
*    September 30, 1994
*
*    .. Scalar Arguments ..
     INTEGER          NN, I
*    ..
*    .. Array Arguments ..
     DOUBLE PRECISION   B( 80,50 ), D( 80,50 ), DL( 80,50 ),
*                                    DU( 80,50)

*
*    .. Parameters ..
     DOUBLE PRECISION   ZERO
     PARAMETER        ( ZERO = 0.0D+0 )
*    ..
*    .. Local Scalars ..
     INTEGER          K
     DOUBLE PRECISION   MULT, TEMP
*    ..
*    .. Intrinsic Functions ..
     INTRINSIC        ABS, MAX

*
     DO 30 K = 2, NN - 1
*       IF( DL( I, K ).EQ.ZERO ) THEN
*
*          Subdiagonal is zero, no elimination is required.
*
*          IF( D( I,K ).EQ.ZERO ) THEN
*
*             Diagonal is zero: set INFO = K and return; a unique
*             solution can not be found.
*
C              INFO = K
C              RETURN
*          END IF
       IF( ABS( D( I,K ) ).GE.ABS( DL( I,K ) ) ) THEN
*
*          No row interchange required
*
           MULT = DL( I,K ) / D( I,K )
           D( I,K+1 ) = D( I,K+1 ) - MULT*DU( I,K )
           B( I,K+1 ) = B( I,K+1 ) - MULT*B( I,K )

           IF( K.LT.( NN-1 ) )
     $        DL( I,K ) = ZERO
```

```
      ELSE
*
*        Interchange rows K and K+1
*
         MULT = D( I,K ) / DL( I,K )
         D( I,K ) = DL( I,K )
         TEMP = D( I,K+1 )
         D( I,K+1 ) = DU( I,K ) - MULT*TEMP
         IF( K.LT.( NN-1 ) ) THEN
           DL( I,K ) = DU( I,K+1 )
           DU( I,K+1 ) = -MULT*DL( I,K )
         END IF
         DU( I,K ) = TEMP

           TEMP = B( I,K )
           B( I,K ) = B( I,K+1 )
           B( I,K+1 ) = TEMP - MULT*B( I,K+1 )

      END IF
   30 CONTINUE
*
*    Back solve with the matrix U from the factorization.
*
       B( I,NN ) = B( I,NN ) / D( I,NN )
      IF( NN.GT.1 )
     $   B( I,NN-1 ) = (B(I,NN-1)-DU(I,NN-1)*B(I,NN)) / D(I,NN-1)
      DO 40 K = NN - 2, 2, -1
        B( I,K ) = ( B( I,K )-DU( I,K )*B( I,K+1 )-DL( I,K )*
     $             B( I,K+2 ) ) / D( I,K )
   40   CONTINUE

*
     RETURN
*    End of DGTSV2

     END
```

APPENDIX B – STEADY STATE ONE-DIMENSIONAL MODEL

```
      Program Steady state gas migration in soils

c     ++++++++++++++++++++++++++++++++++++++++++++++++++++++++++++++++++++++++
c
c     One Dimensional case, with time
c     Non-equal discritization
c     Steady state
c
c     Developed by M.D.N. Perera, Dept. of Civil Engineering, U. of Calgary
c
c     ++++++++++++++++++++++++++++++++++++++++++++++++++++++++++++++++++++++++

      DOUBLE PRECISION X1(80),X2(80),P(80),DPZ(80),V(80),PE,CO,
     * DD,DISP(80),DZ(80),CK,CK1(80),PHI,RT,A1(80),B1(80),C1(80),
     * D1(80),Q1(80),Q2(80),DEPTH,Z(80),QBOT,U1,U2,VCN,ADZ(80),
     * WM1,WM2,T,DT,A2(80),B2(80),C2(80),D2(80),CK1I(80),VC,DIS,
     * RDT,RADZ(80),R1ADZ(80),R2ADZ(80)
      INTEGER I,J,N,L
      CHARACTER Filename*20

      WRITE (*,*) 'Give the Filename:  '
      READ (*,*) Filename
      OPEN (unit = 8, file = Filename, status = 'UNKNOWN')
      OPEN (unit = 9, file = 'b7.txt')

      QBOT = 6.135D-5


      TIME1 = TIMEF()

c     Assign parameters
c     k=kr*k(zz)
c     CK=kkr/(mu)
c     CK1 - z dir
c     DDZ = molecular diffusion
c     Mechanical dispersion = ALFA*V
c     Hydrodynamic dispersion = DDZ + ALFA*V
c     DPZ is first derivative of pressure P

      N = 28
      DEPTH = 0.54D0


      DO J=1,N
      DZ(J) = 2D-2
```

```
      END DO

      DT = 0.0001D0
      PHI = 0.35D0
      CK = 1D-10
      DD = 4.60D-5
      ALFA = 0.5D0
      RT = 24.0427D0
      U1 = 1.519D-10
      U2 = 1.755D-10
      WM1 = 44D0
      WM2 = 28.94D0

      T = 0.0
      Z (1) = 0.0
      Z(2) = DZ(1)

c     Initial guesses
      DO J = 2,N
C       X1(J) = 0.04157*Z(J)/DEPTH
C       X2(J) = 0.0415-0.0412*Z(J)/DEPTH
C       P(J) = 24.0427D0*(X1(J)+X2(J))+(0.56D0-Z(J))*1.1D0*9.81D0
C     *          /1.014D5
        Z(J+1) = Z(J)+DZ(J)
        ADZ(J) = DZ(J-1)+DZ(J)
      END DO

      DO J = 1,N+1
       READ (9,*) X1(J), X2(J)
      END DO

      X1(1) = 1.46D-5
      X2(1) = 0.0415781D0

      THETA1 = (1D0+DSQRT(U1/U2)*((WM2/WM1)**0.25D0))**2D0/(DSQRT(8D0*
     *          (1D0+WM1/WM2)))
      THETA2 = (1D0+DSQRT(U2/U2)*((WM1/WM2)**0.25D0))**2D0/(DSQRT(8D0*
     *          (1D0+WM2/WM1)))

      RDT = PHI/DT

      DO J = 2,N
      RADZ(J) = 1D0/ADZ(J)
      R1ADZ(J) = 1D0/(DZ(J-1)*ADZ(J))
      R2ADZ(J) = 1D0/(DZ(J)*ADZ(J))
      END DO
```

```
      I = 1
      PN = 0.0D0
      CN = 0.0D0
  5   L = 2

c     Calculation of pressure and gradient

      DO J = 1, N+1
       P(J) = RT*(X1(J)+X2(J))+(0.56D0-Z(J))*1.204D0*9.81D0/1.014D5
      END DO

      DO J = 1,N
       DPZ(J) = (P(J+1)-P(J))/DZ(J)
      END DO

c     velocities, dispersion

      IF ((I.EQ.1).OR.(I/100.EQ.I/100.0)) THEN
      DO J = 1, N+1
       IF (X1(J).EQ.0.0) THEN
       VIS = U2
       ELSE IF (X2(J).EQ.0.0) THEN
       VIS = U1
       ELSE
       VIS = U1/(1D0+THETA1*X2(J)/X1(J))+U2/(1D0+THETA2*X1(J)/X2(J))
       END IF

       CK1(J) = CK/VIS
       VC = -CK1(J)*(DPZ(J-1)+DPZ(J))/PHI
       DIS = DD+ALFA*DABS(VC)

       IF ((J.GT.1).AND.(J.LT.N+1)) THEN
       PE = DABS(VC)*DZ(J)/DIS
       CO = DABS(VC)*DT/DZ(J)
       IF (PE.GT.PN) PN = PE
       IF (CO.GT.CN) CN = CO
       END IF
    END DO


c     interface permeability

      DO J = 1,N
       CK1I(J) = 2D0/(1D0/CK1(J+1)+1D0/CK1(J))
      END DO

      END IF
```

```
      DO J = 1,N
       V(J) = -CK1I(J)*DPZ(J)
       DISP(J) = DD+ALFA*DABS(V(J))/PHI
      END DO


c     Diagonals of coefficient matrix
c     Top boundary condition
      B1(2) =0.5D0*(V(1)-V(2))*RADZ(2)-DISP(2)*R2ADZ(2)-DISP(1)*
     *   R1ADZ(2)-RDT
      C1(2) = -0.5D0*V(2)*RADZ(2)+DISP(2)*R2ADZ(2)
      D1(2) = (-V(1)*RADZ(2)-2D0*DISP(1)*R1ADZ(2))*X1(1)-(B1(2)+2D0*RDT)
     *          *X1(2)-C1(2)*X1(3)

      B2(2) = B1(2)
      C2(2) = C1(2)
      D2(2) = (-V(1)*RADZ(2)-2D0*DISP(1)*R1ADZ(2))*X2(1)-(B2(2)+2D0*RDT)
     *          *X2(2)-C2(2)*X2(3)


c     Intermediate points

      DO J = 3,N-1
       A1(J-1)= 0.5D0*V(J-1)*RADZ(J)+DISP(J-1)*R1ADZ(J)
       B1(J) = 0.5D0*(V(J-1)-V(J))*RADZ(J)-DISP(J)*R2ADZ(J)-
     *    DISP(J-1)*R1ADZ(J)-RDT
       C1(J) = -0.5D0*V(J)*RADZ(J)+DISP(J)*R2ADZ(J)
       D1(J) = -A1(J-1)*X1(J-1)-(B1(J)+2D0*RDT)*X1(J)-C1(J)*X1(J+1)

       A2(J-1) = A1(J-1)
       B2(J) = B1(J)
       C2(J) = C1(J)
       D2(J) = -A2(J-1)*X2(J-1)-(B2(J)+2D0*RDT)*X2(J)-C2(J)*X2(J+1)
      END DO

c     Bottom boundary condition

      VCN = -CK1(N)*(P(N+1)-P(N-1))/ADZ(N)
      A1(N-1) = 0.5D0*(-V(N)+V(N-1))*RADZ(N)+DISP(N)*R2ADZ(N)+
     *          DISP(N-1)*R1ADZ(N)
      B1(N) = 0.5D0*(V(N-1)-V(N))*RADZ(N)-DISP(N)*R2ADZ(N)-
     *   DISP(N-1)*R1ADZ(N)-RDT+(-0.5D0*V(N)+DISP(N)/DZ(N))
     *          *VCN/(DD+DABS(VCN)*ALFA/PHI)
      D1(N) = -(-V(N)+2D0*DISP(N)/DZ(N))*QBOT/(DD+DABS(VCN)*ALFA/PHI)
     *          -A1(N-1)*X1(N-1)-(B1(N)+2D0*RDT)*X1(N)
```

```
      A2(N-1) = A1(N-1)
      B2(N) = B1(N)
      D2(N) = -A2(N-1)*X2(N-1)-(B2(N)+2D0*RDT)*X2(N)


c     Solve the equations by Thomas Algorithm.

      CALL DGTSV(N,A1,B1,C1,D1)

      CALL DGTSV(N,A2,B2,C2,D2)

c     Check convergence

 10   IF (L.GT.N) GOTO 30
      IF ((DABS(X1(L)-D1(L)).GT.1D-12).OR.(DABS(X2(L)-D2(L)).GT.1D-12))
     * GOTO 20
      L = L+1
      GOTO 10

 20 DO J = 2,N
       X1(J) = D1(J)
       X2(J) = D2(J)
      END DO

      X1(N+1) = X1(N)+X1(N)-X1(N-1)
      X2(N+1) = X2(N)+X2(N)-X2(N-1)


      T = T+DT
      I = I+1


      GOTO 5
 30 CONTINUE
      DO J = 2,N
       X1(J) = D1(J)
       X2(J) = D2(J)
      END DO
      X1(N+1) = D1(N)+(D1(N)-D1(N-1))*DZ(N)/DZ(N-1)
      X2(N+1) = D2(N)+(D2(N)-D2(N-1))*DZ(N)/DZ(N-1)

c     Gas transport to check contnuity

      DO J=2,N
      Q1(J) = V(J)*(X1(J)+X1(J+1))/2D0-DISP(J)*(X1(J+1)-X1(J))/DZ(J)

    Q2(J) = V(J)*(X2(J)+X2(J+1))/2D0-DISP(J)*(X2(J+1)-X2(J))/DZ(J)
```

```
      END DO


      WRITE(8,*) 'CK= ', CK, '  DDZ= ', DD, '  ALFA= ',ALFA, '  PHI= '
     *     ,PHI, '  DT= ', DT
      DO J = 1,N+1
        WRITE(8,35) Z(J),X1(J),X2(J),P(J),Q1(J),Q2(J), X1(J)/(X1(J)+X2(J))
      END DO
      WRITE (8,*) PN, CN, T
   35 FORMAT(7F10.7)

      END


    SUBROUTINE DGTSV( NN, DL, D, DU, B )
*
* -- LAPACK routine (version 2.0) --
*    Univ. of Tennessee, Univ. of California Berkeley, NAG Ltd.,
*    Courant Institute, Argonne National Lab, and Rice University
*    September 30, 1994
*
*    .. Scalar Arguments ..
     INTEGER            NN
*    ..
*    .. Array Arguments ..
     DOUBLE PRECISION   B(80), D(80), DL(80), DU(80)
*    ..
*
* Purpose
* =======
*
* DGTSV  solves the equation
*
*    A*X = B,
*
* where A is an N-by-N tridiagonal matrix, by Gaussian elimination with
* partial pivoting.
*
* Note that the equation  A'*X = B  may be solved by interchanging the
* order of the arguments DU and DL.
*
* Arguments
* =========
*
* N      (input) INTEGER
*        The order of the matrix A.  N >= 0.
```

```
*
* NRHS   (input) INTEGER
*        The number of right hand sides, i.e., the number of columns
*        of the matrix B.  NRHS >= 0.
*
* DL     (input/output) DOUBLE PRECISION array, dimension (N-1)
*        On entry, DL must contain the (n-1) subdiagonal elements of
*        A.
*        On exit, DL is overwritten by the (n-2) elements of the
*        second superdiagonal of the upper triangular matrix U from
*        the LU factorization of A, in DL(1), ..., DL(n-2).
*
* D      (input/output) DOUBLE PRECISION array, dimension (N)
*        On entry, D must contain the diagonal elements of A.
*        On exit, D is overwritten by the n diagonal elements of U.
*
* DU     (input/output) DOUBLE PRECISION array, dimension (N-1)
*        On entry, DU must contain the (n-1) superdiagonal elements
*        of A.
*        On exit, DU is overwritten by the (n-1) elements of the first
*        superdiagonal of U.
*
* B      (input/output) DOUBLE PRECISION array, dimension (LDB,NRHS)
*        On entry, the N-by-NRHS right hand side matrix B.
*        On exit, if INFO = 0, the N-by-NRHS solution matrix X.
*
* LDB    (input) INTEGER
*        The leading dimension of the array B.  LDB >= max(1,N).
*
* INFO   (output) INTEGER
*        = 0:  successful exit
*        < 0:  if INFO = -i, the i-th argument had an illegal value
*        > 0:  if INFO = i, U(i,i) is exactly zero, and the solution
*              has not been computed.  The factorization has not been
*              completed unless i = N.
*
* =====================================================================
*
*    .. Parameters ..
      DOUBLE PRECISION   ZERO
      PARAMETER          ( ZERO = 0.0D+0 )
*    ..
*    .. Local Scalars ..
      INTEGER            K
      DOUBLE PRECISION   MULT, TEMP
*    ..
*    .. Intrinsic Functions ..
```

```
      INTRINSIC       ABS, MAX
*     ..
*     .. External Subroutines ..
C     EXTERNAL        XERBLA
*     ..
*     .. Executable Statements ..

*
      DO 30 K = 2, NN - 1
C        IF( DL( K ).EQ.ZERO ) THEN
*
*           Subdiagonal is zero, no elimination is required.
*
C           IF( D( K ).EQ.ZERO ) THEN
*
*              Diagonal is zero: set INFO = K and return; a unique
*              solution can not be found.
*
C              END IF
C        ELSE
            IF( ABS( D( K ) ).GE.ABS( DL( K ) ) ) THEN
*
*           No row interchange required
*
            MULT = DL( K ) / D( K )
            D( K+1 ) = D( K+1 ) - MULT*DU( K )

              B( K+1 ) = B( K+1 ) - MULT*B( K )

            IF( K.LT.( NN-1 ) )
     $         DL( K ) = ZERO
          ELSE
*
*           Interchange rows K and K+1
*
            MULT = D( K ) / DL( K )
            D( K ) = DL( K )
            TEMP = D( K+1 )
            IF( K.LT.( NN-1 ) ) THEN
            D( K+1 ) = DU( K ) - MULT*TEMP
              DL( K ) = DU( K+1 )
              DU( K+1 ) = -MULT*DL( K )
            END IF
            DU( K ) = TEMP

              TEMP = B( K )
              B( K ) = B( K+1 )
```

```
            B( K+1 ) = TEMP - MULT*B( K+1 )

         END IF
      30 CONTINUE

*
*     Back solve with the matrix U from the factorization.
*

         B( NN ) = B( NN ) / D( NN )
         IF( NN.GT.1 )
        $    B( NN-1 ) = ( B( NN-1 )-DU( NN-1 )*B( NN ) ) / D( NN-1 )
         DO 40 K = NN - 2, 2, -1
            B( K ) = ( B( K )-DU( K )*B( K+1 )-DL( K )*
        $             B( K+2 ) ) / D( K )
      40 CONTINUE

*
      RETURN
*
*     End of DGTSV
*
      END
```